DESIGN AND SIMULATION OF GRID CONNECTED PV SYSTEM

A DISSERTATION SUBMITTED IN PARTIAL FULFILLMENT OF THE REQUIREMENTS FOR THE AWARD OF THE DEGREE OF

MASTER OF TECHNOLOGY
IN
POWER SYSTEM

(ELECTRICAL ENGINEERING)

SUBMITTED BY:

MANOJ KUMAR
(2K14/ PSY/ 13)

UNDER THE SUPERVISION OF

Dr. Rachana Garg

DEPARTMENT OF ELECTRICAL ENGINEERING

DELHI TECHNOLOGICAL UNIVERSITY
(Formerly Delhi College of Engineering)
Bawana Road, Delhi-110042
INDIA
2016

DEPARTMENT OF ELECTRICAL ENGINEERING

DELHI TECHNOLOGICAL UNIVERSITY

(Formerly Delhi College of Engineering)

Bawana Road, Delhi-110042

CERTIFICATE

I, **Manoj Kumar** Roll No. 2K14/PSY/13, a student of M. Tech. (Power System), hereby declare that the dissertation titled "**Design and Simulation of Grid Connected PV System**" is a bonafide record of the work carried out by me under the supervision of **Dr. Rachana Garg,** Associate Professor, of Electrical Engineering Department, Delhi Technological University in partial fulfilment of the requirement for the award of the degree of Master of Technology and has not been submitted elsewhere for the award of any other Degree or diploma.

Place: Delhi **(Manoj Kumar)**

Date:

(Dr. Rachana Garg)

SUPERVISOR

ACKNOWLEDGEMENT

I would like to express my sincere gratitude to Dr. Rachana Garg for her guidance and assistance in the dissertation. The technical discussions with her were always been very insightful, and I will always be indebted to her for all the knowledge she shared with me. Her prompt responses and availability despite her constantly busy schedule were truly appreciated. She always helped me in all the technical and non-technical issues. Without her consistent support, encouragement and valuable inputs, this dissertation would not have become possible.

I would like to express my deep gratitude to Prof. Madhusudan Singh, Head of Department of Electrical Engineering for providing his support during my project. I would also like to thank all the faculty members and staff of Electrical Engineering Department, DTU.

I would also like to thank to Ms Nikita Gupta (Research Scholar DTU), my batch-mates and friends who encouraged and helped me in completing the dissertation.

Finally, I express my deep sincere thanks to my Parents who motivated and encouraged me for higher studies, without which it wouldn't have been possible.

Delhi, 2016 Manoj Kumar

ABSTRACT

The human activities contribute to the global warming of the planet. As a result, every country strives to reduce carbon emissions. The world is facing not only the depletion of fossil fuels, but also its rise in prices which causes the worldwide economic instability. Several measures are being undertaken by the Governments around the world to explore alternative energy sources and to achieve pollution reduction. Solar photovoltaic system is one of the most important renewable and green energy source to generate electrical power and the fastest growing power generation in the world. Solar photovoltaic system may be standalone system or grid connected system.

In recent years, there has been a rapid increase in the grid connected PV systems being connected to the distribution network. As a result, high quality, low harmonic distortion current injection into the grid is essential. To achieve this, careful consideration of the inverter control is necessary.

In this work, design and simulation of grid connected 8 kW solar photovoltaic system is presented under various load and atmospheric conditions. The inverter control for integrating the PV system to the grid is also presented. The three phase inverter works as a multi-functional device, used to supply the power to the grid as power converter as well as harmonic eliminator. The inverter control is simulated using three control algorithms viz. SRFT, ISCT, Icos $\emptyset$, under various load and different environmental conditions in MATLAB/SIMULINK. The inverter control schemes reduce the harmonics in the source current due to various loads in the system and the unity power factor on the supply side is maintained. Thus, the power quality is improved due to reduced THD.

TABLE OF CONTENTS

COVER PAGE			i
CERTIFICATE			ii
ACKNOWLEDGEMENT			iii
ABSTRACT			Iv
TABLE OF CONTENTS			V
LIST OF FIGURES			viii
LIST OF TABLES			xi
LIST OF ABBREVIATIONS			xii
CHAPTER 1	**INTRODUCTION**		**1-8**
	1.1 General		1
	1.2 Classification of sources of energy		1
	1.2.1	Non-renewable resource of energy	1
	1.2.2	Renewable energy sources	2
	1.3 Motivation		6
	1.4 Objective		6
	1.5 Thesis Organization		7
CHAPTER 2	**LITERATURE REVIEW**		**9-14**
	2.1 General		9
	2.2 PV cell modeling		9
	2.3 MPPT algorithms for maximum power extraction		10
	2.4 Inverter control schemes		11
	2.5 Conclusion		14
CHAPTER 3	**MATHEMATICAL MODELLING OF GRID CONNECTED PV SYSTEM**		**15-30**
	3.1 General		15
	3.2 Solar PV system		15

3.2.1 Standalone solar PV system 15

3.2.2 Grid Connected Solar PV system 16

3.3 Components of Grid connected PV system 17

3.3.1 Photovoltaic Array 17

3.3.1.1 Characteristics of PV array 21

3.3.1.2 Effect of temperature and irradiation change on I-V and P-V characteristics 22

3.3.2 DC-DC converter 24

3.3.2.1 DC-DC boost converter 24

3.3.2.2 Designing of boost converter 25

3.3.3 Maximum power point techniques(MPPT) 26

3.3.3.1 Perturb and observe algorithm 26

3.3.4 Photovoltaic inverter 28

3.3.4.1 Design of VSI 29

3.4 Conclusion 30

CHAPTER 4 CONTROL ALGORITHMS FOR PV INVERTER 31-44

4.1 General 31

4.2 Control Algorithms 31

4.2.1 Synchronous reference frame theory 31

4.2.1.1 Phase locked loop 34

4.2.1.2 Hysteresis current controller (HCC) 35

4.2.2 Instantaneous symmetrical component theory 37

4.2.3 Icosø control algorithm 40

4.3 Conclusion 44

CHAPTER 5 SIMULATION RESULTS AND DISCUSSION 45-74

5.1 General 45

5.2 Proposed system 45

5.3 Simulation results of the proposed system for 46

5.3.1 SRF theory based control algorithm 46

5.3.2 ISCT theory based control algorithm 56

5.3.3 Icosø theory based control algorithm 65
5.4 Comparison of THD under SRF, ISCT and Icosø algorithms 73
5.5 Conclusion 74
CHAPTER 6 CONCLUSION AND FUTURE SCOPE OF WORK 75
6.1 Conclusion 75
6.2 Future scope 75
REFERENCES 76
APPENDIX I 82
LIST OF PUBLICATIONS 83

LIST OF FIGURES

Figure No.	Name	Page no.
Fig. 1.1	Non-renewable energy resources	2
Fig. 1.2	Renewable energy sources	2
Fig. 1.3	Status of renewable energy in India	3
Fig. 1.4	Status of solar energy in India	4
Fig. 1.5	Solar photovoltaic system	4
Fig. 1.6	Grid connected solar PV system	6
Fig. 3.1	Direct coupled standalone PV system	15
Fig. 3.2	Block diagram of standalone PV system with battery storage	16
Fig. 3.3	General block diagram of grid connected solar PV system	17
Fig. 3.4	Photovoltaic cell, Module and array	18
Fig. 3.5	Photocurrent generation principle	19
Fig. 3.6	Single-diode model of the theoretical PV cell and equivalent circuit of a practical PV cell including the series and parallel resistance	19
Fig. 3.7	I-V curve of the PV cell	20
Fig. 3.8	Characteristics a) I-V curve b) P-V curve of a practical PV device	22
Fig. 3.9	I-V and P-V characteristics of PV cell at constant temperature and variable irradiance	23
Fig. 3.10	I-V and P-V characteristics of PV cell at variable temperature and constant irradiance	23
Fig. 3.11	Circuit diagram of Boost converter	24
Fig. 3.12	P &O Algorithm for MPPT	26
Fig. 3.13	Voltage Source Converter	29
Fig. 4.1	Reference current extraction using SRF theory	33
Fig. 4.2	Diagram of 3-φ PLL	35
Fig. 4.3	Hysteresis current control	36
Fig. 4.4	Schematic Diagram of Hysteresis Current Controller	36
Fig. 4.5	Block Diagram for Extracting Source Current	38
Fig. 4.6	Block diagram of extracting reference source currents using Icosø	41
Fig. 5.1	Grid connected Solar PV system	45
Fig. 5.2	Simulink model of the grid connected PV system	46
Fig. 5.3	Simulink model of SRFT Controller for reference current extraction	47
Fig. 5.4	Performance of grid connected Solar PV system for balanced linear load under load changing and varying irradiation level	48
Fig. 5.5	Performance of grid connected Solar PV system for linear	48

	load under load changing and varying temperature levels	
Fig. 5.6	Waveform and harmonic analysis for Grid Current (I_{grid}) and PCC current (I_{PCC}) for linear load	49
Fig. 5.7	Power flow at different part of the system for linear load under load change and varying irradiation	49
Fig. 5.8	Power flow at different part of the system for linear load under load change and varing temperature	50
Fig. 5.9	In phase grid side voltage and current for linear load conditions.	50
Fig. 5.10	Performance of grid connected SPV system for non-linear load under load changing and varying irradiation levels	51
Fig. 5.11	Performance of grid connected SPV system for non-linear load under load changing and varying temperature levels	52
Fig. 5.12	Waveform and harmonic analysis for Grid Current (I_{grid}) and Load current (I_{Load}) for non- linear load	52
Fig. 5.13	In phase grid side voltage and current for non-linear load conditions	53
Fig. 5.14	Performance of grid connected SPV system for non-linear load under unbalancing and varying irradiation levels	54
Fig. 5.15	Waveform and harmonic analysis for Grid Current (I_{grid}) for non- linear load during unbalancing time	54
Fig. 5.16	Performance of grid connected SPV system for dynamic load under torque variation and varying irradiation levels	55
Fig. 5.17	Waveform and harmonic analysis for Grid Current (I_{grid}) and PCCcurrent (I_{PCC}) for dynamic load	55
Fig. 5.18	ISCT controller for reference current extraction	56
Fig. 5.19	Performance of grid connected SPV system for linear load under load changing and varying irradiation level	57
Fig. 5.20	Performance of grid connected SPV system for linear load under load changing and varying temperature levels	58
Fig. 5.21	Waveform and harmonic analysis for Grid Current (I_{grid}) and PCC current (I_{PCC}) for linear load	58
Fig. 5.22	In phase grid side voltage and current for linear load conditions.	59
Fig. 5.23	Performance of grid connected SPV system for non-linear load under load changing and varying irradiation levels	60
Fig. 5.24	Performance of grid connected SPV system for non-linear load under load changing and varying temperature levels	61
Fig. 5.25	Waveform and harmonic analysis for Grid Current (I_{grid}) and Load current (I_{Load}) for non- linear load	61
Fig. 5.26	In phase grid side voltage and current for non-linear load conditions	62

Fig. 5.27	Performance of grid connected SPV system for non-linear load under unbalancing and varying irradiation levels	63
Fig. 5.28	Waveform and harmonic analysis for Grid Current (I_{grid}) for non- linear load during unbalancing time	63
Fig. 5.29	Performance of grid connected SPV system for dynamic load under torque variation and varying irradiation level	64
Fig. 5.30	Waveform and harmonic analysis for Grid Current (I_{grid}) and PCC current (I_{PCC}) for dynamic load	65
Fig. 5.31	Icos∅ controller for reference current extraction	65
Fig. 5.32	Performance of grid connected SPV system for linear load under load changing and varying irradiation levels	66
Fig. 5.33	Performance of grid connected SPV system for linear load under load changing and varying temperature levels	67
Fig. 5.34	Waveform and harmonic analysis for Grid Current (I_{grid}) and PCC current (I_{PCC}) for linear load	67
Fig. 5.35	In phase grid side voltage and current for linear load conditions	68
Fig. 5.36	Performance of grid connected SPV system for non-linear load under load changing and varying irradiation levels	69
Fig. 5.37	Performance of grid connected SPV system for non-linear load under load changing and varying temperature levels	69
Fig. 5.38	Waveform and harmonic analysis for Grid Current (I_{grid}) and Load current (I_{Load}) for non- linear load	70
Fig. 5.39	In phase grid side voltage and current for non-linear load conditions	70
Fig. 5.40	Performance of grid connected SPV system for non-linear load under unbalancing and varying irradiation levels	71
Fig. 5.41	Waveform and harmonic analysis for Grid Current (I_{grid}) for non- linear load during unbalancing time	71
Fig. 5.42	Performance of grid connected SPV system for dynamic load under torque variation and varying irradiation levels	72
Fig. 5.43	Waveform and harmonic analysis for Grid Current (I_{grid}) and PCC current (I_{PCC}) for dynamic load	73

LIST OF TABLES

Table no.	Title	Page no.
I	Present status of installed PV system in India	5
II	THD of source current, PCC current and load current under various loads	73

LIST OF ABBREVIATIONS

KWh	Kilowatt hour
GW	Giga watt
RE	Renewable energy
JNNSW	Jawaharlal Nehru National Solar mission
MNRE	Ministry of New and Renewable Energy
PV	Photovoltaic
MPPT	Maximum power point tracking
P&O	Perturb and observe
VSI	Voltage source inverter
CCVSI	Current controlled voltage source inverter
IGBT	Insulated Gate Bipolar Transistor
PWM	Pulse Width Modulation
SRFT	Synchronous Reference Frame Theory
ISCT	Instantaneous symmetrical component theory
PFC	Power factor correction
PLL	Phase Locked Loop
HCC	Hysteresis Current Controller
PCC	Point of Common Coupling
DC	Direct Current
AC	Alternating Current
W	Watts
VAr	Volt Ampere reactive
THD	Total Harmonic Distortions
DG	Distributed generation

CHAPTER 1

INTRODUCTION

1.1 General

Electrical energy plays a pivotal role in our daily activities. The degree of development and civilization of a country is measured by the amount of utilization of energy by human beings. Electrical energy demand is increasing day by day due to increase in population, urbanization and industrialization. To meet this growing energy demand, electric generation must be increased. The world's net electricity generation has been increased from 17.3 trillion kWh in 2005 to 24.4 trillion kWh in 2015 and will be 33.3 trillion kWh in 2030 [1]. Currently, most of the electricity generation is from fossil fuels (Non-Renewable resource).With increasing rate of energy consumption, fossil fuel supply is fast depleting resulting in inflation and energy crisis. Also, the use of non-renewable resources can cause environmental pollution and greenhouse gas emission, which results in global warming. To overcome environmental pollution and greenhouse gas emissions like carbon-dioxide and mercury, the world is now moving from conventional energy sources to the renewable energy sources. Renewable energy sources are known to be much cleaner and produce energy without harming the environment. Hence, alternative or renewable source of energy have to be developed to meet the future energy requirement.

1.2 Classification of Sources of Energy

The energy resources are classified into following categories:

i. Non-renewable sources of energy
ii. Renewable energy source

1.2.1 Non-Renewable Sources of Energy

Non-renewable energy sources are mostly the sources from fossil fuel. They took millions of years to form, and will run out one day. Non-renewable energy resources are exhaustible

in nature and cannot be recreated in a short period of time. Fig. 1.1 shows different types of non-renewable energy sources.

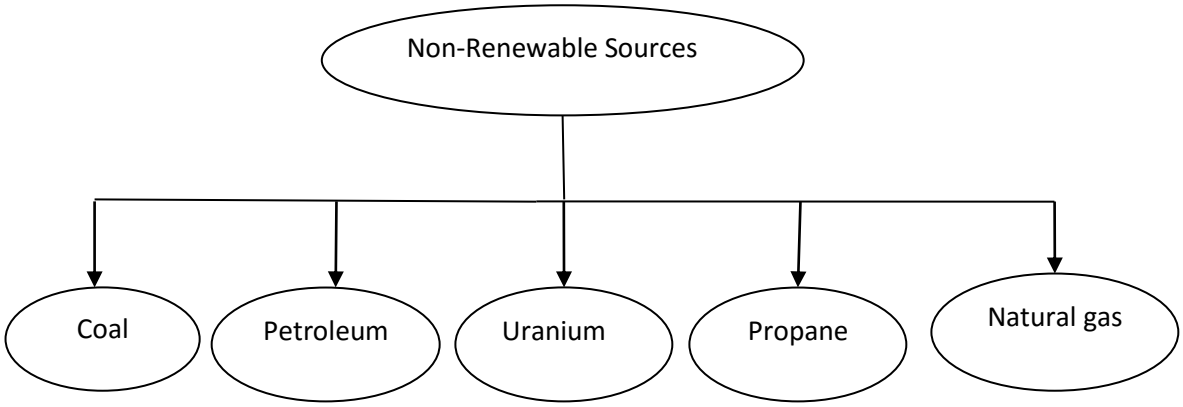

Fig. 1.1 Non-Renewable Energy Sources

1.2.2 Renewable Energy Sources

Renewable energy sources are non-exhaustible in nature. These types of sources exist freely in nature and may never run out and can be used to generate energy again and again. Fig 1.2 shows different types of renewable energy sources includes Biomass, Wind, Hydro-Power, Geothermal and Solar etc.

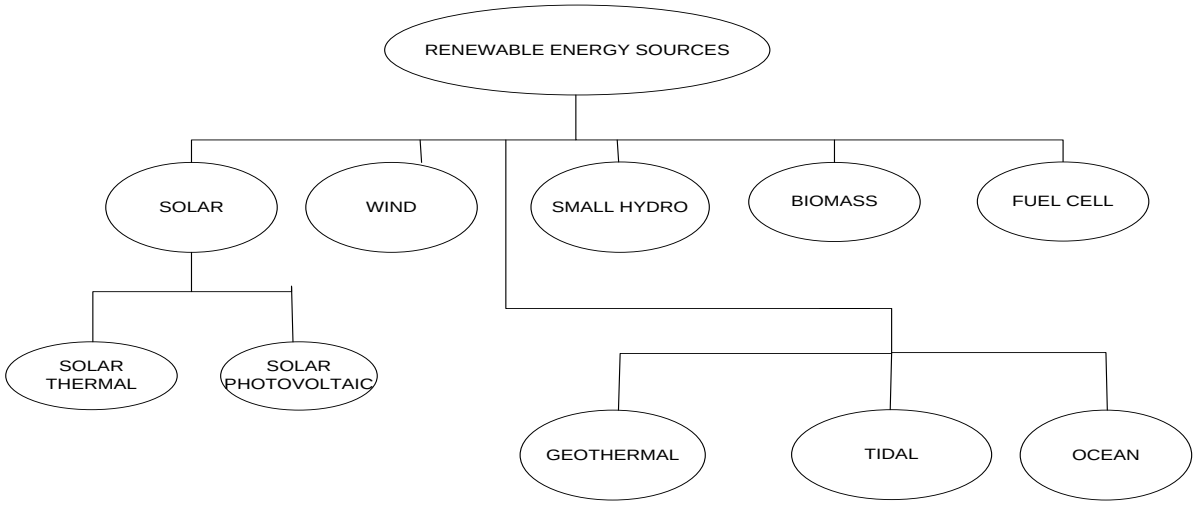

Fig. 1.2 Renewable Energy Sources

India has a total installed capacity of 263.66 GW and RE (Renewable energy) capacity of 34.35 GW (11% of Installed capacity (as on March 2015)) and has a vast potential of renewable energy sources. The status of renewable energy in India is shown in Fig. 1.3[2]

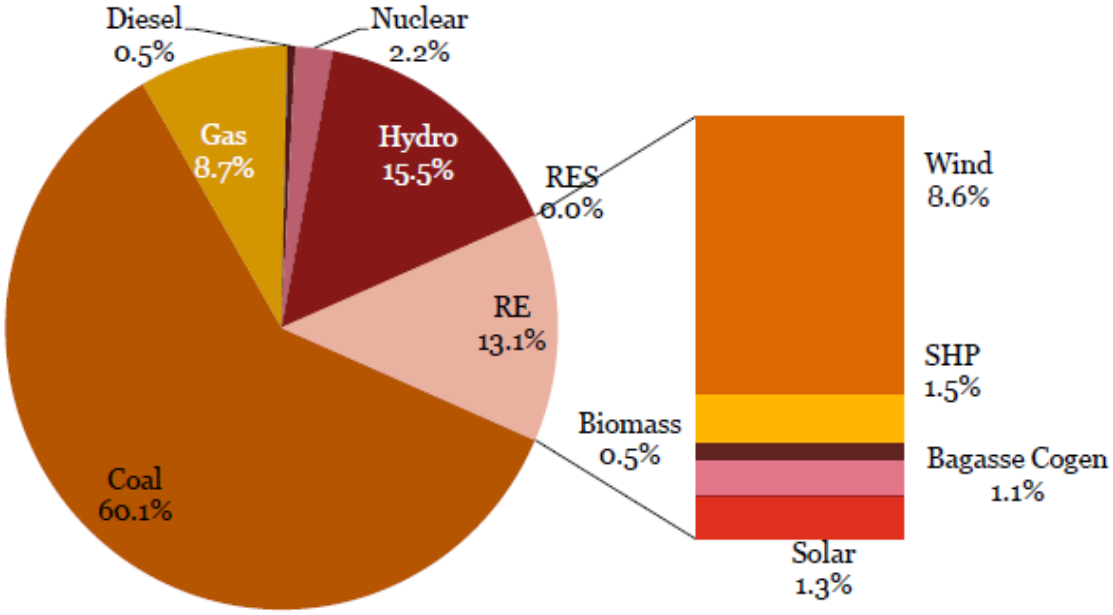

Fig. 1.3 Status of Renewable Energy in India [2]

One of the most important renewable energy source is solar energy. The geographical location of India is quite favourable for implementation of solar energy technologies. Present solar energy utilization in India stands far from being adequate. From this perspective, India has formulated its solar energy utilization roadmap for future through Jawaharlal Nehru National Solar Mission (JNNSM) with a target of deploying 20GW of grid connected solar power generation by 2022[3-4].The solar energy source is a practical solution to address the persistent demand supply gap in the power industry with the help of photovoltaic (PV) system. The PV approach is particularly suitable for the geographical and social-economic feature of this country. The present status of solar energy in India is shown in Fig. 1.4.

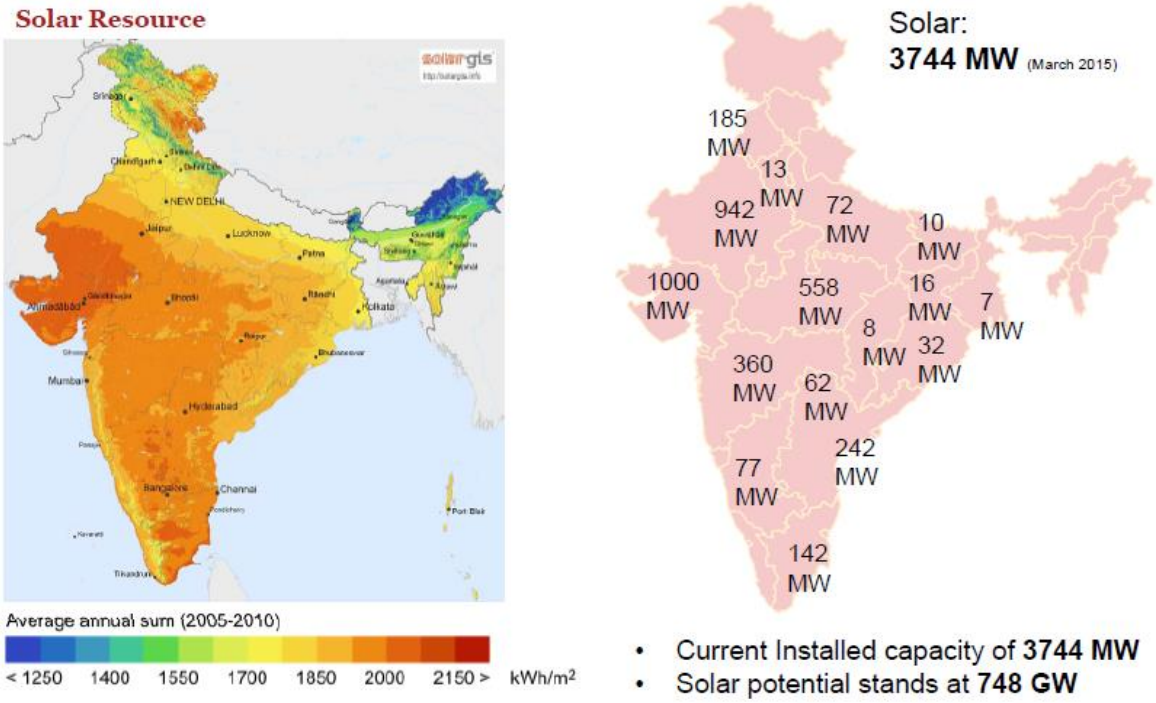

Fig. 1.4 Status of Solar Energy in India [2]

Solar Photovoltaic system can be utilized to produce electricity. With the help of photovoltaic process, solar energy can be converted into electric energy and such system is called solar photovoltaic (PV) system as shown in Fig.1.5. Large scale application of photovoltaic system for power generation, either on the rooftops of houses or in large fields connected to the utility grid provide clean and safe method of electricity generation.

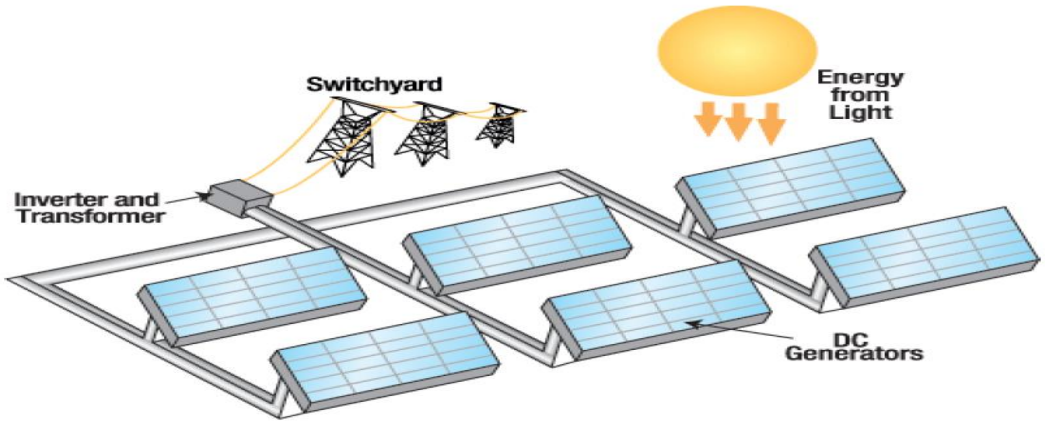

Fig. 1.5 Solar Photovoltaic System

The photovoltaic system is used in: (i) off-grid application where PV panels supply local loads (loads which are not connected to grid). Such systems are called standalone system (ii) Grid connected application where PV system is connected to grid and such type of systems are called grid connected PV system. Grid-connected PV systems can be installed on the facades and rooftops of buildings. They can also be installed in big fields to produce large amount of power. PV system has a variety of application in India. Some major photovoltaic power plants in India are Kamuthi solar power projects having 360 MW capacity, Charanka solar park Gujrat having capacity 221 MW, Welspun solar MP project in Madhya Pradesh having capacity 151 MW, Sakri solar plant Maharashtra etc. Hence solar PV is progressively becoming more attractive, than other renewable source of power.

PV installation in India also consist of off-grid connectivity and small capacity application used mostly for public lighting, traffic lighting and domestic power back-up in urban areas and small solar lanterns in the rural areas. In recent years, it is also used for powering water pumps for farming and small industrial areas. Government organizations like railways, telecom and other agencies are major consumers of PV solar system in India. Table I shows the present status of installed PV system in various sectors in which 360 MW of Solar Rooftop Projects sanctioned by MNRE and 49.677 MW Commissioned are presented.

Table I Present status of installed Rooftop PV system in India [2]

Sector	**Installed by SECI(MW)**	**Installed by States(MW)**	**Total Installed (MW)**
Commercial	11.36	12.71	24.07
Government	2.36	4.893	7.253
Hospital	1.6	0.47	2.07
Institutional	3.215	4.131	8.346
Religious institution	0.12	7.52	7.64
Residential	0	0.298	0.298
Total	**18.655**	**31.022**	**49.677**

1.3 Motivation

Solar energy is becoming an important source of energy all over the world and especially in India. To see India as SOLAR INDIA as stated in JNNSM, it is important to focus on setting up an enabling environment for solar energy penetration in the country.

Over the last decade there has been significant rise in the PV electrification projects both grid-connected and Standalone. So, it is important to investigate the performance of solar PV system and knowledge about the performance of solar power plants will result in correct investment decisions, a better regulatory framework and favourable government policies.

1.4 Objective

The main objective of this thesis is to design, simulate and study the performance of a grid interfaced solar PV system under various loads and atmospheric conditions. Fig. 1.6 shows the block diagram of grid connected PV system.

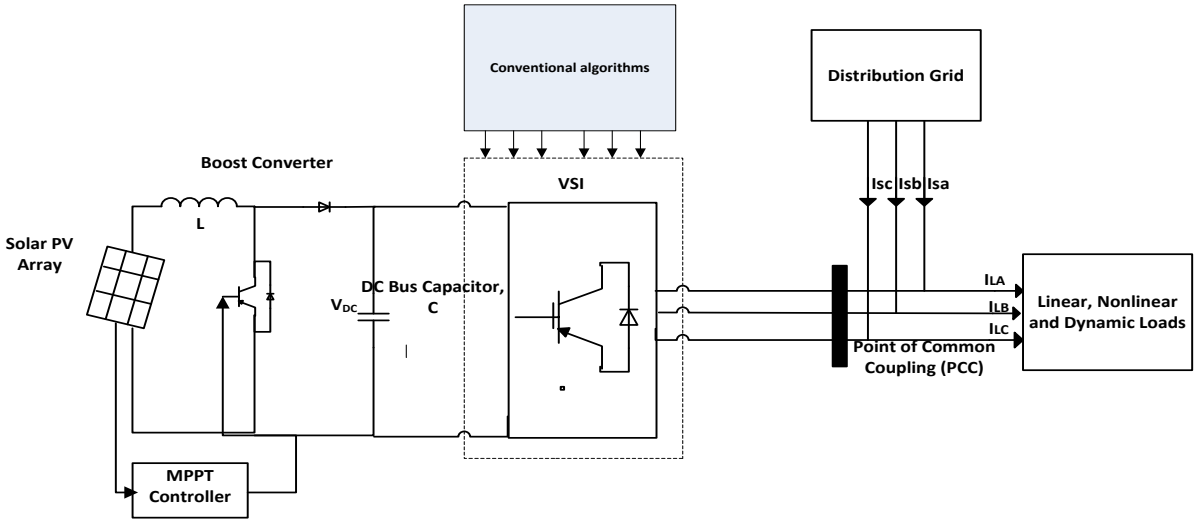

Fig. 1.6 Grid connected Solar PV system

Being a distributed generation, solar photovoltaic system integration to grid involves many power quality challenges viz. voltage fluctuation, harmonics, reactive power compensation voltage dips/swells, flicker, voltage unbalance, harmonics etc. The grid-side controller (DC-AC converter) reduces these power quality problems. Thus, the quality of the output

power to the grid is maintained. The grid-side controller must also regulate the DC-link voltage (the DC link that is between the two power converters) so that the power flow in the system is balanced.

Other challenge in the application of PV system is to extract the maximum power from sun under changing environment conditions. PV cell has nonlinear behavior and its output power is influenced by solar irradiation and temperature. To match the nonlinear output of PV modules with the load under changing atmospheric conditions, maximum power point tracking (MPPT) technique is usually implemented to always find and track the maximum power point of the PV panel [5].

In this thesis, following work has been carried out:

i. Grid connected PV system has been designed for an active power of 8 kW and simulated in MATLAB Simulink version 15.
ii. MPPT technique (P&O) has been implement to extract maximum power from the PV panel
iii. Control algorithms for PV inverter control have been investigated.

1.5 Thesis Organization

This thesis consists of six chapters, with the first chapter introducing the importance of solar energy, motivation and objective of this work.

Chapter 2, deals with the literature review of the recent achievements and current research activities in the field of the grid-connected PV systems and its control.

Chapter 3, presents the basics of Photovoltaic system, DC-DC converter, MPPT techniques, and PV inverter.

Chapter 4, presents the different control algorithms to control the PV inverter.

In Chapter 5, simulation results of grid connected PV system under various load condition for power factor correction mode (PFC) in MATLAB environment using SIMULINK are presented.

Chapter 6, presents the summary of the dissertation and conclusion as well as the future scope of this work.

CHAPTER 2

LITERATURE REVIEW

2.1 General

This chapter intends to give a brief literature review of grid connected PV system. A wide range of research work has been reported in area of maximum power point techniques and control techniques for ac- dc converter used grid connected PV system. The main focus of literature review is on following points:

i. PV cell modeling
ii. MPPT algorithms for maximum power extraction
iii. Inverter control schemes.

2.2 PV Cell Modeling

An ideal PV cell can be represented by a constant current source and a diode. Its output depends on the atmospheric condition and it exhibits non-linear behavior.

Pritam et al. [6] presents the modelling of a solar based non-conventional energy generation system. A grid-connected solar cell (PV) system with the functionality of harmonic compensation is introduced in this paper. Based on this, a test bed is built up to validate the practicability of the proposed scheme.

S. Sumathi et al. [7] book provide a comprehensive account of solar and wind energy modeling methods. For this purpose, explanatory background material has been introduced with MATLAB based simulation models. This book presents the recent trends in solar and wind energy based on soft computing techniques along with practical examples and Simulink models.

Haitham Abu Rub et al.[8], dasgupta et al [9] and Augustin McEvoy et al.[10] presents a comprehensive overview of grid-connected PV systems, including power curves, grid-connected configurations, different converter topologies (both single and three phases), control schemes, maximum power point tracking (MPPT), and anti-islanding detection methods.

B. Boukezata et al. [11] proposes the effective utilization of active power filter (APF) for interconnecting the PV modules to the grid using direct power control method. Its main feature is the capability to compensate the reactive power and harmonic currents drawn by nonlinear loads and simultaneously inject the maximum power available from the PV array into the grid.

M. G. Villalva et al. [12] proposes a method of modeling and simulation of photovoltaic arrays to find the parameters of the nonlinear I–V equation by adjusting the curve at three points: open circuit, maximum power, and short circuit.

2.2 MPPT Algorithms for Maximum Power Extraction

PV cells show the non-linear characteristics. Under changing weather conditions, its output changes and so it is essential to track the maximum power of a solar cell under varying atmospheric conditions. Lots of work has been done in developing the maximum power point techniques.

J. A. Gow et al. [13] develop a complete solar photovoltaic power electronic conversion system in simulation in order to allow the interaction between a proposed converter and the PV array. The model accepts irradiance and temperature as variable parameters and outputs the I-V characteristic for that particular cell.

Wei Jiang et al. [14] introduces the operation principle of current mode control Boost converter. The equation of two different work states are built by applying the theory of KCL and KVL. Two models working in CCM and DCM are respectively established using MATLAB and Simulink and the nonlinear phenomenon of Boost converter can be observed through simulation.

Nikita Gupta et al [15] propose a asymmetrical fuzzy logic control for PV module connected micro grid. In this paper author explain that during load change transients, there is considerable variation in dc link voltage in case of conventional controller whereas with asymmetrical fuzzy logic control, transient performance is improved considerably.

Sachin et al. [16] and Mukhtiar Singh et al. [17] presents a different approach for evaluating the performance of Photovoltaic Array and grid connected DC-AC converter control topology. A model is developed through converting basic circuit equation of solar

cell into simplified form including the effect of changing solar irradiation and temperature. In this paper an efficient MPPT control approach and grid interfacing of Photovoltaic array through DC/DC/AC Converter

S. Rustemli et al. [18], Kinal Kachhiya et al. [19] and H. Atlas et al. [20] presents the performance comparison of boost and interleaved boost converter for Maximum Power Point Tracking (MPPT) and various MPPT algorithms.

Trishan Esram et al. [21] presents the different techniques for maximum power point tracking of photovoltaic (PV) arrays.

Tarek Selmi et al. [22] and M.A Elgendy et al. [23] presents the mathematical analysis of a photovoltaic cell for the single diode and double diode cell configurations. The model of the double diode representation was implemented using a proprietary algorithm and MATLAB/Simulink. To track the point of maximum power perturb and observe (P&O) algorithm method was implemented.

2.3 Inverter Control Schemes

For a grid connected PV system, it is essential that the output of inverter is of proper magnitude and frequency. Also, by proper designing the control scheme of inverter the THD can be reduced.

S. B. Kjaer [24], in his research project developed an inverter for AC module applications. The project results in an inverter for a single PV module, with rating from 120 W to 160 W.

R. Mechouma et al. [25] presents a review on different technologies for connecting photovoltaic (PV) modules to a three-phase- grid and explain the inverters. The inverters are categorized into some classifications: the number of power processing stages; the use of decoupling capacitors and their locations.

Bhim Singh et al. [26] presents the design of a three phase DSTATCOM (Distribution Static Compensator) and its control algorithm based on correlation and cross correlation function approach for power quality improvement under linear/ nonlinear loads in a distribution system.

B. N. Singh et al. [27] used three-pole/four-pole topologies of current-controlled voltage source inverters (CC-VSI) as active filter (AF). The proposed AF system employs power balance theory, which is implemented using a TMS320C31 DSP

El-Samahy et al. [28] investigates the effect of the Distributed Generation (DG) on power quality pointing out its positive and negative impacts.

Bhattacharya et al. [29] proposes a synchronous reference frame based controller for a hybrid series active filter system. This paper discusses the basic synchronous reference frame controller structure and addresses its operation under non-unity controller loop gain conditions.

Bhim singh et al. [30] presents a novel concept of utilising SPV generating system to improve the power factor to unity or to regulate a voltage at PCC. Rejil et al. [31] presents simulation and design of active filter using synchronous frame theory.

Nikita Gupta et al. [32] presents a characterization study of 10 kW photovoltaic module under various load conditions. Control algorithm related to synchronous reference frame theory (SRFT) is used to generate gate signal for voltage source converter (VSC).

Ravi Nath Tripathi et al. [33] presents the concept of interconnection of Solar Photovoltaic (SPV) power generating system using Synchronous Reference Frame (SRF) theory based control in indirect current control mode of operation.

Da silva et al. [34] and [35] proposes a phase-locked loop (PLL) control strategy to synthesize unit vector using the synchronous reference frame (SRF).

MohamayeeMohapatra et al. [36] presents the comparative study between fixed and sinusoidal hysteresis current controller for PWM voltage source inverter.

U. Koteswara Rao et al. [37] and Sunil Kumar et al. [38] have explained the theory of instantaneous symmetrical components. ISCT is applied to explore various control strategies of load compensation, under different supply voltages. When the supply voltages are balanced and sinusoidal, all of these strategies converge to the same compensation characteristics.

Arindam Ghosh et al. [39] presents a new approach for generating reference currents for an active filter and/or a static compensator. It is assumed that the compensator is connected to a load that may either be connected in star or in delta. The load can be unbalanced and may

also draw harmonic currents. The purpose of the compensating scheme is to balance the load, as well as make the supply side power factor a desired value. The theory of instantaneous symmetrical components is used to obtain an algorithm to compute three phase reference currents which, when injected to the power system, produce desired results. Authors also proposes a suitable compensator structure that will track the reference currents in a hysteresis band control scheme.

Mahesh K. Mishra et al. [40], Naresh K. Kummari, Asheeshet al. [41] and Dinesh Kumar, Rajesh et al. [42] have been discussed load compensation techniques under unbalanced and distorted voltages. Two kinds of compensation methods are considered. In the first category, synchronous detection and modified equal current strategies are used under the unbalanced but sinusoidal source voltages. In the second method, load compensation based on instantaneous symmetrical component theory with positive sequence extraction is proposed and is shown to work under unbalanced and the non-sinusoidal source voltages.

Arun Kumar Verma et al. [43] describes a 4-leg VSC (Voltage Source Converter) based SPV(Solar Photovoltaic) power generating system, integrated to a 4-wire distribution system using Modified Instantaneous Symmetrical Component Theory based control algorithm. This MISCT is used to estimate reference currents to control 4-legVSC. The control algorithm is used to balance the loads and to improve the power factor of ac mains.

Manoj Kumar et al [44] presents a dual voltage source inverter (DVSI) scheme to enhance the power quality and reliability of the microgrid system. The control algorithms are developed based on instantaneous symmetrical component theory (ISCT) to operate DVSI in grid sharing and grid injecting modes.

G. Bhuvaneswari et al. [45] proposed Icos∅ algorithm which is applied to a three-phase shunt active filter to provide harmonics and reactive power compensation as demanded by the non-linear. The design is verified in simulation as well as signals implemented in hardware using simple analog circuits and results are compared.

Bhim Singh et al. [46] presents A DSTATCOM (Distributed Static Compensator) consisting of a 3-leg VSC (voltage source converter) and a zigzag transformer is used for the load compensation and the neutral current compensation in 3-phase 4-wire distribution system. The IcosΦ algorithm is modified for controlling the DSTATCOM for power factor

correction (PFC) and zero voltage regulation (ZVR) modes at PCC (point of common coupling) with indirect current control technique.

Kamatchi Kannan et al. [47] presents a three-phase three-wire DSTATCOM which is fed by Photovoltaic (PV) array or battery operated DC-DC boost converter is proposed for reactive power compensation, source current harmonic reduction and load compensation in the distribution system. The two control methods are Synchronous Reference Frame (SRF) theory and Icosø algorithm are used the switching of VSC will occur by comparing the source current with the reference current using Hysteresis based Pulse Width Modulation (PWM) current controller.

G. Bhuvaneswari et al. [48] and [49] also proposed Icosø algorithm which is applied to a three-phase shunt active filter to provide harmonics and reactive power compensation as demanded by the non-linear. The design is verified in simulation as well as signals implemented in hardware using simple analog circuits and results are compared.

2.5 Conclusion

Lots of work has been done in the area of grid connected PV system. In this chapter a brief literature review of the previous work done on the relevant topics viz. PV modelling, MPPT techniques, inverter control has been carried out.

CHAPTER 3
MATHEMATICAL MODELLING OF GRID CONNECTED PV SYSTEM

3.1 General

Solar energy is one of the most important source of renewable energy. The Photovoltaic system uses the solar energy to produce electricity. The main components of a PV system are solar cells or PV cells, DC-DC Boost converter, DC-AC inverter etc. This chapter presents the fundamentals of PV cells and modelling of a PV cell using an equivalent electrical circuit, and an overview of the DC-DC boost converter, MPPT techniques, PV inverter and its design etc.

3.2 Solar PV System

Solar PV system can be broadly classified as standalone and grid connected PV system [6- 9]:

3.2.1 Standalone Solar PV system

The PV system not connected to the electric utility grid is known as off-Grid PV system or 'Stand-alone PV systems'. Stand-alone system may be direct coupled PV system which is designed to supply DC or AC electrical loads. It is called direct coupled system because the output of a PV system is directly connected to the load. There is no electrical energy storage (batteries) in direct-coupled systems. The maximum power point tracking (MPPT) is used between the array and load. Fig. 3.1 shows the direct-coupled standalone solar PV system.

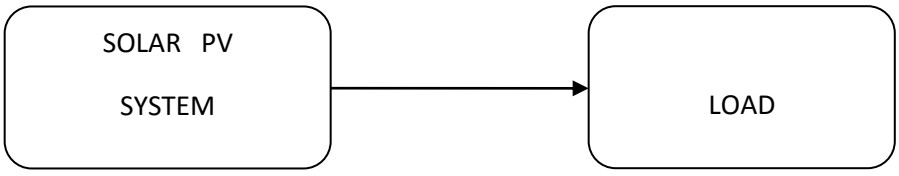

Fig. 3.1 Direct-Coupled Standalone PV System

An example of direct coupled solar PV systems is in agriculture applications where solar PV array can be directly connected to run the pump.

In some standalone systems battery is used as storage element. Fig. 3.2 shows the block diagram of a typical stand-alone PV system powering DC and AC loads with battery storage option.

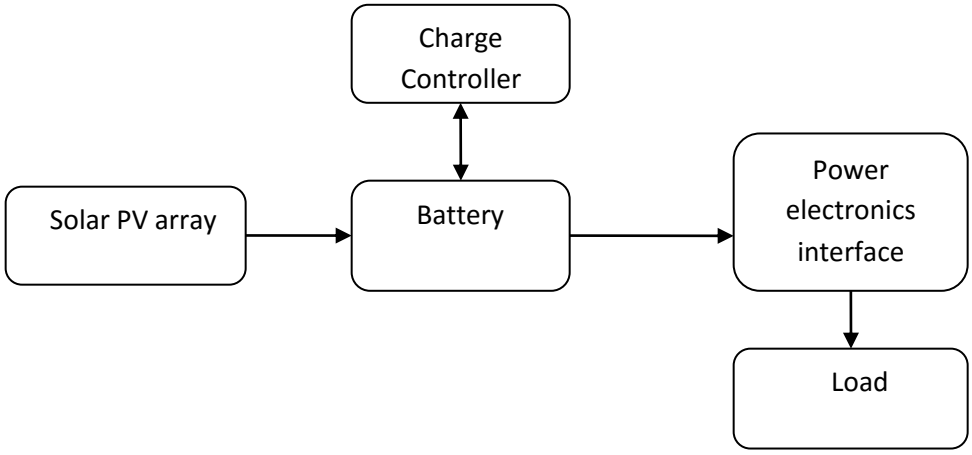

Fig. 3.2 Block diagram of Standalone PV system with battery storage

When batteries are implemented in the system, charge controllers have to be added. These controllers avoid discharge and overcharge of the battery. The charge controller regulates the current output and prevents the voltage level from exceeding the maximum value for charging the batteries. The output of the charge controller is connected to the battery bank. During the sunshine hours, the load is supplied with DC power while simultaneously charging the battery. The controller will ensure that the DC power output from the PV arrays should be adequate to sustain the connected load while sizing the batteries. Battery bank sizing depends on a number of factors, such as the duration of an uninterrupted power supply to the load when there is less or no radiation from the sun.

3.2.2 Grid-connected Solar PV system

The PV system which interface with the electric utility grid is called grid connected PV system. In grid connected PV system, there is bi-directional flow of energy. If the load is less than the output of PV system, the excess power from PV is fed to the grid. When the load is more than the PV output, the remaining load power is supplied by the grid as shown

in Fig. 3.3. The primary component in grid-connected PV systems is the inverter. The inverter converts the DC power produced by the PV array into AC power consistent with the voltage, frequency and power quality requirements of the utility grid.

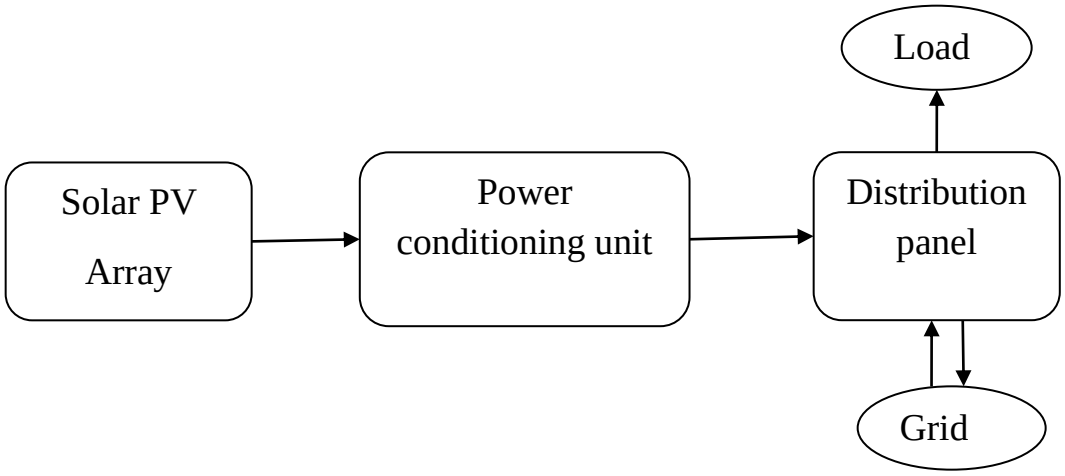

Fig. 3.3 General block diagram of Grid connected Solar PV system

3.3 Components of Grid connected PV system

The various components of grid connected PV system are:

i. Photovoltaic array
ii. DC-DC converter
iii. MPPT Techniques
iv. PV Inverter and its design

3.3.1 Photovoltaic Array

The basic component of a PV system is a PV cells. For higher power output, number of cells are combined and grouped to form PV modules and a number of PV modules can be grouped to form large photovoltaic arrays as shown in the Fig. 3.4

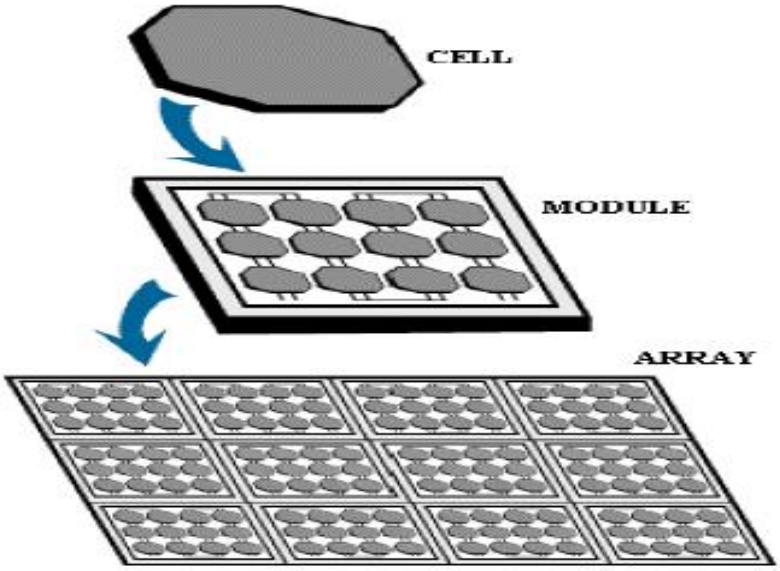

Fig. 3.4 Photovoltaic cell, Module and Array.

The Solar PV system usually consists of several solar arrays. Also, apart from the solar arrays, the solar PV system comprise of battery charge controller, MPPT controller and inverter and the entire system performance is based on the efficiency or the performance of the individual components [7].

PV cell is made up of various semiconductor materials but mono-crystalline silicon and polycrystalline silicon are mainly used for commercial use and each PV cell generates approximately 0.6V. The photovoltaic (PV) cell is basically a semiconductor diode whose p–n junction is exposed to light. Fig.3.5 shows the photocurrent generation principle of PV cells. In a photovoltaic cell when sunlight strikes its surface, some portion of the solar energy is absorbed in the semiconductor material. If absorbed energy is greater than the band gap energy of the semiconductor, the electrons from the valence band jumps to the conduction band. By this, pair of hole electrons are created in the illuminated region of the semiconductor. The electrons thus created in the conduction band are now free to move. These free electrons are forced to move in a particular direction by the action of electric field present in the PV cell. These flowing electrons constitutes current and can be drawn for external use by connecting a metal plate on top and bottom of PV cell. This current and voltage created because of its built in electric fields produces required power.When sun light hits the cell, the photons are absorbed by the semiconductor atoms, freeing electrons

from the negative layer. This free electron finds its path through an external circuit toward the positive layer resulting in an electric current from the positive layer to the negative one [10].

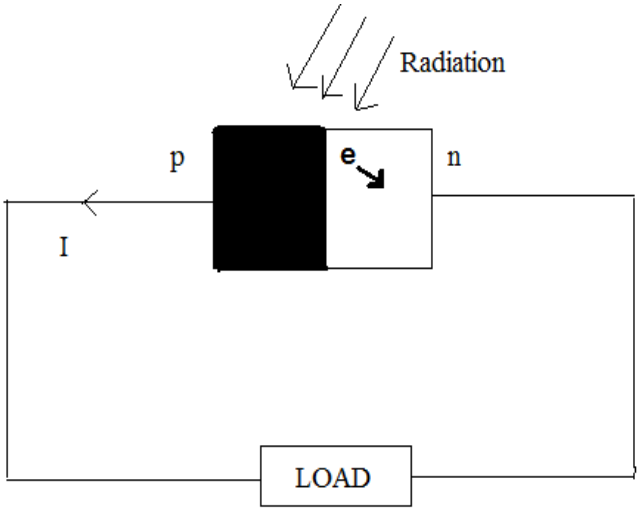

Fig.3.5. Photocurrent generation principle

The simple equivalent circuit of an ideal PV cell and practical PV cell is as shown in Fig.3.6. Ideal PV cell consists of ideal current source in parallel with the diode. The practical model of PV cells consists of ideal cell along with series resistance (R_s) and parallel resistance (R_p).

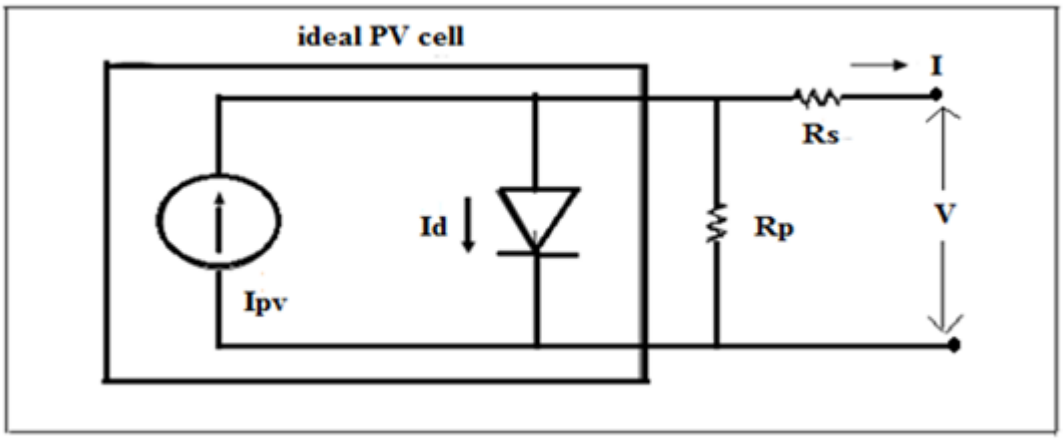

Fig. 3.6 Single-diode model of the theoretical PV cell and equivalent circuit of a practical PV cell including the series and parallel resistances.

The basic eqn. from the theory of semiconductors [11-12], that mathematically describes the I-V characteristics of the ideal PV cell are given by eqn. (3.1) to eqn. (3.3):

$$I = I_{pv} - I_d \tag{3.1}$$

Here, $I_d = I_O \left[exp\left(\frac{qv}{aKT}\right) - 1\right]$ (3.2)

Thus, $I = I_{pv} - I_O[exp\left(\frac{qv}{aKT}\right) - 1]$ (3.3)

where, I_{pv} is the current generated by the incident light which is directly proportional to the sun irradiation. So, I_{pv} represents the cell photocurrent, I_d is the diode eqn., I_O is the reverse saturation or leakage current of the diode, q is the electron charge ($1.60217646 \times 10^{-19}$C), K is the Boltzmann constant ($1.3806503 \times 10^{-23}$ J/K), T (inKelvin) is the temperature of the p-n junction and 'a' is the diode ideality constant. Fig.3.7 shows the I-V curve originated from eqn. (3.1).

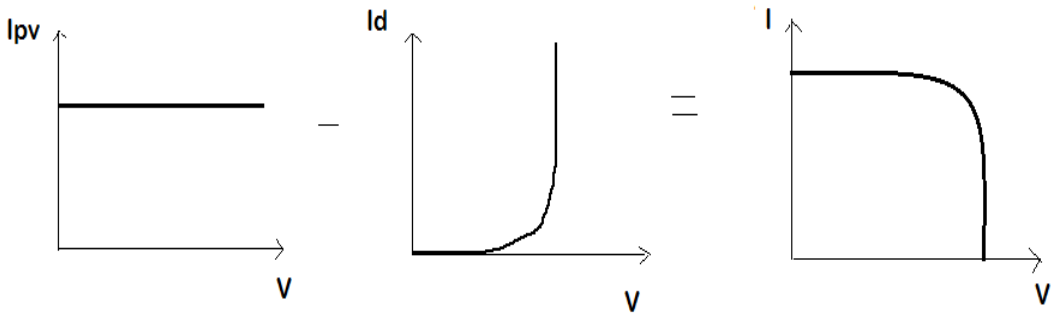

Fig. 3.7 I–V curve of the PV cell

The eqn. (3.3) represents the ideal PV cell and does not represent the I-V characteristic of a practical PV array. Further, the Practical arrays are composed of several connected PV cells and the observation of the characteristics at the terminals of the PV array requires the inclusion of additional parameters to the basic eqn. (3.3). Hence, the modified eqn. for practical PV array is shown in eqn. (3.4):

$$I = I_{pv} - I_o \left[exp\left\{\frac{(V+R_SI)}{V_ta}\right\} - 1\right] - \frac{V+R_SI}{Rp} \tag{3.4}$$

Now, if the array is composed of N_p parallel connections of cells the PV and saturation currents may be expressed as$I_{PV} = I_{PV}N_P$, $I_O = I_ON_P$. Thus, the eqn. (3.4) can be written as eqn. (3.5):

$$I = I_{pv}N_p - N_p I_o \left[exp\left\{\frac{q(V+IRs)}{N_s akT}\right\} - 1\right] - \frac{V+IR_S}{R_P} \quad (3.5)$$

The photo-current mainly depends on the solar irradiance and cell temperature as shown in eqn. (3.6)

$$I_{pv} = I_{sc} * \frac{I_{rr}}{1000}\left[1 + \left(T - T_{ref}\right) * \alpha\right] \quad (3.6)$$

Where $V_t = \frac{N_s kT}{q}$ is the thermal voltage of the array with *N*s cells connected in series, $R_S$is the equivalent series resistance of the array and Rp is the equivalent parallel resistance, T_{ref} is module reference temperature of 25^0 C and T is the module operating temperature (K) of 25 to 70 ^{0}C and α is the short-circuit current temperature coefficient at short circuit condition and I_{sc} is the Short-circuit current of PV cell at 25°C

3.3.1.1 Characteristics of PV Array

The PV cell photocurrent depends on the radiation and the temperature. The current-voltage (I-V) characteristics and power-voltage characteristics (P-V) of the PV system are shown in Fig. 3.8, (a) and (b) respectively under radiation 1000 W/m^2 and temperature 25^0 C. The characteristics show that both I-V and P-V curves are nonlinear. The output power of PV array is maximum at certain value of voltage (V_{mpp}) and this point is called as maximum power point (MPP). The corresponding voltage (V_{mpp}) and current (I_{mpp}) at Maximum Power Point (MPP) are also shown in Fig. 3.8.

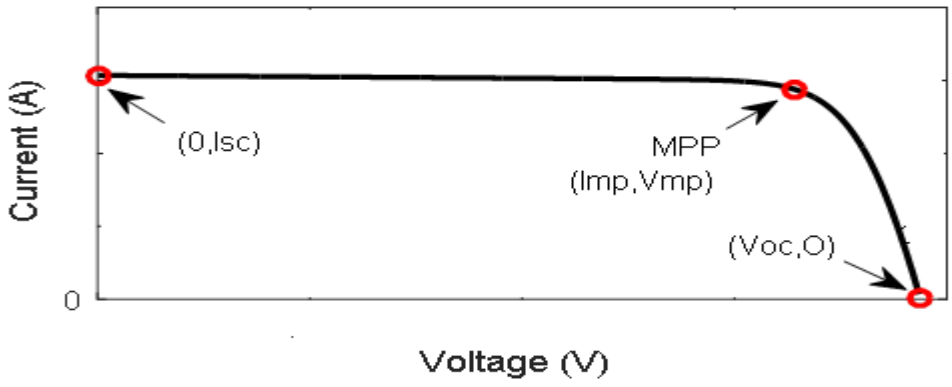

(a)

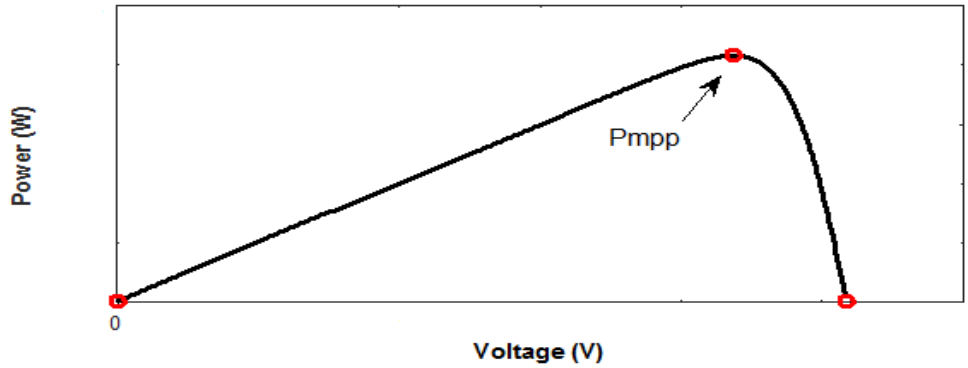

(b)

Fig. 3.8. Characteristic a) I-V curve b) P-V curve of a practical PV device

The power available from a photovoltaic module at any point along the curve is expressed in watts. There is a point on the knee of the curve where maximum power output is located. This power will decide the rating of the PV panel. This output power of PV module depends on PVs output voltage $V_{mp}$and PVs output current I_{mp} as $P_{mp} = V_{mp} * I_{mp}$.

Solar PV array is designed for maximum 8kW at 1kW/m2 of solar radiation, and at 25^0C in this thesis. The rating and specifications of devices and components are presented in appendix-I.

3.3.1.2 Effect of temperature and irradiation change on I-V and P-V characteristics

The current-voltage behaviour of solar panels is nonlinear and depends on the solar irradiation intensity and environmental temperature [13-15].

A) Effect of Irradiance Change

The output power of PV array is the function of voltage and current. At constant temperature 25^0C and variable irradiance, the I-V and P-V characteristics are plotted as shown Fig. 3.9. It is observed that as irradiance is increased from 100 W/m^2 to 1000 W/m^2, the generated voltage and hence the output power of PV array is also increased.

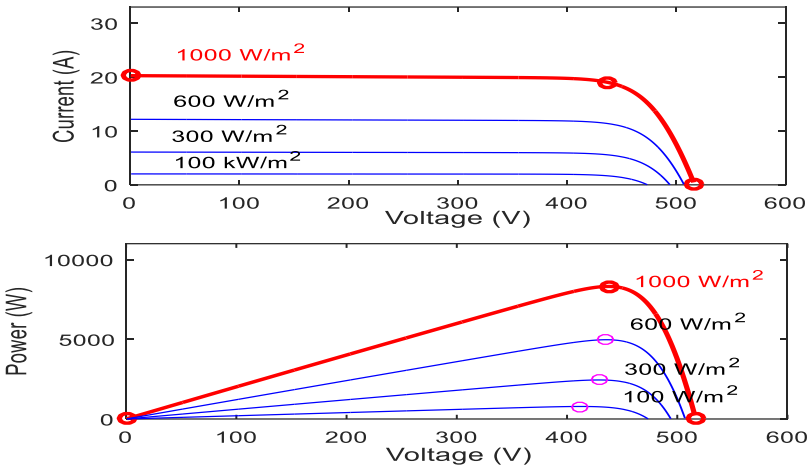

Fig 3.9. I-V and P-V Characteristics of the PV cell at constant temperature and Variable irradiance

B) Effect of temperature Change

The Fig. 3.10 shows I-V characteristics and P-V characteristics of PV array at irradiance of 1000W/m^2 and different temperature condition. From the Figure it is evident that increasing temperature from 15^{0}C to 60^{0}C results in reduction of voltage and there is slight increase in current. Hence output power is reduced.

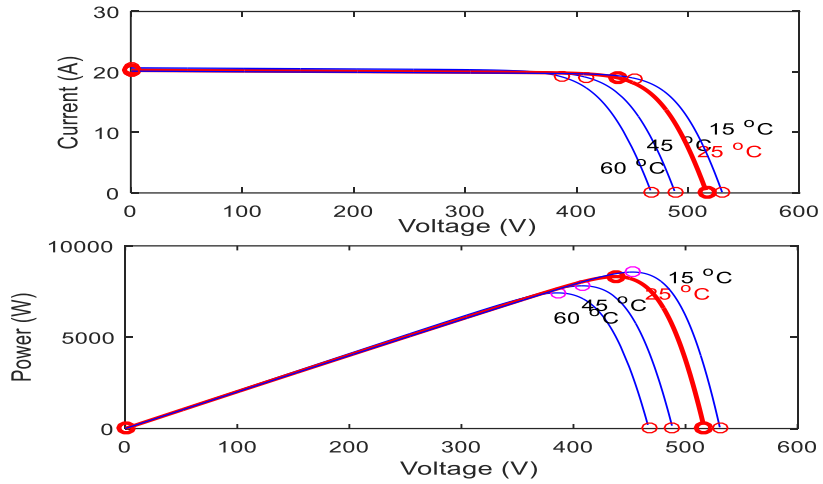

Fig. 3.10 I-V and P-V Characteristics of the PV cell at variable temperature and Constant irradiance

Thus, solar irradiance has direct relation and temperature has reverse relation with output power of PV module. It means with increase in the sunlight intensity, the output power rises up and with increase in the temperature, the power comes down.

3.3.2 DC-DC Converter

The voltage produced by the photovoltaic cells will vary according to the sunlight intensity (irradiance) and temperature, but the system output requires a constant voltage value to be able to process and control the electric energy in the system (i.e. the voltages, currents, frequency). So, there is a need for a power electronic interface. The power electronics converters used are DC-DC converter and DC-AC converter.

The purpose of DC-DC Converters is to convert unregulated DC input to regulated or controlled DC output at a desired voltage level. With the help of MPP Tracking (which will be explained later) the converter adjusts its operation according to the output value to find the optimal operating voltage of the PV module.

The different types of DC-DC converters used in the grid connected PV system are:

i. Buck converter,
ii. Boost converter ,
iii. Buck –boost converter, etc.

In this work DC-DC boost converter is used.

3.3.2.1 DC-DC Boost Converters

The Boost converter is also called as step-up converter which has an output DC voltage greater than its input DC voltage. Boost converter has two semiconductor switches and one storage element [16]. Fig.3.11 shows the circuit diagram of a boost converter.

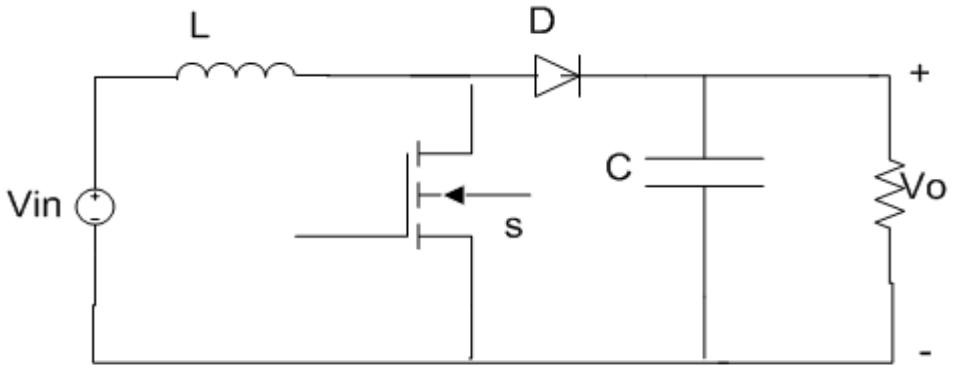

Fig 3.11 Circuit diagram of Boost Converter

When the switch is closed the inductor gets charged by the PV or battery and stores the energy. In this case diode blocks the current flowing, so that the load current remains constant which is being supplied due to the discharging of the capacitor. When the switch is open the diode conducts and the energy stored in the inductor discharges and charges the capacitor. Therefore, the load current remains constant throughout the operation. The Boost converter is used to regulate the electric power generated by solar cell with maximum power point tracking (MPPT) techniques. A converter without MPPT system only regulates the output voltage of PV module, but it does not ensure that PV system is operating at the maximum power point MPP. Thus, power loss occurs, if the PV system is not operating at or near to the MPP. Therefore, it is extremely important to follow the MPP in any condition to ensure that the available maximum power is obtained from the PV array.

3.3.2.2 Design of Boost Converter

DC-DC boost converter has two tasks to perform. First one is to boost the dc voltage level to the appropriate level so that it is easily converted into the desired ac voltage and second is to operate the PV panel at maximum power point. A boost converter provides the control of the PV panel output voltage so that the PV Panel operate at maximum output operating point and maintain the Voltage input to the Inverter. In this thesis DC-DC boost converter increases the voltage value of PV array to 800 V and also performs the maximum power tracking function. The design specification of the DC-DC boost converter can be computed [15] using the eqn. (3.7) and (3.8):

$$L_b = \frac{V_i D_c}{\Delta i_n f_s} \tag{3.7}$$

where, L_b is the value of an inductor for boost converter, D_C is the Duty cycle given by eqn.3.8

$$D_c = 1 - \frac{V_{in}}{V_{oc}} \tag{3.8}$$

$$C_b = \frac{I_{oc} D_C}{\Delta v_r f s} \tag{3.9}$$

and V_i, V_o,are the input and output voltages of boost converter, Δi_n is the input ripple current and it may take as 6% of input current, f_s is the switching frequency is 10kHz,Δv_r is output ripple voltage and it is taken as 3% of the output voltage V_o. $I_1 = (\frac{P_{mp}}{V_{mp}})$ is the input current.

3.3.3 Maximum Power Point tracking (MPPT) Techniques

The output of PV cell depends hugely on environmental conditions. Under different environment condition, the output voltage of photovoltaic cell will be different. So, environmental variations change the maximum output power of solar array. The output power of photovoltaic array arrives at maximum value only at a certain output voltage value, called the maximum power point. Therefore, making the PV system work at around the maximum power point is called the maximum power point tracking (MPPT). The Maximum Power Point Tracking (MPPT) technique or algorithms are used with power electronic circuits like boost converter to extract maximum energy from the Photovoltaic (PV) Systems.There are various MPPT algorithms. These algorithms are based on the voltage and current signal of the PV system which are adjusted by varying the duty cycle of DC-DC Boost converter in order to achieve maximum power point.

There are different algorithms used to track the maximum power point (MPP). Some of the most popular algorithms are [16-17]:

1) Perturb and Observe,
2) Incremental Conductance method,
3) Fractional short circuit current,
4) Fractional open circuit voltage, etc.

The choice of the algorithm depends on the time taken by the algorithm in order to track the MPP, implementation cost and the ease of implementatiosn. The Perturb and Observe technique is very simple to apply. So, in this work the boost converter is used with Perturb and Observe (P&O) MPPT algorithm for tracking maximum power point.

3.3.3.1 Perturb and Observe Algorithm

In this method the voltage and current of PV array are sensed and fed to the MPPT controller to track MPP and generates control signal for DC-DC boost converter. This

control signal is compared with saw-tooth waveform of 10 kHz and its output signal controls the duty cycle of a DC-DC boost converter in order to track the maximum power of solar photovoltaic system.

The P&O algorithm [18-22] works on the idea of introducing perturbation to the system's operating point to generate maximum output power. It is based on the constant measuring of the PV current and voltage and calculation of its power output while the working point is moving in order to reach the maximum power. The PV array is perturbed by adding small increments until the maximum power point is reached. Initially P_1 (power output) is calculated by measuring the values of V_1 and I_1 of the solar module. Then a small perturbation is added in the form of d. Then P_2 is calculated by measuring the new values of V_2 and I_2. If the P_2 reads positive, the system will keep perturbing in the same direction. Once P_2 reads negative, the algorithm will bring the output power value back towards the maximum power point by adding a negative increment. When the maximum power point is reached, the system operating point will start to oscillate constantly around that maximum power point. The controller will track this operating point and try to bring the V of the solar module to perform on this maximum power point. The algorithm for P &O MPPT is shown in Fig. 3.12.

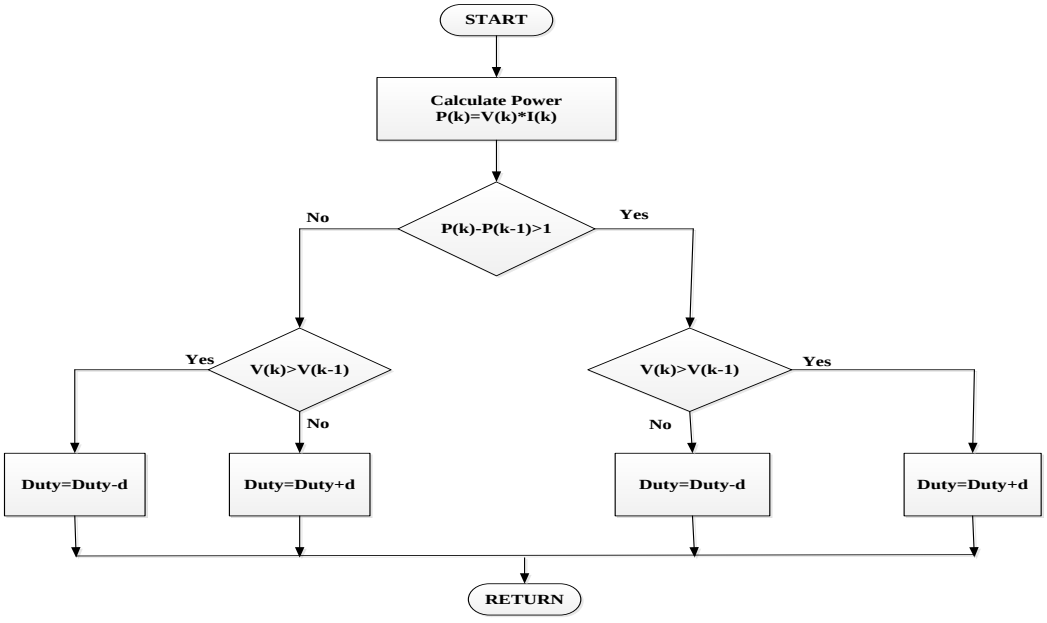

Fig 3.12 P &O Algorithm for MPPT

The algorithm shows that the voltage and current are taken as input to the MPPT unit and duty cycle is obtained as the output. A slight perturbation (d = 0.01) is introduced in the system. This perturbation causes the power of the solar module to change. If the power increases due to the perturbation, then the perturbation is continued (Duty + d) in that direction. After the peak power is reached, the power at the next instant decreases and after that the perturbation reverses (Duty − d).

The disadvantage of the P&O method is that, it doesn't give a stable response when there are rapid changes in irradiance levels.

3.3.4 Photovoltaic Inverter

The PV System can be connected to the 3-Phase grid via a DC-DC Boost converter and a PV inverter which is basically a Voltage Source Inverter (VSI) to convert the dc voltage output of the boost converter to 3 phase ac voltage of desired magnitude and frequency. VSI are largely used in DG systems because of its high efficiency, compact size and good control on power flow. VSI are broadly classified into two types: Voltage controlled Voltage Source Inverter (VCVSI) and Current controlled Voltage source Inverter (CCVSI) [23]

In VCVSI the size of the filter or Decoupling Inductor is a matter of concern as it is an essential part of the system which makes the power flow possible. In weak grid where the voltage drops considerably, the inverter has to supply both the active and the reactive power there by increasing the size of the inductor. Moreover, power factor correction is not possible in VCVSI [24]. On the contrary the unity power factor operation is possible in case of CCVSI. So, the CCVSI has been chosen for the present work.

The PV inverter is basically a three-phase dc-ac current controlled voltage source inverter which consists of six IGBT switches with anti-parallel diodes which are switched on and off through a gate driver circuit as shown in Fig 3.13.

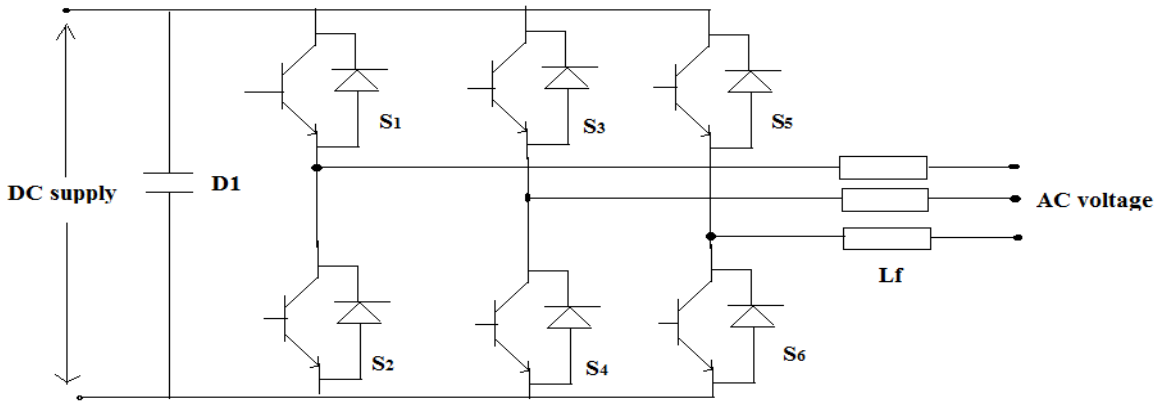

Fig 3.13 Voltage Source Inverter (IGBT Based)

The VSI consists of capacitors to filter the DC link voltage. In the VSI, IGBT semiconductor switches are used. IGBT improves efficiency and reduces dynamic performance and the level of audible noise. IGBT is available for low switching loss. It has a very low on-state voltage drop. It can be easily controlled in high voltage and high current applications. The PV inverter or VSI may act as the active shunt compensator and provide the reactive power compensation, harmonics compensation and load balancing.

3.3.4.1 Design of VSI

Three leg VSI is used as PV inverter, have six IGBTs with anti-parallel diodes connected in a bridge formation. The ratings of IGBTs used are 2500kV and 1500A. The calculations for DC bus voltage to be maintained across the VSI, interfacing inductor rating are as follows [25-27]:

i. DC Bus Voltage

The instantaneous energy fed to the PV inverter decides the DC terminal voltage magnitude and it must be greater than amplitude of voltage at PCC. For a three leg VSC with a DC capacitor, the DC link voltage is given by eqn.(3.9).

$$v_{dc} = (2\sqrt{2}v_{line})/\sqrt{3}m \quad (3.9)$$

Where, *m* is the modulation index and taken as 0.9, and v_{line} is AC terminal voltage of VSI and is equal to 415 V (RMS line to line). With these values the calculated value of v_{dc} is 752.99V. The selected magnitude of dc terminal voltage is 800V in this project.

ii. Coupling Inductor (L_f)

The calculation of the coupling inductance L_f for VSI depends on the current ripple Δi , DC bus voltage v_{dc} and switching frequency $f_{sw} = 10kHz$, and L_f is given by eqn. (3.10), $L_f = \frac{\sqrt{3}\, m\, v_{dc}}{12hfsw\Delta i}$ (3.10)

Where, Δi=5% of phase current, h (=1.2) is overload factor and m (= 0.9) is modulating index. The calculated value of is 6.34mH and L_f = 7mH is taken in this investigation.

The inductors (L_f) will limit the amount of circulating current flowing through the circuit.

3.4 Conclusion

The photovoltaic cell modeling and basic I-V and P-V characteristics of a cell have been presented. These characteristics show that output of a PV cell changes with the environmental conditions. The mathematical model of DC-DC boost converter and PV inverter are presented. The Perturb and Observe algorithm to track the maximum power is also presented.

CHAPTER 4

CONTROL ALGORITHMS FOR PV INVERTER

4.1 General

The increased use of power electronic converters and non-linear loads in the power system leads to the generation of harmonic currents which deteriorates the power-quality [28]. Here, the PV system is connected to the grid through a three-phase inverter to connect PV system to three phase grid and also compensate power quality problems. Several algorithms exists to control the inverter, mainly differing in the sensed parameters and the processing involved. This chapter presents three algorithms for controlling the grid interfacing inverter to compensate power quality problems.

4.2 Control Algorithms for PV Inverter

The objective of inverter control schemes is to extract fundamental component of required current from the sensed parameters according to the system's need. The conventional control algorithms studied are:

(i) Synchronous Reference Frame (SRF) Theory

(ii) Instantaneous Symmetrical Component Theory(ISCT)

(iii) Icosineφ control algorithm

The mathematical description of the algorithms is described in this section.

4.2.1 Synchronous Reference Frame (SRF) theory

The synchronous reference frame theory (SRFT) or d-q theory is based on time-domain reference signal estimation techniques. It performs the operation in steady-state or transient state as well as for generic voltage and current waveforms. It allows controlling the active power filters. Another important characteristic of this theory is the simplicity of the calculations, which involves only algebraic calculation. The basic structure of SRF controller consists of direct (d-q) and inverse $(d\text{-}q)^{-1}$ park transformations [29].

The SRFT is an indirect control technique used to generate gate pulses for controlling PV inverter. In this method sensed values of Load current, PCC voltage and dc bus voltage are taken as the feedback signal. The block diagram representation of control technique based on SRF theory is shown in Fig.4.1.The SRF theory is related to extraction of synchronously rotating d-q components. The currents from load end are sensed and using Park's transformation, the 3-φ load currents (i_{Labc}) are converted to (d-q-0) frame [29-31]. The AC side terminal voltages are given in eqn. (4.1) to eqn. (4.3)

$$v_{sa} = V_m \sin(\omega t) \tag{4.1}$$

$$v_{sb} = V_m \sin(\omega t - \frac{2\pi}{3}) \tag{4.2}$$

$$v_{sc} = V_m \sin(\omega t + \frac{2\pi}{3}) \tag{4.3}$$

And fundamental component of load current are given in eqn. (4.4) to eqn. (4.6):

$$i_{La} = I_m \sin(\omega t - \theta_n) \tag{4.4}$$

$$i_{Lb} = I_m \sin(\omega t - \frac{2\pi}{3} - \theta_n) \tag{4.5}$$

$$i_{Lc} = I_m \sin(\omega t - \frac{2\pi}{3} - \theta_n) \tag{4.6}$$

SRF extracts the fundamental component of load currents by transformation of current signals into d-q reference frame using park's transformation given by eqn. (4.7)

$$\begin{bmatrix} i_{Ld} \\ i_{Lq} \\ i_{L0} \end{bmatrix} = \frac{2}{3} \begin{bmatrix} \cos\omega t & \cos\left(\omega t - \frac{2\pi}{3}\right) & \cos\left(\omega t + \frac{2\pi}{3}\right) \\ \sin\omega t & \sin\left(\omega t - \frac{2\pi}{3}\right) & \sin\left(\omega t + \frac{2\pi}{3}\right) \\ 1/2 & 1/2 & 1/2 \end{bmatrix} * \begin{bmatrix} i_{La} \\ i_{Lb} \\ i_{Lc} \end{bmatrix} \tag{4.7}$$

The d-axis and q- axis currents consist of fundamental and harmonic components given by eqn. (4.8) and eqn. (4.9):

$$i_d = i_{ddc} + i_{dac} \tag{4.8}$$

$$i_q = i_{qdc} + i_{qac} \tag{4.9}$$

For harmonics terms, all harmonics are included behaving as an ac component. While the fundamental terms behaves as dc component. These components are then passed through

LPF to extract dc components i.e. harmonics are separated from reference signal. Now, dc quantities are in the reference signals.

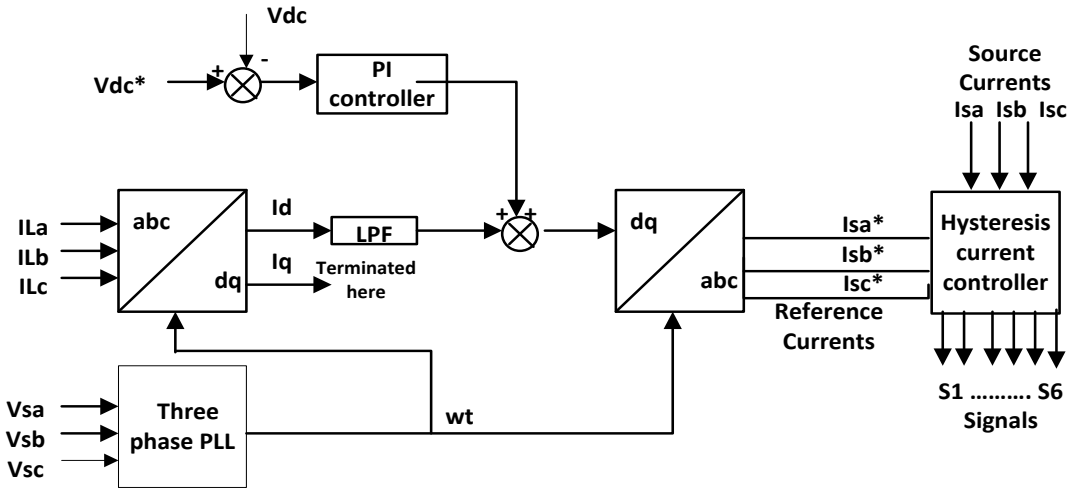

Fig. 4.1 Reference current extraction using SRF theory

Under the operation of grid connected system in power factor(PFC) correction mode, the control algorithm considers that grid must supply direct axis component of load current and active power component of current which are required to regulate the DC bus voltage to constant and to feed inverter losses (i_W). The PI controller regulates the dc bus voltage to desired reference level and provides the active power transfer for compensation of inverter losses [33]. Hence load's active power requirement and the power required to maintain constant DC voltage at inverter DC terminals is to be fulfilled by the grid and therefore these two are added. To maintain DC voltage constant, the error between reference signal and sensed DC voltage is fed into a PI controller, thus generating an output current (i_W) equal to the loss in DC voltage and i_W which is the value of current required to compensate the losses is given in eqn.(4.10)

$$i_W(n) = i_W(n-1) + K_p\big(V_{de}(n) - V_{de}(n-1)\big) + K_i * V_{de}(n) \quad (4.10)$$

Where,K_p and $K_i$are the gains for PI controller and $V_{de}(n)$ is error between the measured DC terminal voltage signal and reference DC voltage of 800V given by eqn. (4.11),

$$V_{de}(n) = V_{dc}^*(n) - V_{dc}(n) \quad (4.11)$$

Therefore the total active power comprised in the grid current can be given by eqn. (4.12),

$$i_{active}^* = i_{dc} + i_W \quad (4.12)$$

Where i^*_{active} is the amplitude of reference AC mains current. The active power component of reference AC main currents must be in phase of PCC voltage. So, a 3-φ PLL is used to synchronize these signals with the voltages at PCC. The angle ωt of park's transformation is the synchronous angular position determined by the PLL. The resultant currents in the *d-q-0* reference frame($i^*_d = i^*_{active},\ i^*_q = 0, i^*_0$) are reverse transformed into reference source current ($i^*_{sa}, i^*_{sb}, i^*_{sc}$) in *a-b-c* frame using reverse Park's transformation given by eqn. (4.13)

$$\begin{bmatrix} i^*_{sa} \\ i^*_{sb} \\ i^*_{sc} \end{bmatrix} = \begin{bmatrix} \cos\omega t & \sin\omega t & 1 \\ \cos\left(\omega t - \frac{2\pi}{3}\right) & \sin\left(\omega t - \frac{2\pi}{3}\right) & 1 \\ \cos\left(\omega t + \frac{2\pi}{3}\right) & \sin\left(\omega t + \frac{2\pi}{3}\right) & 1 \end{bmatrix} * \begin{bmatrix} i^*_d \\ i^*_q \\ i^*_0 \end{bmatrix} \tag{4.13}$$

These reference source currents, calculated from eqn. (4.13) are fed to hysteresis current controller (HCC) along with sensed source currents, thus generating switching signal for PV inverter. The hysteresis band current controller controls the source currents (i_{sa}, i_{sb}, i_{sc}) close to three phase reference currents($i^*_{sa}, i^*_{sb}, i^*_{sc}$).

4.2.1.1 Phase Locked Loop

A phase locked loop (PLL) is a system which synchronizes its output signal with a given input signal or reference signal both in frequency and in phase. It is a non-linear closed loop control which automatically changes the frequency of a controlled oscillator depending on the frequency and phase of the input signal such that the output is matched both in frequency and phase with the reference or the input signal.

A synchronous Reference Frame PLL (SRF PLL) is mainly used for tracking the phase angle in case of 3-phase signals which works in a similar way as a linear PLL with only difference in the Phase Detector (PD) block. It uses Park's Transformation of a 3-phase signal as the PD. The schematic diagram of the Three-phase Phase locked loop is shown in Fig 4.2. This PLL is used in controlling the PV inverter. PLL generates ωtangle varying between 0 and 2π, and synchronized to zero crossing of the fundamental of phase 'a' [34-35]

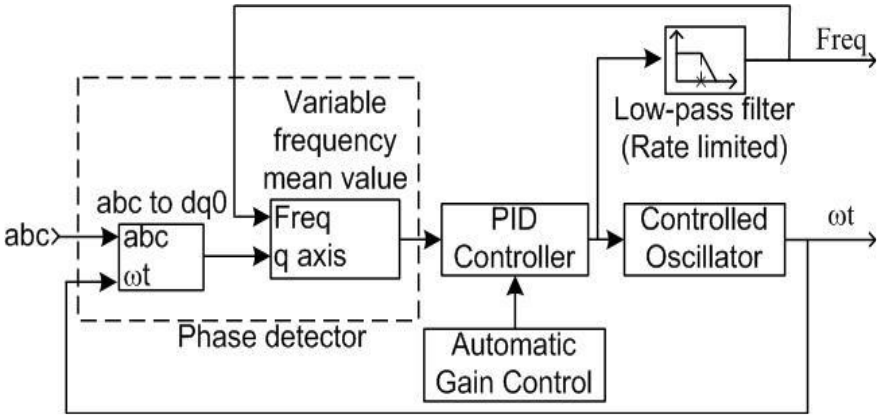

Fig 4.2 Schematic Diagram of 3-φ PLL

The 3-φ input signal to the PLL is transformed to the *d-q-0* rotating frame, the angular speed required for this conversion is provided by an internal oscillator. Then q-axis component of transformed signal, which is proportional to the phase difference between the *a-b-c* signal and the internal oscillator rotating frame, is filtered with a mean (variable frequency) block. The output of this block is fed to a PID controller having an optional automatic gain control (AGC), it keeps the phase differences to 0 by acting on a controlled oscillator. The PID output, corresponding to the angular velocity, is filtered and converted to frequency in Hz and output of the controlled oscillator is the angle (ωt) varying between 0 & 2π rad.

4.2.1.2 Hysteresis Current Controller (HCC)

Gating pulses for a inverter are generated using synchronized pulse width modulation (PWM) method or hysteresis current control method [36]. Hysteresis current controller is used because of its simplicity in implementation and fast response with peak current limiting capability. But hysteresis current control scheme suffers with the disadvantage of wide variation in switching frequency, which may be prohibitively high, and can cause higher losses of the converter switches due to increased number of switching per cycle. The two level scheme is simplest in implementation, requiring the value of tracking error alone, which is the difference between the references ($i_{sa}^{*}, i_{sb}^{*}, i_{sc}^{*}$) and the actual values (i_{sa}, i_{sb}, i_{sc}) of the grid side current.

In this method switching is done in an asynchronous way to ramp the actual current up and down so that it will follow the reference current. When the source current is exceeding the

upper hysteresis limit, it turns on a negative voltage switching function and causes the source current to decrease. And if the current violates the lower hysteresis limit, then it turns on a positive voltage switching function to increase the source current. The hysteresis band limit used in this investigation is 0.2. The tracking of the actual current wave using a hysteresis current controller is shown in Fig. 4.3

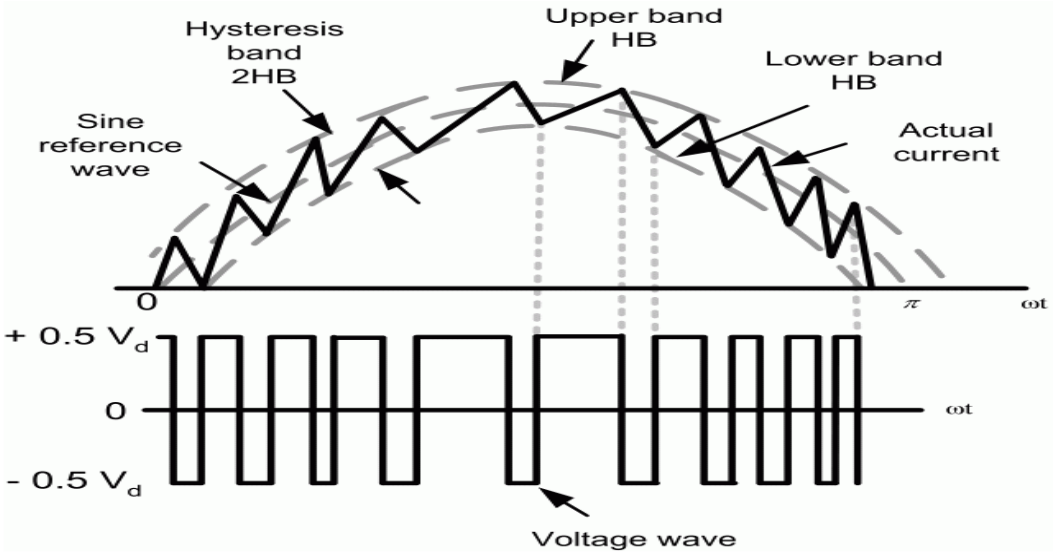

Fig. 4.3 Hysteresis current control

The internal architecture of hysteresis current controller is shown in Fig 4.4. the six pulses are generated for six IGBT switches in VSC, as each phase is connected to two switches, the output pulses also contains one pulse for upper switch and one pulse for lower switch.

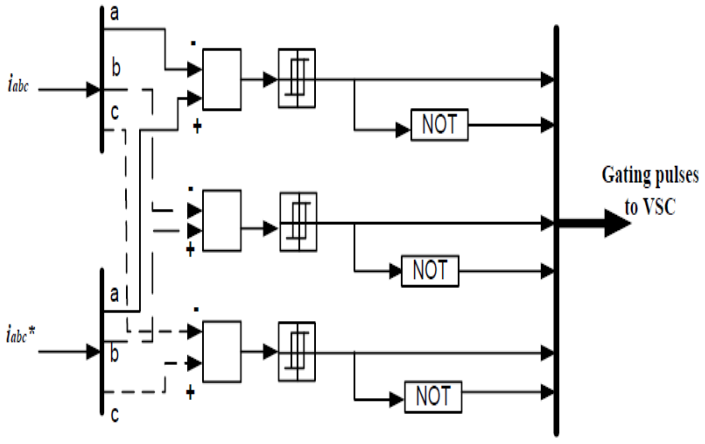

Fig 4.4 Schematic Diagram of Hysteresis Current Controller

4.2.2 Instantaneous Symmetrical Component Theory (ISCT)

The theory of instantaneous symmetrical components can be used for the purpose of harmonic suppression and power factor correction [37-39] etc. The control algorithms based on instantaneous symmetrical component theory can practically compensate any kind of unbalance and harmonics in the load. For any set of three-phase instantaneous currents or voltages, the instantaneous symmetrical components are defined by eqn. (4.14) and eqn. (4.15),

$$\begin{bmatrix} i_{a_0} \\ i_{a_1} \\ i_{a_2} \end{bmatrix} = \frac{1}{\sqrt{3}} \begin{bmatrix} 1 & 1 & 1 \\ 1 & a & a^2 \\ 1 & a^2 & a \end{bmatrix} \begin{bmatrix} i_a \\ i_b \\ i_c \end{bmatrix} \tag{4.14}$$

Similarly for three-phase instantaneous voltages, we have

$$\begin{bmatrix} v_{a_0} \\ v_{a_1} \\ v_{a_2} \end{bmatrix} = \frac{1}{\sqrt{3}} \begin{bmatrix} 1 & 1 & 1 \\ 1 & a & a^2 \\ 1 & a^2 & a \end{bmatrix} \begin{bmatrix} v_{sa} \\ v_{sb} \\ v_{sc} \end{bmatrix} \tag{4.15}$$

In the above equation, a is a complex operator and it is given by$a = e^{\frac{j2\pi}{3}}$,$a^2 = e^{\frac{j4\pi}{3}}$.It is to be noted that the instantaneous components of currents, $i_{a_1}$and $i_{a_2}$are complex time varying quantities also they are complex conjugate of each other. This same is true for $v_{a_2}$and v_{a_2} quantities. The terms i_{a_0} and v_{a0} are real quantities. These instantaneous symmetrical components are used to formulate equation for load compensation etc.

Hence the reference current estimation, load balancing, harmonics reduction and power factor correction is done by PV inverter using instantaneous symmetrical component theory control algorithm. The block diagram for the ISCT control algorithm is shown in the Fig.4.5.The PCC voltage ($\mathrm{v_{sa}}, \mathrm{v_{sb}}, \mathrm{v_{sc}}$) source current ($\mathrm{i_a}, \mathrm{i_b}, \mathrm{i_c}$), load currents ($\mathrm{i_{la}}, \mathrm{i_{lb}}, \mathrm{i_{lc}}$) and DC bus voltage ($\mathrm{v_{dc}}$) of the PV system are used for extraction of reference source current. The first part of control strategy of inverter is based on computing of instantaneous positive sequence of load side currents and utility side voltages using instantaneous symmetrical component theory.

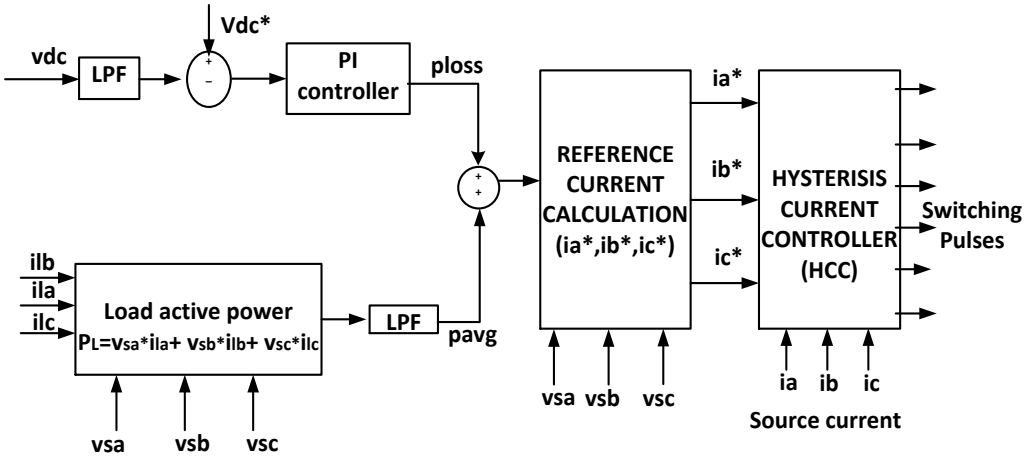

Fig. 4.5. Block Diagram for Extracting Source Current

The objective of the algorithm is to provide balanced supply current. So, the source current is given by eqn. (4.16):

$$i_a + i_b + i_c = 0 \tag{4.16}$$

Positive sequence quantities of voltage and current are to be considered to obtain the balanced source current. Using symmetrical component theory, positive component can be obtained using the eqn. (4.17) and also from power factor of the source point of view, we have

$$\angle v_{a1} = \angle i_{a1} + \emptyset \tag{4.17}$$

$$\angle\{v_{sa} + a v_{sb} + a^2 v_{sc}\} = \angle\{i_a + a i_b + a^2 i_c\} + \emptyset \tag{4.18}$$

Where v_{a1} and i_{a1} are positive sequence quantities and $\emptyset$ is the phase between supply voltage and current. Under the supply voltage is balanced, the above eqn. can be written using the eqn. (4.19):

$$\tan^{-1}\left(\frac{k_1}{k_2}\right) = \tan^{-1}\left(\frac{k_3}{k_4}\right) + \emptyset \tag{4.19}$$

Where,

$$k_1 = \sqrt{3/2}\,(v_{sb} - v_{sc})\ ,\ k_2 = (3/2)(v_{sb})$$

$k_3 = \sqrt{3/2}\,(i_b - i_c)$, $k_4 = (i_a - i_{b/2} - i_{c/2})$(4.20)

$\beta = \tan\emptyset/\sqrt{3}$ (4.21)

After solving eqn. (4.17), (4.18), (4.19) and (4.20) it results in eqn. (4.22):

$(v_{sb} - v_{sc} - \beta v_{sa})i_a + (v_{sc} - v_{sa} - \beta v_{sb})i_b + (v_{sa} - v_{sb} - \beta v_{sc})i_c = 0$ (4.22)

When $\beta = 0$, source current (i_a, i_b, i_c) are to be in phase of voltages(v_{sa}, v_{sb}, v_{sc})which implies that the reactive power demand of the load is supplied by the inverter. But in the case of other than zero, the source may supplies or absorbs the reactive power [40-44].

The source should supply the active power to the load in PFC mode. The average power demand is given in eqn. (4.23)

$P_{avg} = v_{sa}i_a + v_{sb}i_b + v_{sc}i_c$ (4.23)

where P_{avg} is average active power which is obtained after filtering the harmonics using LPF filter. The load active power can be calculated from eqn. (4.24):

$P_l = v_{sa}i_{la} + v_{sb}i_{lb} + v_{sc}i_{lc}$ (4.24)

The DC bus voltage is maintained constant using PI (proportional integral) controller, given by eqn. (4.25):

$P_{loss} = K_{pdc}\,V_{dcei} + K_{idc}\int V_{dcei}\,dt$ (4.25)

Where $V_{dcei} = v_{dc}^{*} - v_{dc}$= error. v_{dc}^{*} and v_{dc} are the reference voltage and sensed voltage of DC bus respectively. K_{pdc} and K_{idc} are the proportional and integral gain of the PI controller over the DC bus voltage of DC-AC converter.

With the PI controller the loss component due to switching is maintained. Hence P_{loss} is provided which compensate the switching losses in the converter. Therefore, the total power given by eqn. (4.26):

$P_{avg} + P_{loss} = v_{sa}i_a + v_{sb}i_b + v_{sc}i_C$ (4.26)

After solving eqn. (4.16), (4.21) and (4.25), the reference current can be obtained using eqn. (4.27):

$$i_a^* = [v_{sa} + (v_{sb} - v_{SC})\beta](P_{avg} + P_{loss})/A$$

$$i_b^* = [v_{sb} + (v_{sc} - v_{sa})/\beta](P_{avg} + P_{loss})/A$$

$$i_c^* = [v_{sc} + (v_{sa} - v_{sb})/\beta](P_{avg} + P_{loss})/A \quad (4.27)$$

Where $A = \sum(v_{sa}^2 + v_{sb}^2 + v_{sc}^2)$ and $\beta = 0$ (PFC) in the grid connected PV system.

The reference currents are then compared with actual source currents (i_a, i_b, i_c) using hysteresis current controller (HCC) that results in the required six pulses for controlling PV Inverter.

4.2.3 Icosø Control Algorithm:

The 'Icosø' algorithm deduced the fundamental component of the active part of the load current, i.e. 'Icosø' in each phase using a LPF tuned to fundamental frequency and sample & hold circuits. It gives the amplitude of the desired mains current in each phase. The three-phase mains voltages are used as templates to generate unit amplitude sine waves in phase with the mains voltages. The desired currents are then calculated as the product of the amplitude Icosø and the unit sine wave for each phase [45-49].

For a self-supporting DC bus of the inverter, the capacitor voltage fluctuations are used to calculate the extra power loss in the inverter. The corresponding current amplitude is calculated and added to the active component of the fundamental load current in each phase.

This algorithm generates reference currents for the three-phase PV inverter based on the real part of the load current. This ensures that the current drawn from the supply mains is purely sinusoidal with no reactive component i.e. at unity power factor. This algorithm is used for harmonic compensation along with achieving unity power factor at the source side.

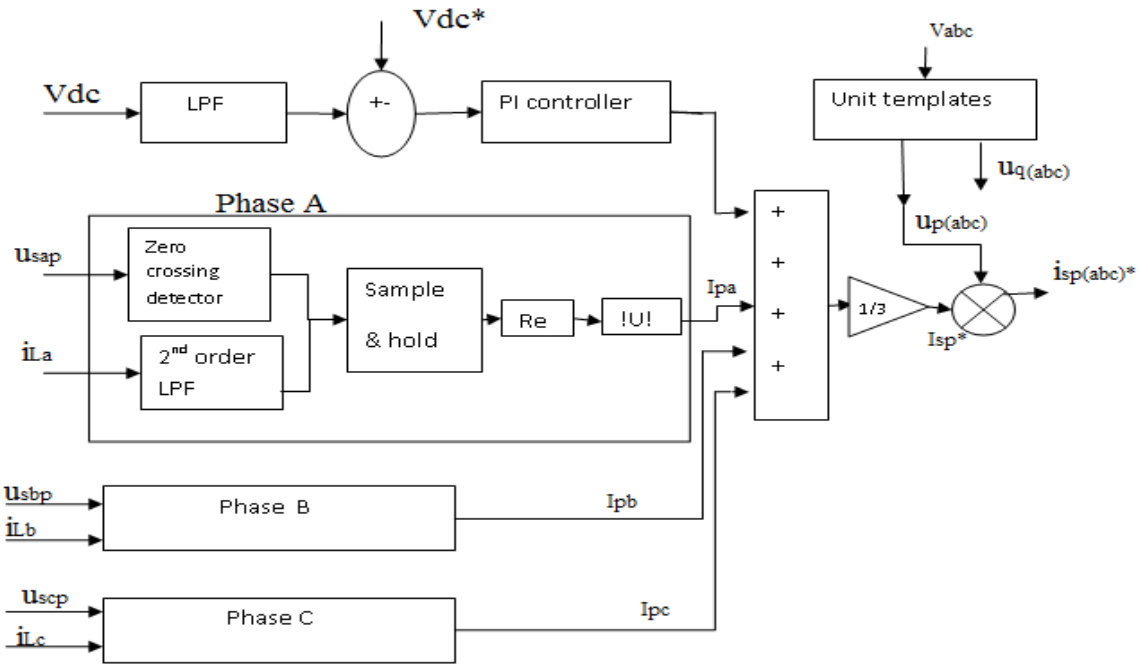

Fig 4.6 Block diagram of extracting reference source currents using Icos∅

The 'Icos∅' based control algorithm is shown in Fig.4.6. The PCC voltage (v_a, v_b, v_c), the source currents(i_a, i_b, i_c),the load currents(i_{la}, i_{lb}, i_{lc}), and the DCbus voltage $(V_{dc})$of the PV inverter are sensed. The product ofIcos∅ andIsin∅ component of load currents with unit templates will generates the reference source currents [44-46].

Let, the load current can be expressed by eqn. (4.28)

$$i_{la} = \sum_{k=1}^{k=\infty} I_{lak}\sin(k\omega t - \varphi_{ak})$$

$$i_{lb} = \sum_{k=1}^{k=\infty} I_{lbk}\sin(k\omega t - \varphi_{bk} - 120^0)$$

$$i_{lc} = \textstyle\sum_{k=1}^{k=\infty} I_{lck}\sin(k\omega t - \varphi_{ck} - 240^0) \quad (4.28)$$

Here$\varphi_{(abc)1}$ and$\varphi_{(abc)k}$ are phase angles of fundamental and k[th] harmonic current in a,b and c phases, $I_{l(abc)1}$ and$I_{l(abc)k}$ are amplitude of fundamental and k[th] harmonic current in a,b, and c phases.

The magnitude of active component of fundamental load currents is given by eqn. (4.29):

$$|Re(I_{la1})| = |I_{la}|cos\emptyset_a$$

$$|Re(I_{lb1})| = |I_{lb}|cos\emptyset_b$$

$$|Re(I_{lc1})| = |I_{lc}|cos\emptyset_c \quad (4.29)$$

The amplitude of active component (Icos∅)of fundamental load current is extracted at the zero crossing of the unit template in phase of PCC voltage from the load currents by shifting the load currents by +90°, using a set of low pass filters. The filters are used with 50Hz cut-off frequency to extract the fundamental load current. A zero crossing detector and a "sample and hold" circuit are used to extract the (Icos∅) (amplitude of fundamental load current atzero crossing of corresponding in phase unit template).

Now, for balanced source currents, the magnitude of active component of reference source currents can be in given in eqn. (4.30):

$$I_{sp}^{*} = (|I_{la}|cos\emptyset_a + |I_{lb}|cos\emptyset_b + |I_{lc}|cos\emptyset_c + I_d)/3 \quad (4.30)$$

Where,$|I_{la}|cos\emptyset_a$,$|I_{lb}|cos\emptyset_b$and$|I_{lc}|cos\emptyset_c$ are the amplitude of the load active currents andI_d is the output of the DC bus voltage PI controller for the self supporting bus of the inverter which can be expressed as:

$$P_{loss} = K_{pdc}\, V_{dcei} + K_{idc} \int \mathrm{V_{dcei}}\, \mathrm{dt} \quad (4.31)$$

where $\mathrm{V_{dcei}} = \mathrm{v_{dc}}* - \mathrm{v_{dc}}$ is the error in DC bus voltage.$\mathrm{v_{dc}}*$ = reference DC bus voltage of inverter and $\mathrm{v_{dc}}$ =actual DCbus voltage of inverter respectively. K_{pdc} and K_{idc} are theproportional and integral gains of the PI controller over theDC bus voltage of inverter given in eqn. (4.31).

Similarly the amplitude of reactive component(Isin∅)of fundamental load currents can be extracted at the zero crossing of the unit template in quadrature of PCC voltage from the filtered fundamental load currents. The magnitude of reactive component of the reference source currents can be expressed as.

$$I_{sp}^{*} = \frac{(|I_{la}|cos\emptyset_a + |I_{lb}|cos\emptyset_b + |I_{lc}|cos\emptyset_c + I_d)}{3} \quad (4.32)$$

Similarly, the magnitude of reactive component of reference source current is given by eqn. (4.33)

$$I_{sq}^{*} = \frac{(|I_{la}|sin\emptyset_a + |I_{lb}|sin\emptyset_b + |I_{lc}|sin\emptyset_c + I_d)}{3} \quad (4.33)$$

For power factor correction,$I_{sq}^{*}$is kept zero.

Now, Unit amplitude templates are in-phase and quadrature component of source voltage, which are of unit magnitude. They are used to provide phase difference to different components of current. For calculation of unit amplitude template, first terminal

voltage,v_m, is calculated by the formula given in eqn.(4.34), where v_a, $v_b$and$v_c$are phase voltages of the supply line.

$$v_m = Sqrt(\{(2/3)(v_{sa}^2 + v_{sb}^2 + v_{sc}^2)\}) \quad (4.34)$$

After that individual phase voltages get divided by terminal voltage, this will give unit amplitude with the phase angle of actual supply of phase voltage. In phase components are represented by u_{pa}, u_{pb}andu_{pc}, respectively for phase a, b and c. Quadrature components are represented by u_{qa}, u_{qb}andu_{qc}, respectively for phase a, b and c. Eqn. for calculation of unit templates are given in eqn.(4.35) to (4.38).

$$u_{pa} = \frac{v_a}{v_m},\ u_{pb} = \frac{v_b}{v_m},\ u_{pc} = \frac{v_c}{v_m} \quad (4.35)$$

$$u_{qa} = -\frac{u_{pb}}{\sqrt{3}} + \frac{u_{pc}}{\sqrt{3}} \quad (4.36)$$

$$u_{qb} = \sqrt{3}\frac{u_{pa}}{2} + \frac{(u_{pb}-u_{pc})}{2\sqrt{3}} \quad (4.37)$$

$$u_{qc} = -\sqrt{3}\frac{u_{pa}}{2} + \frac{(u_{pb}-u_{pc})}{2\sqrt{3}} \quad (4.38)$$

Thus, three phase active component of source currents can be obtained with in-phase unit templates as:

$$i_{sap}^* = I_{sp}^* u_{pa}$$
$$i_{sbp}^* = I_{sp}^* u_{pb}$$
$$i_{scp}^* = I_{sp}^* u_{pc} \quad (4.39)$$

Now, The three phase reference source currents can be obtained from eqn. (4.40) .

$$i_{sa}^* = I_{sap}^*$$
$$i_{sb}^* = I_{sbp}^*$$
$$i_{sc}^* = I_{scp}^* \quad (4.40)$$

The reference currents are then compared with actual source currents(i_{sa}, i_{sb}, i_{sc}) using hysteresis current controller (HCC) that results in the required six pulses for controlling PV Inverter.

4.3 Conclusion

In this chapter, a detailed description of various control algorithms for inverter control is presented. By analyzing the control algorithms, it can be concluded that SRF is based on axis transformation. ISCT is also transform based technique. And Icosø is a technique in which the fundamental component of the active part of the load current, i.e. 'Icosø' is deduced from the load current in each phase using a low pass filter tuned to fundamental frequency and sample and hold circuits.

CHAPTER 5

SIMULATION RESULTS AND DISCUSSION

5.1 General

This chapter presents, simulation analysis of grid connected solar PV system using three-phase inverter with all three inverter control algorithms and P & O algorithm for maximum power point tracking. The comparison of performance of different control algorithms are also presented under various loads and atmospheric conditions.

5.2 Proposed System

For the study purpose, 8 kW solar PV system is connected to a three phase 415V, 50 Hz AC distribution grid with 800 V as dc link voltage. Fig. 5.1 shows the schematic diagram of proposed grid connected solar PV system.

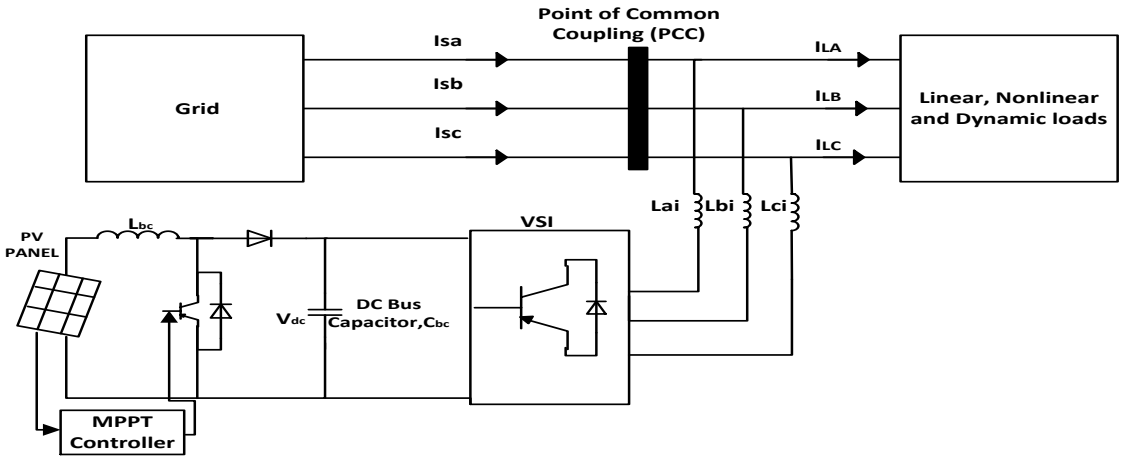

Fig 5.1 Grid connected Solar PV system

Loads connected to the system are balanced linear loads (Star connected), non-linear loads, dynamic loads and unbalanced non-linear loads. The PV inverter is connected to the grid system in shunt at the point of common coupling with an interfacing inductor (L_f).

The grid synchronized photovoltaic system is modeled in MATLAB using Simulink toolbox. A MATLAB model is developed for the grid connected PV system as shown in Fig. 5.2.

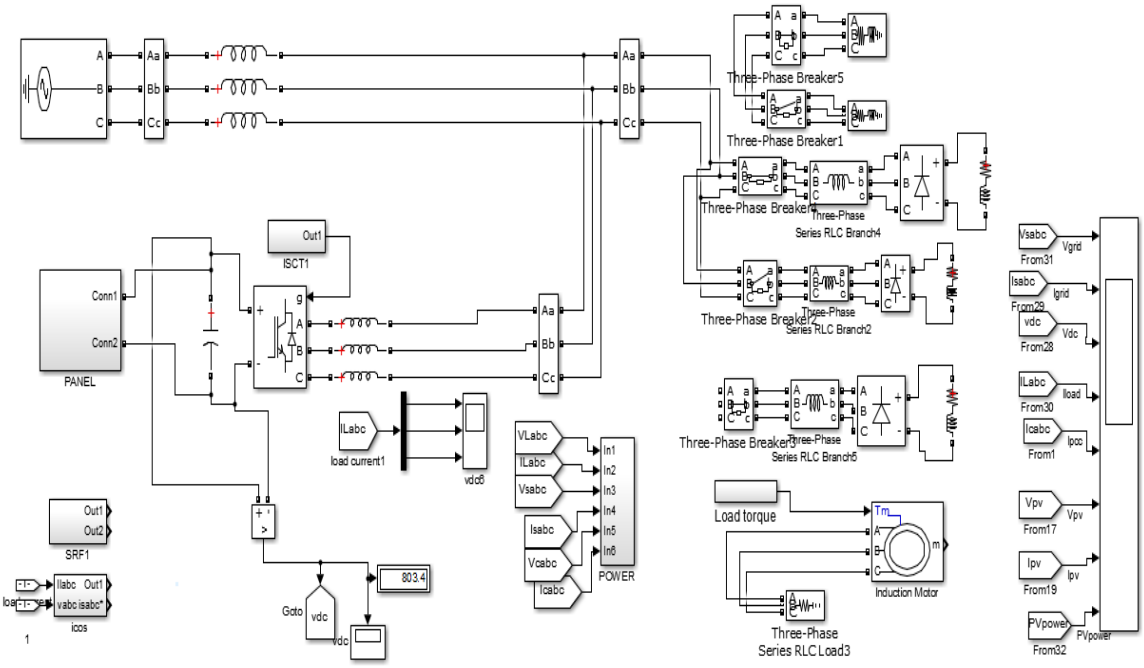

Fig. 5.2 Simulink model of the grid connected PV system

Values of all the parameters are given in the appendix-I. The simulation results of grid side voltage and current, dc bus voltage, PCC voltage and current, load voltage and current, PV voltage and current, PV power for various loads are presented for different algorithms

5.3 Simulation results of the proposed system:

The simulation results of the proposed system for various loads under varying atmospheric conditions are presented. Three different control algorithms viz. SRFT, ISCT and IcosØ are used for controlling the inverter.

5.3.1 Synchronous Reference Frame (SRF) Theory based control algorithm

The theory and its control technique is already explained in section (4.2.1). The Simulink model for the control technique is shown in Fig. 5.3.

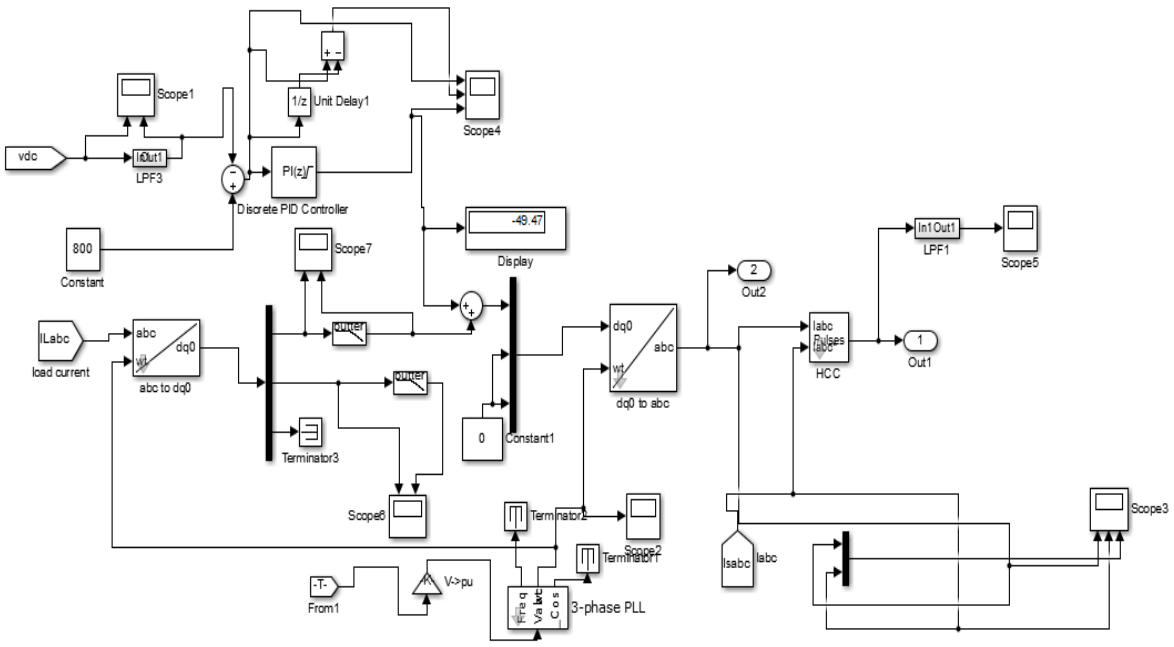

Fig.5.3. Simulink model of SRFT Controller for reference current extraction

A. Performance of grid connected Solar PV system with balanced linear load :

The simulation results of grid connected Solar PV system with balanced linear load are shown in Fig. 5.4 and Fig. 5.5. From 0.3sec to 0.5sec the load is suddenly decreased. The effect of load change on the various parameters can be observed. V_{dc} remains constant and source current decreases to meet the load demand, but remains balanced, sinusoidal and the power factor is maintained to unity. From 0.6 sec. to 0.75 sec, irradiation of the solar PV system is decreased from 1000 W/mm^2 to 600 W/mm^{2}as shown in Fig. 5.4 and temperature is increased from 25^{0}C to 45^{0}C as shown in Fig. 5.5 respectively. Under these conditions, solar PV power is reduced. So, the remaining load demand is supplied from the grid. Under all the above variable conditions, DC link and PCC voltages are maintained and grid current remains balanced. The THD level of grid current is 2.30% and PCC current is 1.32% as shown in Fig.5.6, which is well within the IEEE limits. The active power fed to the load is the sum of the grid power and PV power. For the above variations, the system power balance is shown in Fig. 5.7 and Fig. 5.8. Also unity power factor is maintained for the grid side supply system as shown in Fig. 5.9.

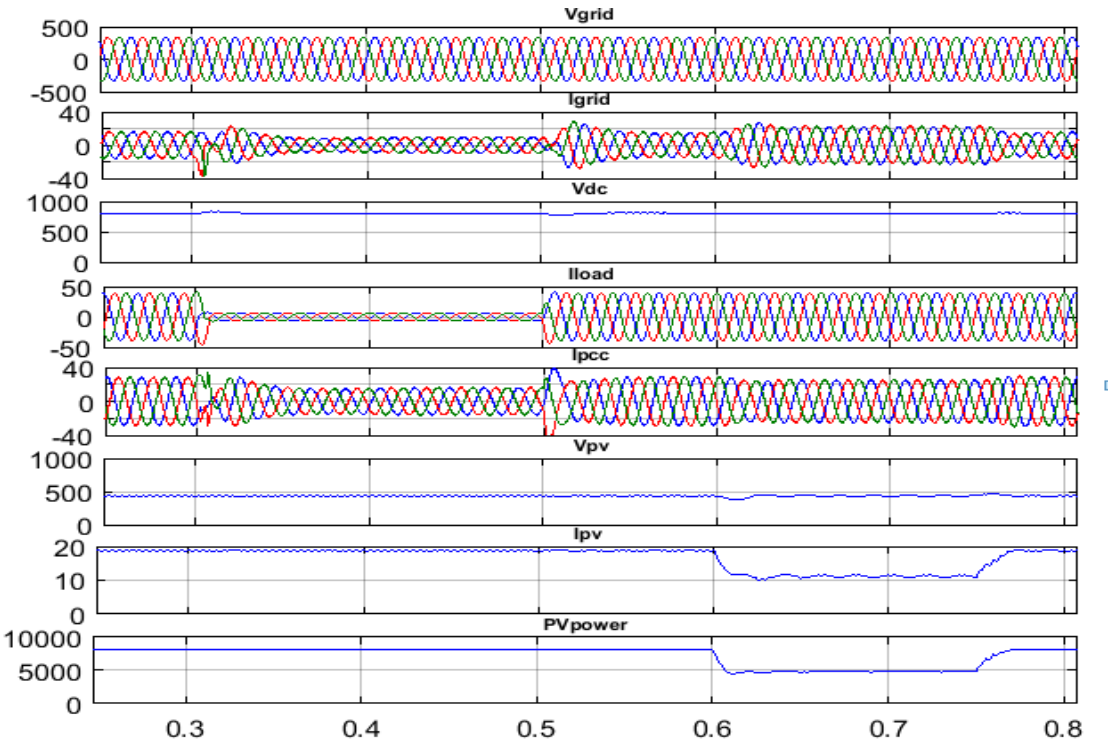

Fig. 5.4. Performance of grid connected Solar PV system for balanced linear load under changing load with varying irradiation level

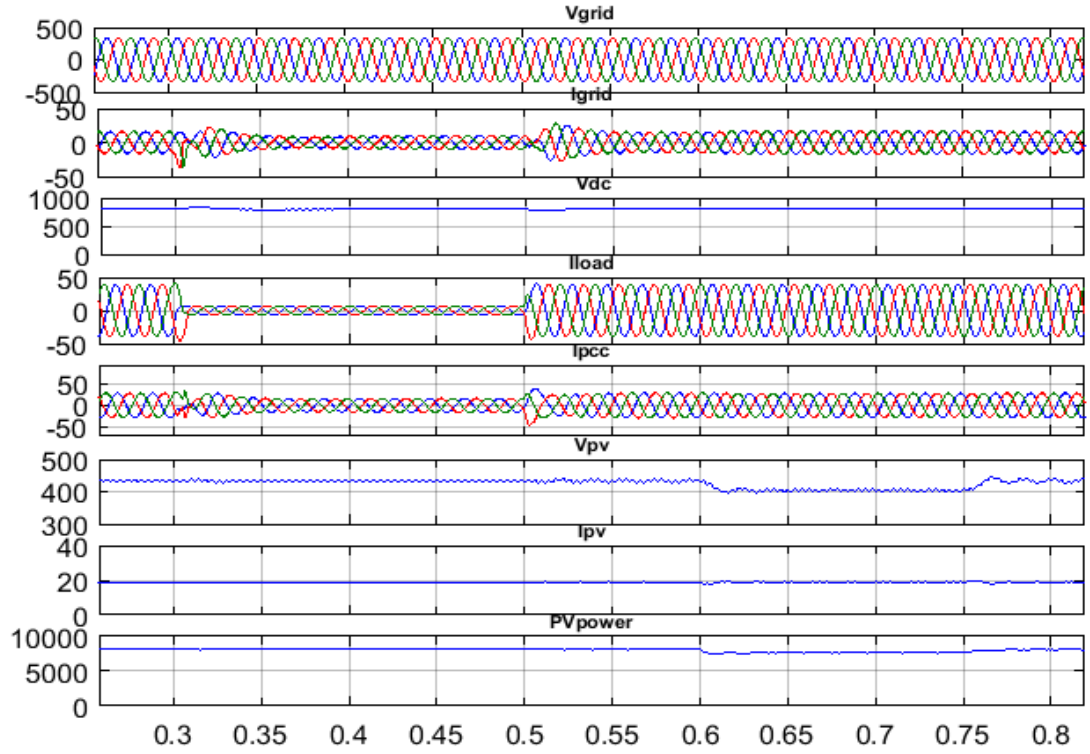

Fig. 5.5. Performance of grid connected Solar PV system for linear load under changing load with varying temperature levels

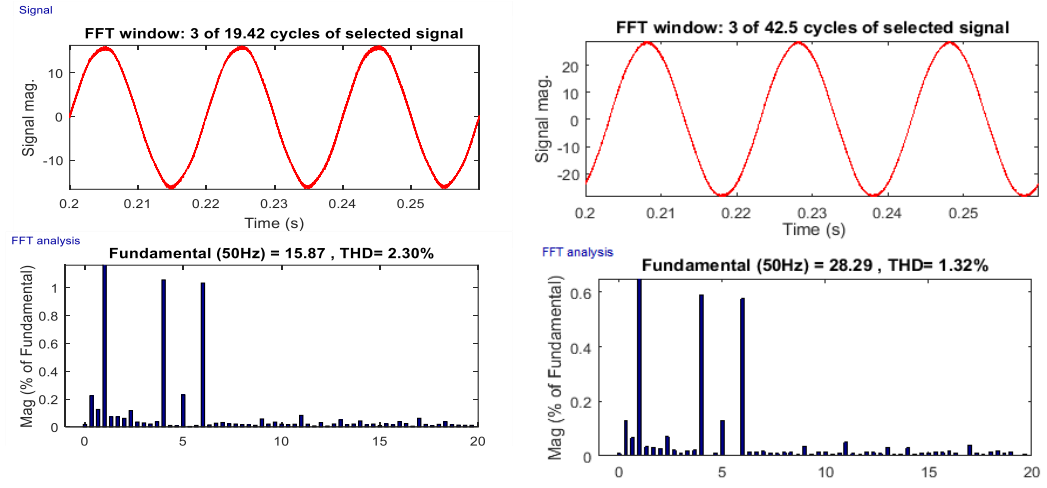

Fig.5.6 Waveform and harmonic analysis for Grid Current (I_{grid}) and PCC current (I_{PCC}) for linear load

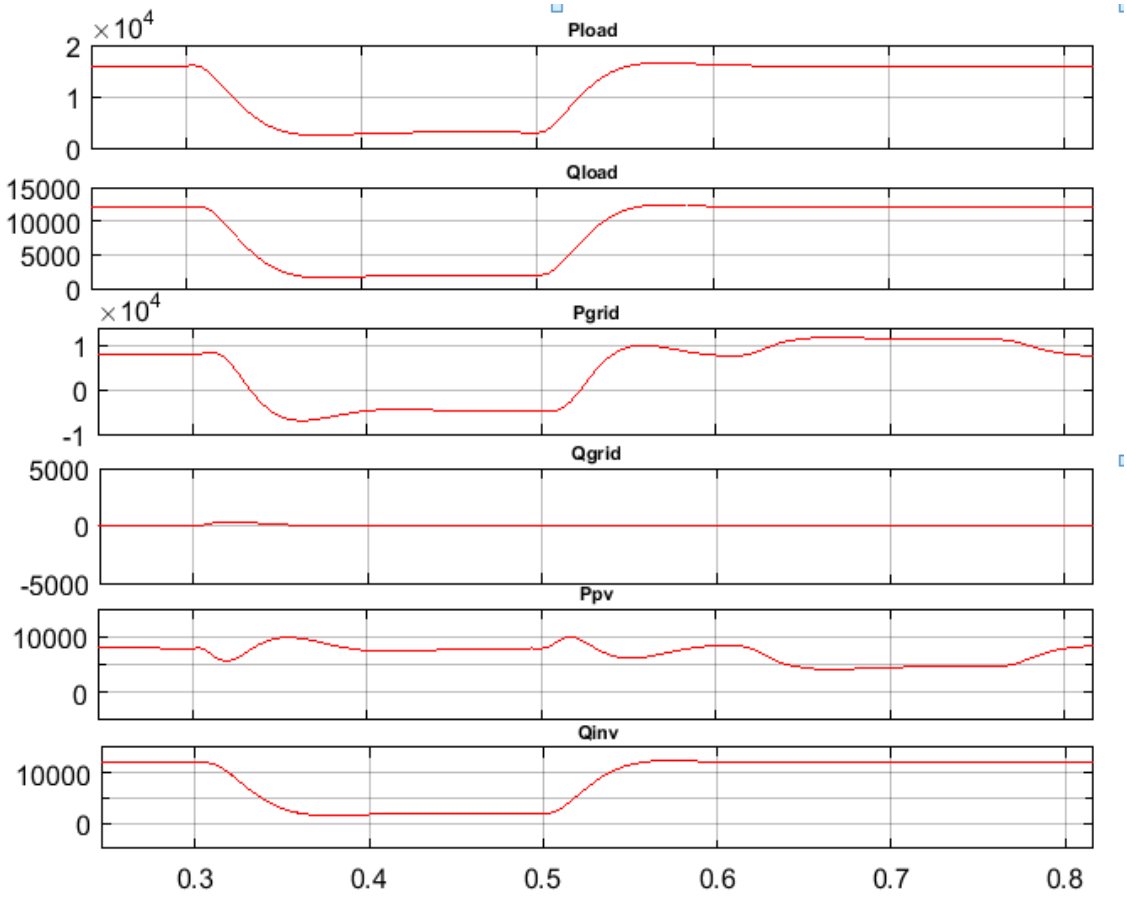

Fig.5.7 Power flow at different part of the system for linear load under load change with varying irradiation

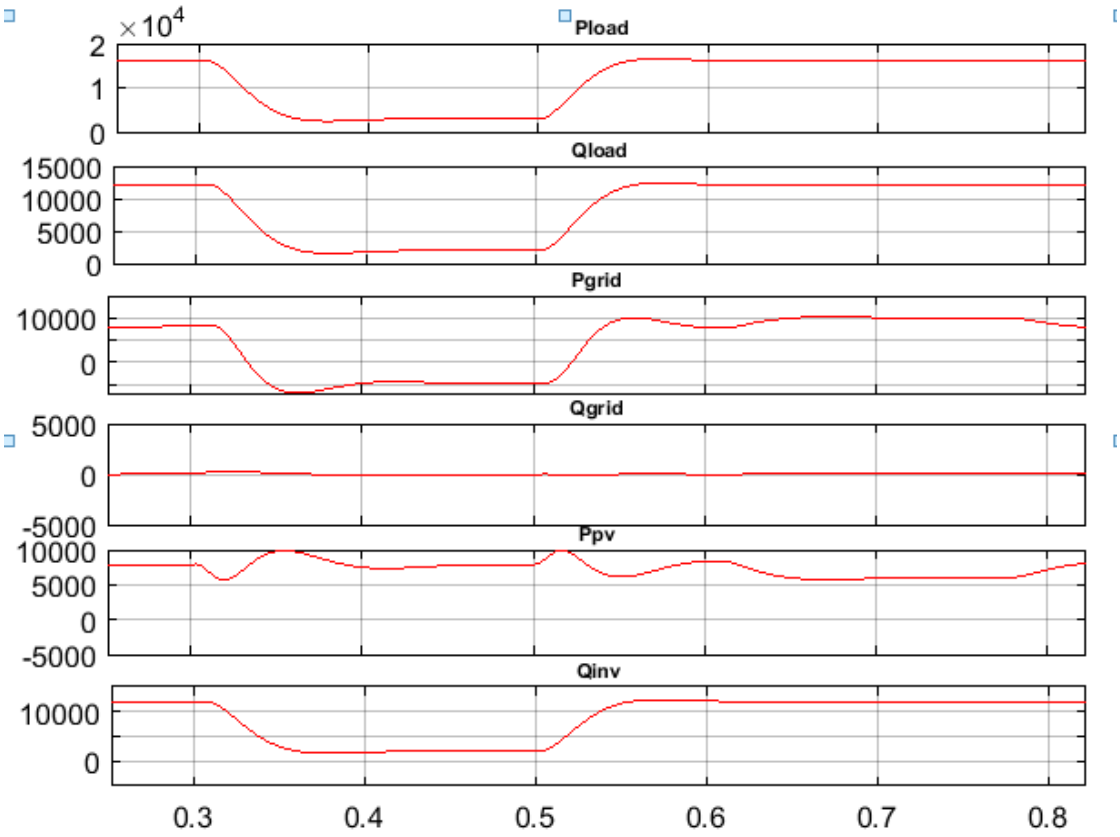

Fig.5.8 Power flow at different part of the system for linear load under load change with varying temperature

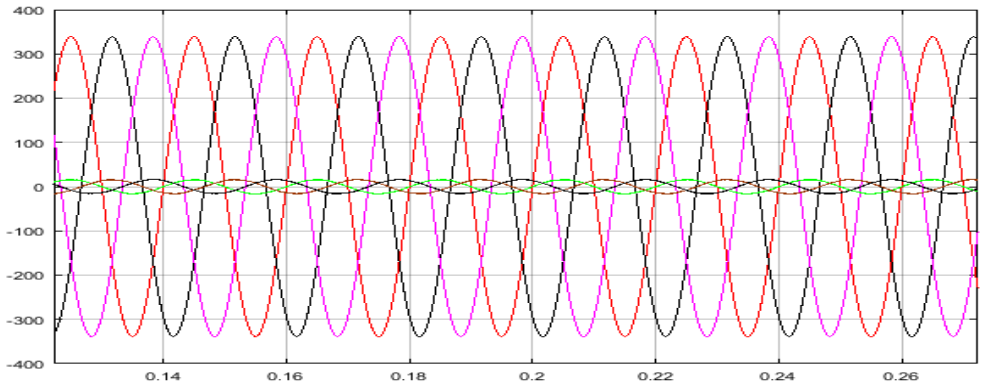

Fig.5.9 In phase grid side voltage and current for linear load conditions.

B. Performance of grid connected Solar PV system with balanced non-linear load:

The simulation results of grid connected Solar PV system with balanced non-linear load are shown in Fig. 5.10 and Fig. 5.11. From 0.3sec to 0.5sec the load is suddenly decreased. The effect of load change on the various parameters can be observed. V_{dc} remains constant and

source current decreases to meet the load demand, but remains balanced, sinusoidal and the power factor is maintained to unity. From 0.6 sec. to 0.75 sec, irradiation of the Solar PV system is decreased from 1000 W/mm^2 to 600 W/mm^{2}as shown in Fig. 5.10 and temperature is increased from 25^{0}C to 45^{0}C as shown in Fig. 5.11 respectively. Under these conditions, solar PV power is reduced. So, the remaining load demand is supplied from the grid. Under all the above variable conditions, DC link and PCC voltages are maintained and grid current remains balanced. The THD level of grid current is 1.18% and THD level of load current is 16.34% as shown in Fig.5.12, which is well within the IEEE limits. Also unity power factor is maintained for the grid side supply system as shown in Fig. 5.13.

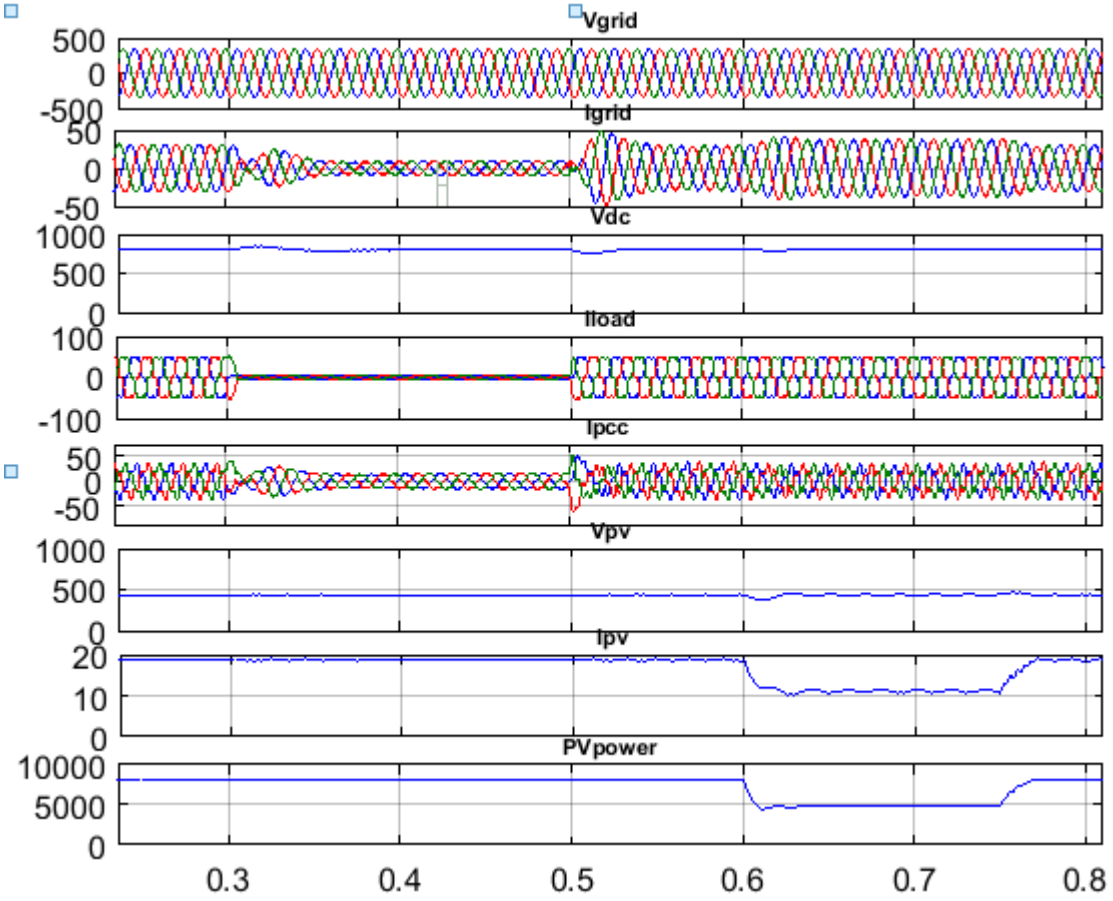

Fig. 5.10. Performance of grid connected SPV system for non-linear load under changing load with varying irradiation levels

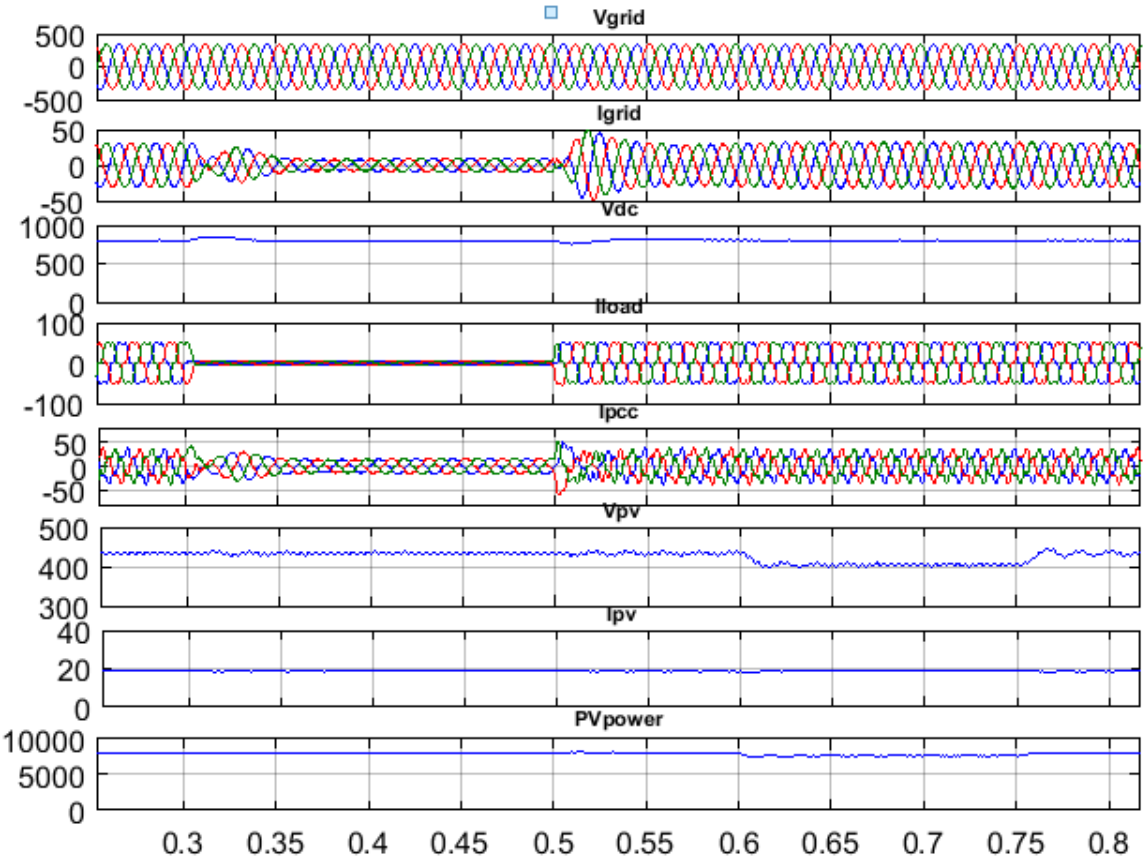

Fig 5.11.Performance of grid connected SPV system for non-linear load under changing load with varying temperature levels

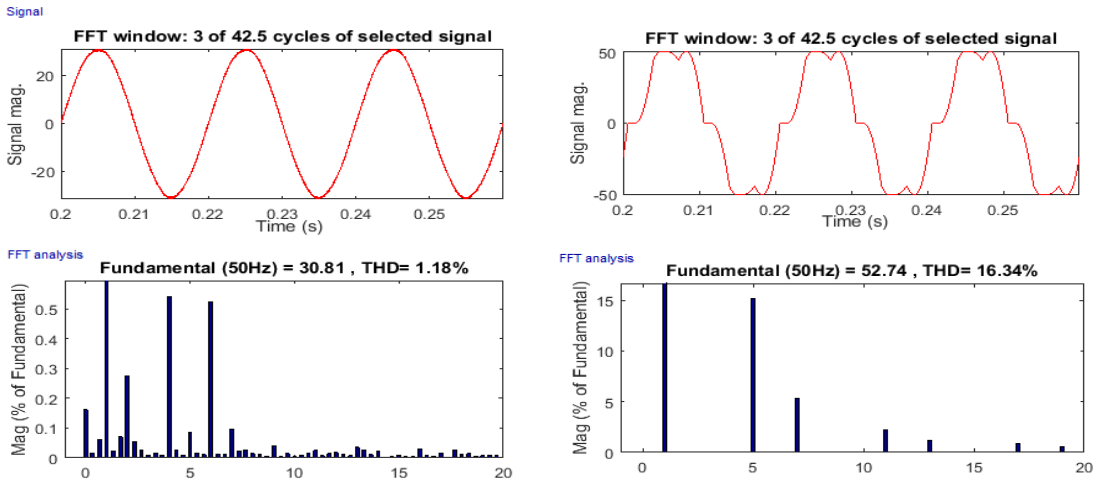

Fig.5.12 .Waveform and harmonic analysis for Grid Current (I_{grid}) and Load current (I_{Load}) for non-linear load

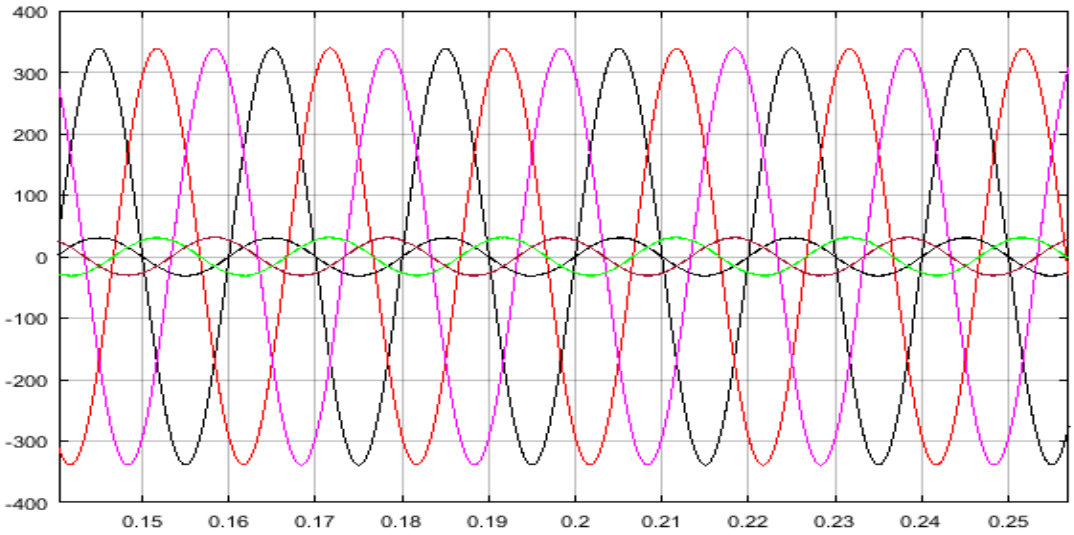

Fig. 5.13. In phase grid side voltage and current for non-linear load conditions

C. Performance of grid connected Solar PV system with unbalanced non-linear load

The performance for non-linear unbalanced load condition is shown in Fig.5.14. From 0.3 sec to 0.5 sec 'a' phase of the load has been disconnected and at t=0.5 sec this 'a' phase load is again applied and the system again comes in the balanced mode. The effect of unbalanced load on the various parameters can be observed. V_{dc} remains constant and source current decreases to meet the load demand, but remains balanced, sinusoidal and the power factor is maintained to unity. From 0.6 sec. to 0.75 sec, irradiation of the SPV system is decreased from 1000 W/mm^2 to 600 W/mm^2 is also shown by fig 5.14. Under this condition, solar PV power is reduced. So, the remaining load demand is supplied from the grid. Under all the above variable conditions, DC link and PCC voltages are maintained and grid current remains balanced. The THD level of grid current is 3.85% which is well within the IEEE limits and THD level of load current is 16.34% as shown in Fig.5.15.

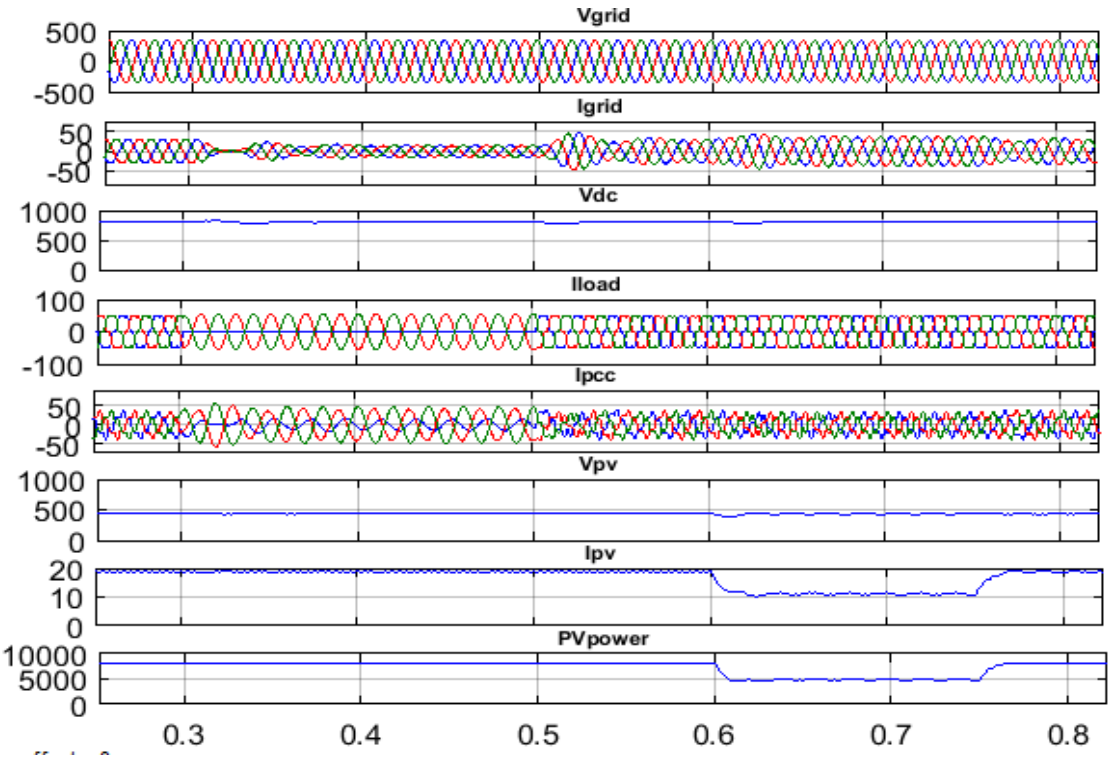

Fig. 5.14. Performance of grid connected SPV system for non-linear load under unbalancing with varying irradiation levels

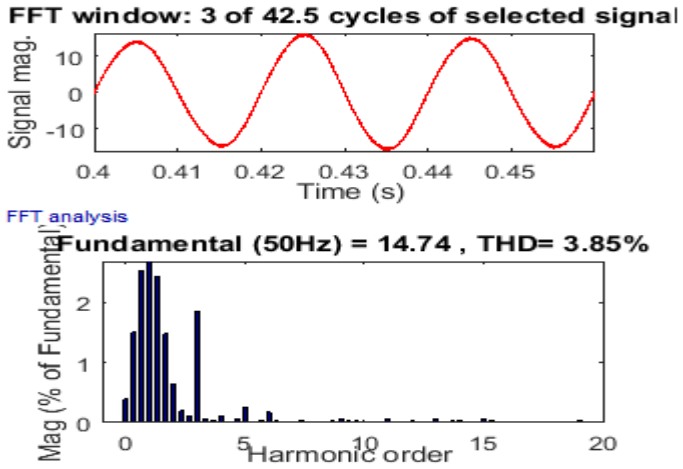

Fig.5.15 .Waveform and harmonic analysis for Grid Current (I_{grid}) for non- linear load during unbalancing time

D. Performance of grid connected Solar PV system with dynamic load.

The performance for dynamic load is shown in Fig. 5.16. At 0.3 sec torque of motor is increased to full load torque value i.e 20 N-m, after 5sec it is decreased to half of the load

torque i.e 10N-m, and its effect on the various parameters can be seen. As seen from the graphs, V_{dc} remains constant, PCC voltage is regulated, current from the grid side decreases to meet the load. DC bus voltage and PCC voltage are well maintained and load currents are balanced and THD level of grid current is 3.32% and PCC current is 2.96%, which is well within IEEE limits as given by Fig. 5.17.

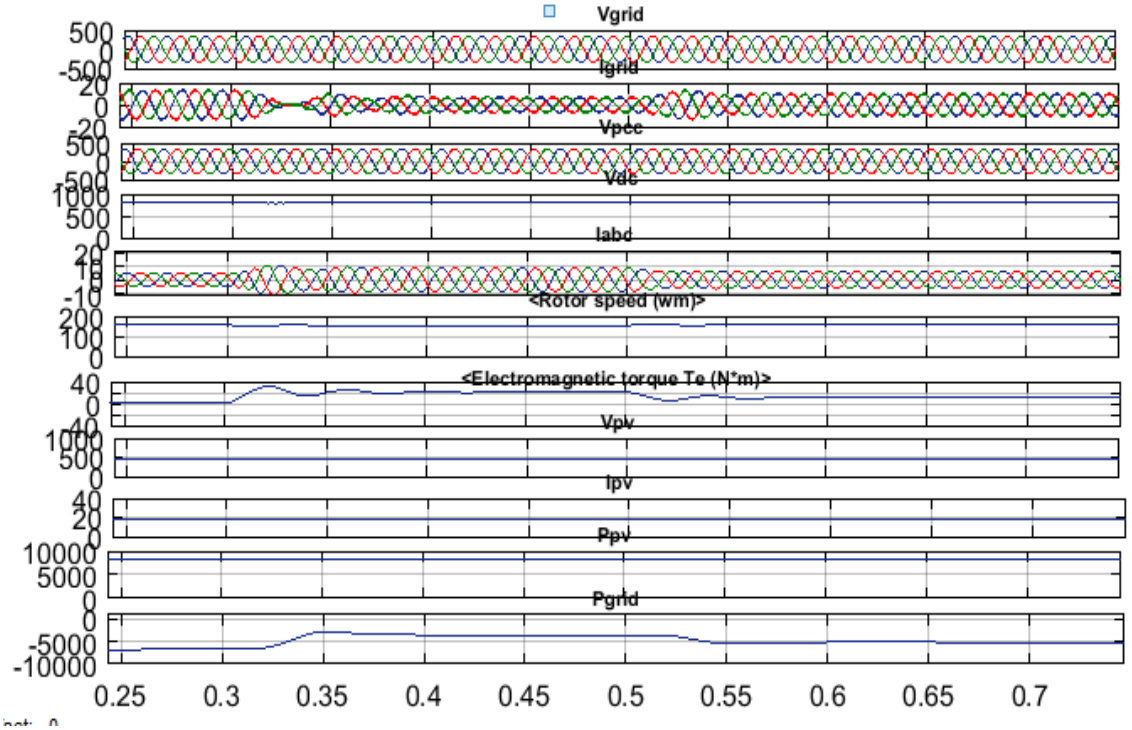

Fig. 5.16.Performance of grid connected SPV system for dynamic load under torque variation with varying irradiation levels

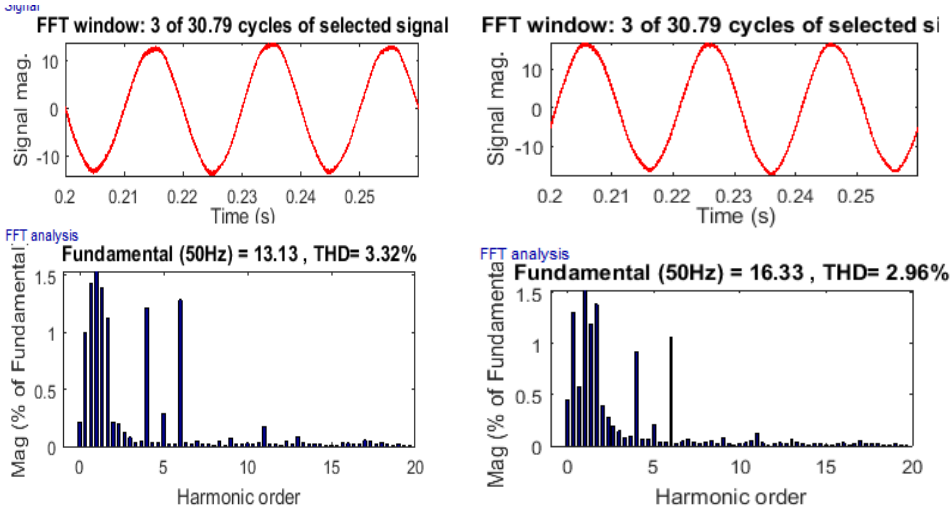

Fig.5.17 .Waveform and harmonic analysis for Grid Current (I_{grid}) and PCCcurrent (I_{PCC}) for dynamic load

5.3.2 Instantaneous Symmetrical Component Theory based control algorithm

The theory and its control technique is already explained in section 4.2.2. The Simulink model for the control technique is shown in Fig. 5.18.

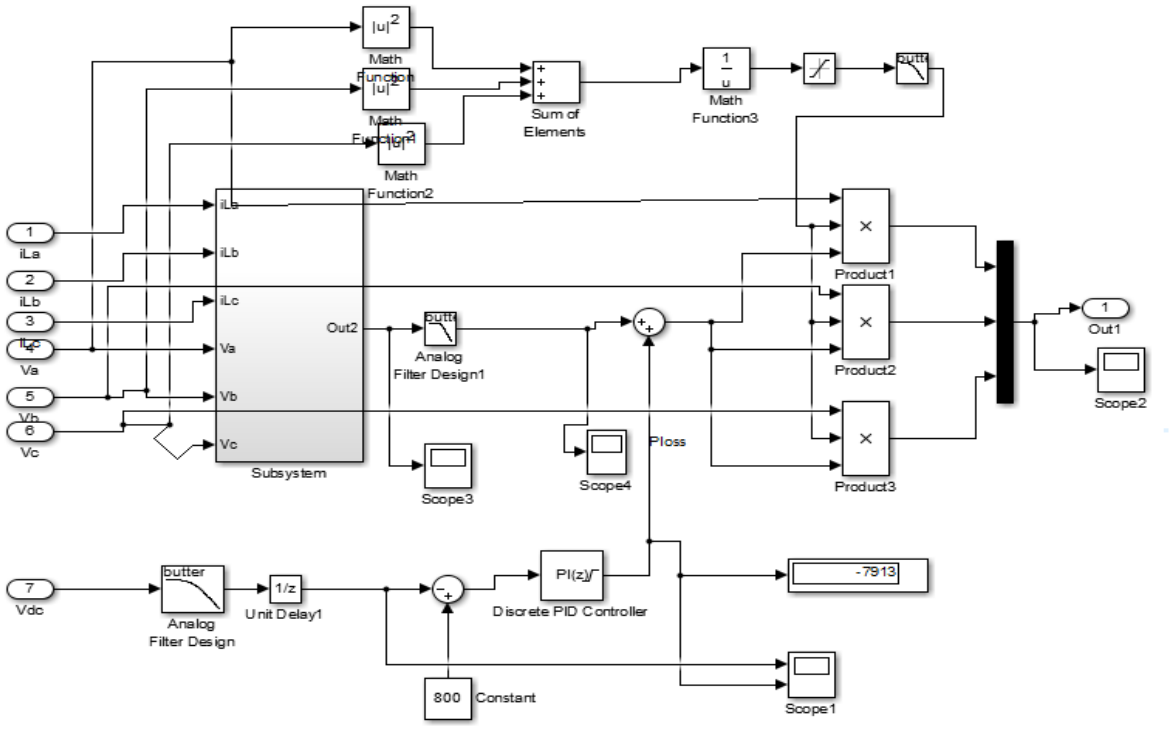

Fig.5.18. ISCT controller for reference current extraction

A) Performance of grid connected Solar PV system with balanced linear load

The simulation results of grid connected SPV system with balanced linear load are shown in Fig. 5.19 and Fig. 5.20. From 0.3sec to 0.5sec the load is suddenly decreased. The effect of load change on the various parameters can be observed. V_{dc} remains constant and source current decreases to meet the load demand, but remains balanced, sinusoidal and the power factor is maintained to unity. From 0.6 sec. to 0.75 sec, irradiation of the Solar PV system is decreased from 1000 W/mm^2 to 600 W/mm^{2}as shown in Fig. 5.19 and temperature is increased from 25^{0}C to 45^{0}C as shown in Fig. 5.20 respectively. Under these conditions, SPV power is reduced. So, the remaining load demand is supplied from the grid. Under all the above variable conditions, DC link and PCC voltages are maintained and grid current

remains balanced. The THD level of grid current is 3.46% and PCC current is 1.97% as shown in Fig. 5.21, which is well within the IEEE limits. Also unity power factor is maintained for the grid side supply system as shown in Fig. 5.22.

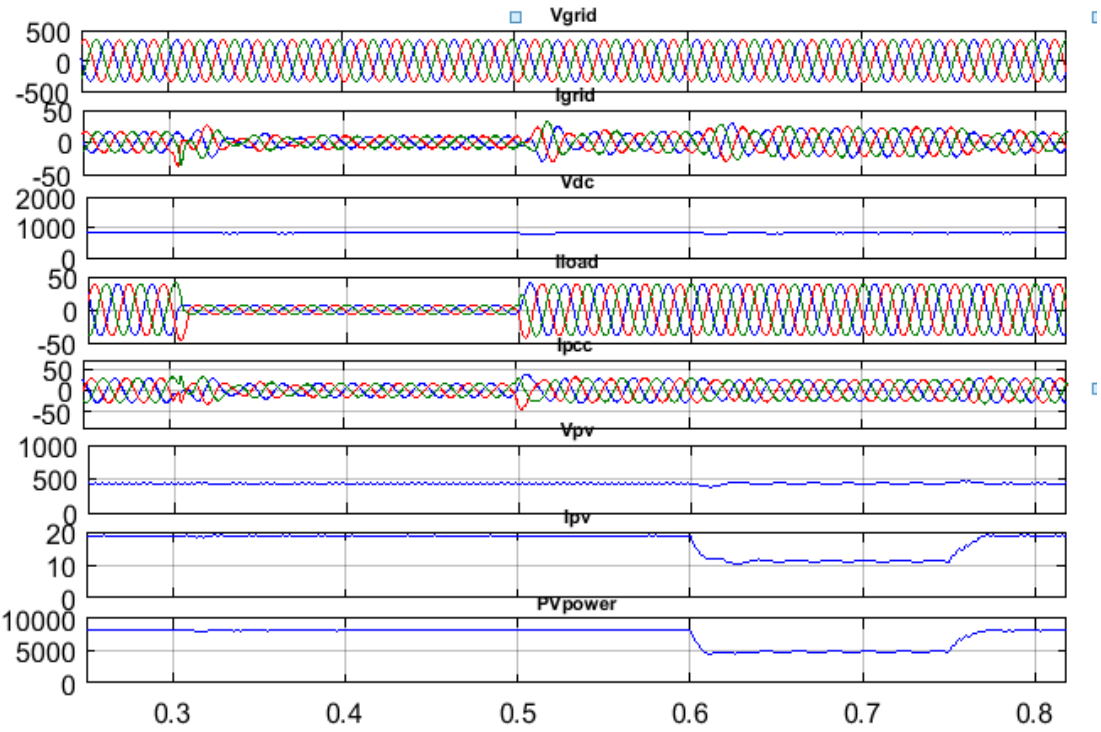

Fig. 5.19. Performance of grid connected SPV system for linear load under changing load with varying irradiation level

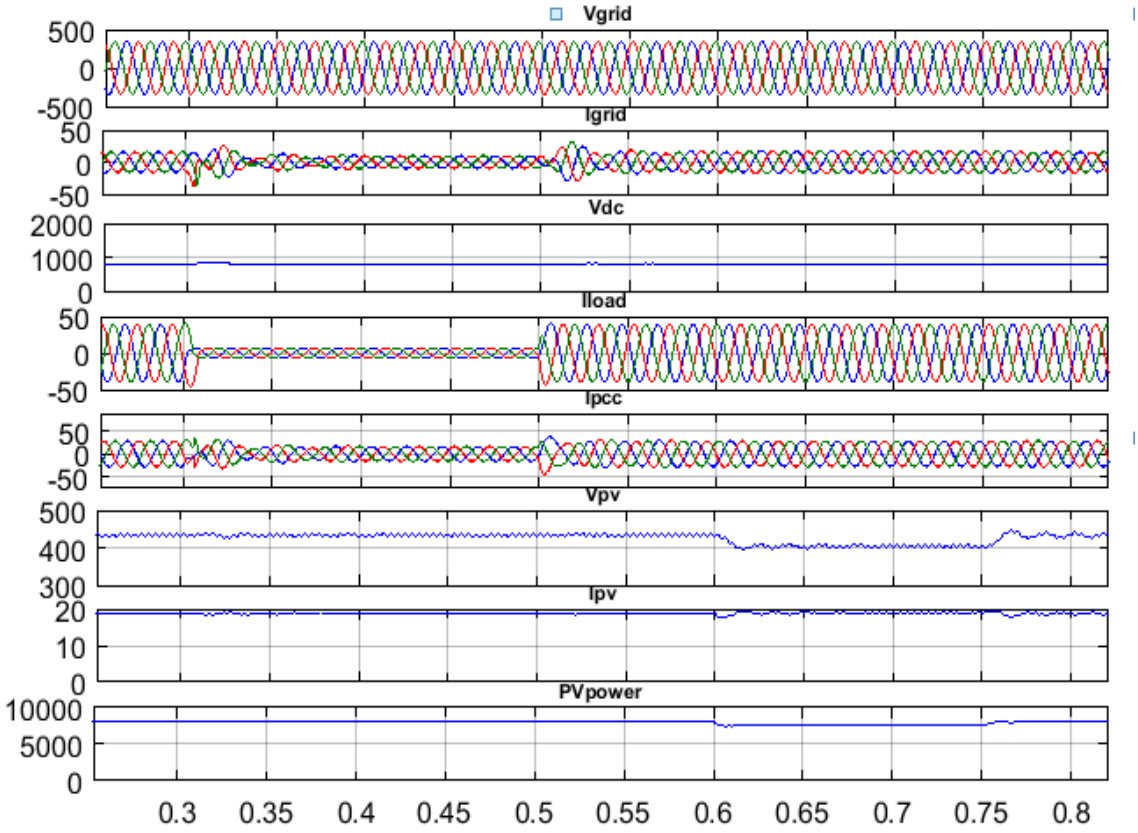

Fig 5.20.Performance of grid connected SPV system for linear load under changing load with varying temperature levels

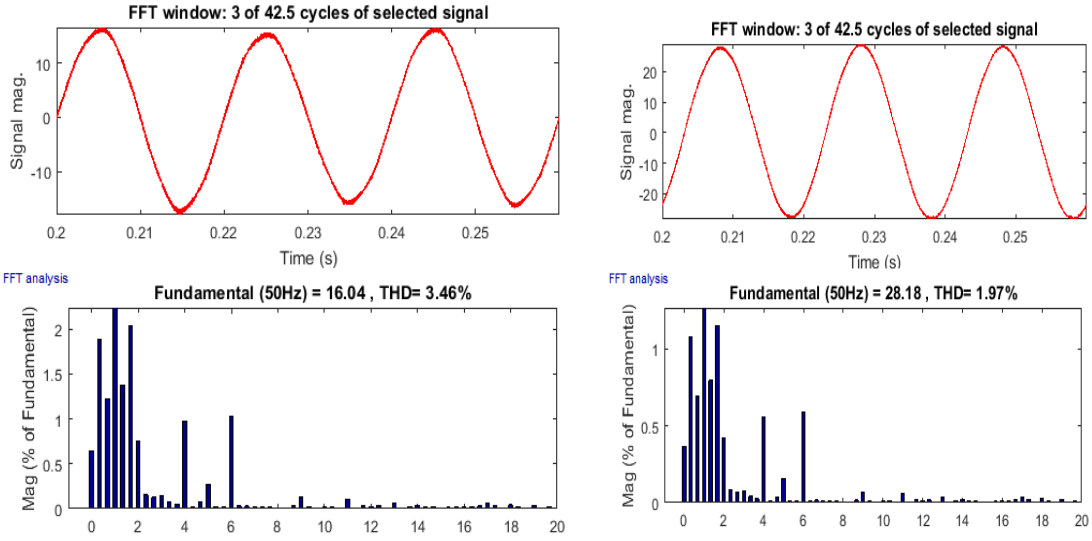

Fig.5.21Waveform and harmonic analysis for Grid Current (I_{grid}) and PCC current (I_{PCC}) for linear load

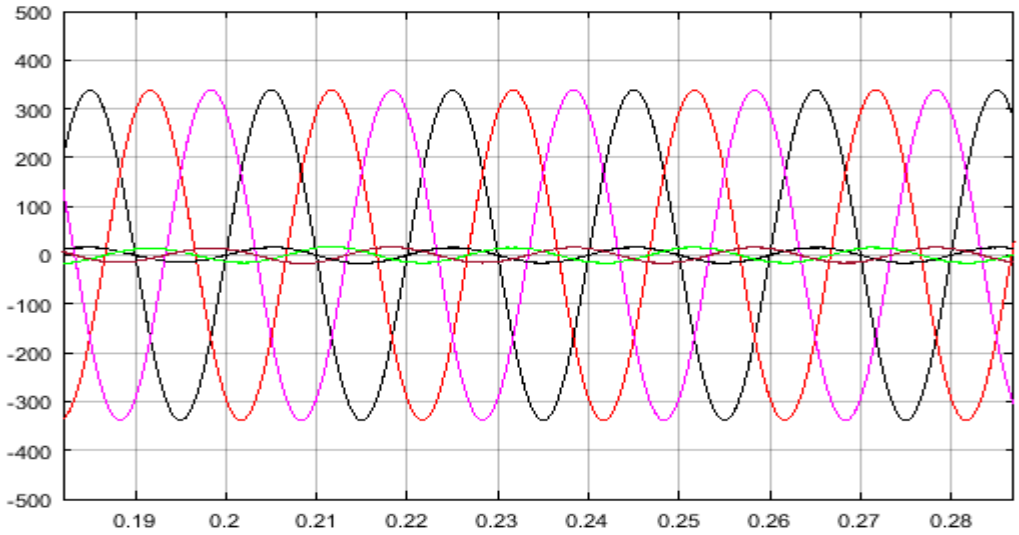

Fig.5.22 In phase grid side voltage and current for linear load conditions.

B. Performance of grid connected Solar PV system with balanced non-linear load

The simulation results of grid connected SPV system with balanced non-linear load are shown in Fig. 5.23 and Fig. 5.24. From 0.3sec to 0.5sec the load is suddenly decreased. The effect of load change on the various parameters can be observed. V_{dc} remains constant and source current decreases to meet the load demand, but remains balanced, sinusoidal and the power factor is maintained to unity. From 0.6 sec. to 0.75 sec, irradiation of the Solar PV system is decreased from 1000 W/mm^2 to 600 W/mm^{2}as shown in Fig. 5.23 and temperature is increased from 25^{0}C to 45^{0}C as shown in Fig. 5.24 respectively. Under these conditions, Solar PV power is reduced. So, the remaining load demand is supplied from the grid. Under all the above variable conditions, DC link and PCC voltages are maintained and grid current remains balanced. The THD level of grid current is 1.78% and THD level of load current is 16.34% as shown in Fig. 5.25, which is well within the IEEE limits. Also unity power factor is maintained for the grid side supply system as shown in Fig. 5.26.

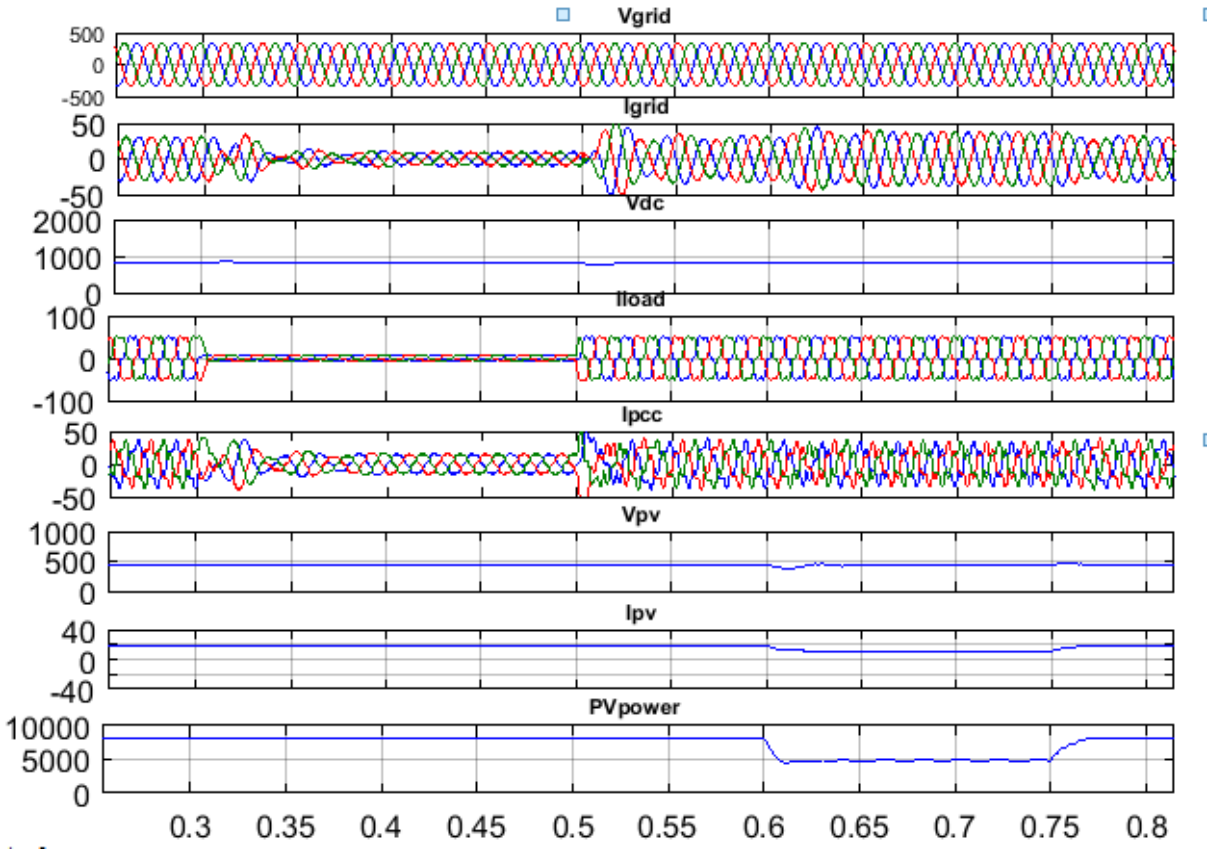

Fig. 5.23. Performance of grid connected SPV system for non-linear load under changing load with varying irradiation levels

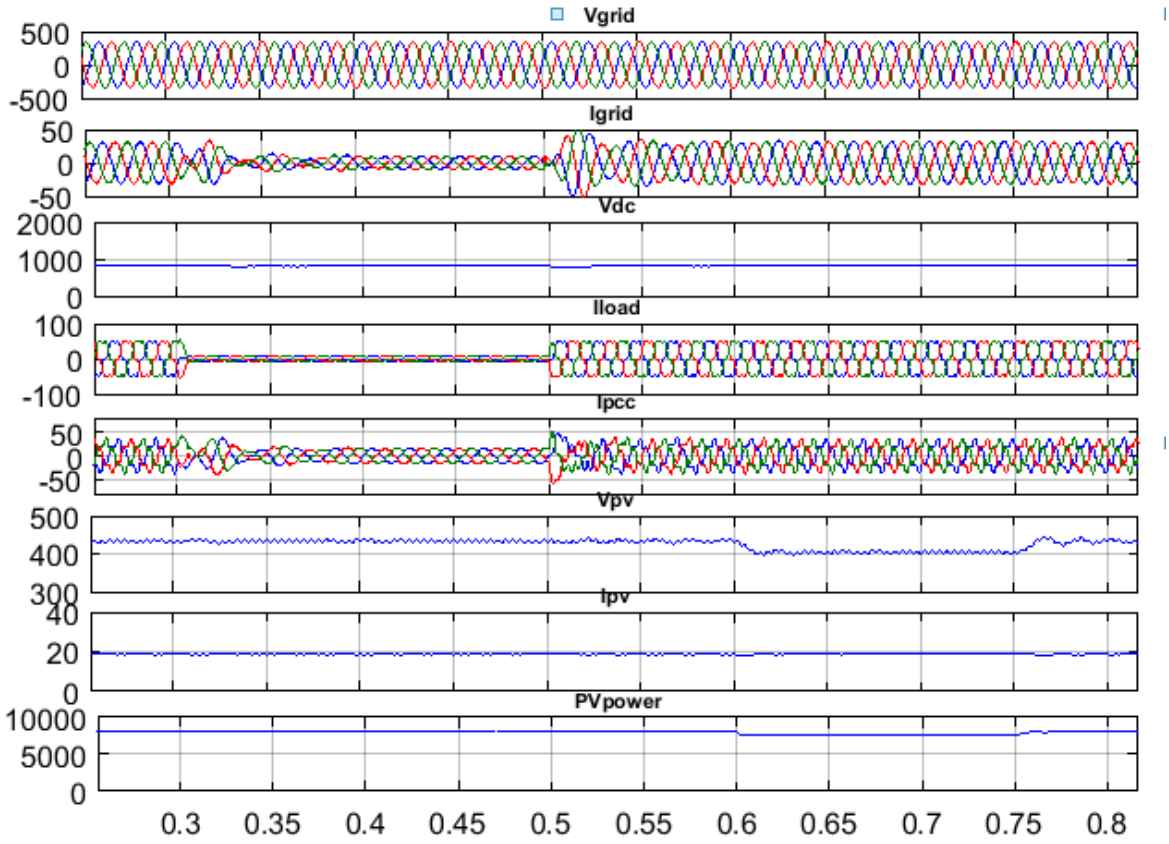

Fig 5.24. Performance of grid connected SPV system for non-linear load under changing load with varying temperature levels

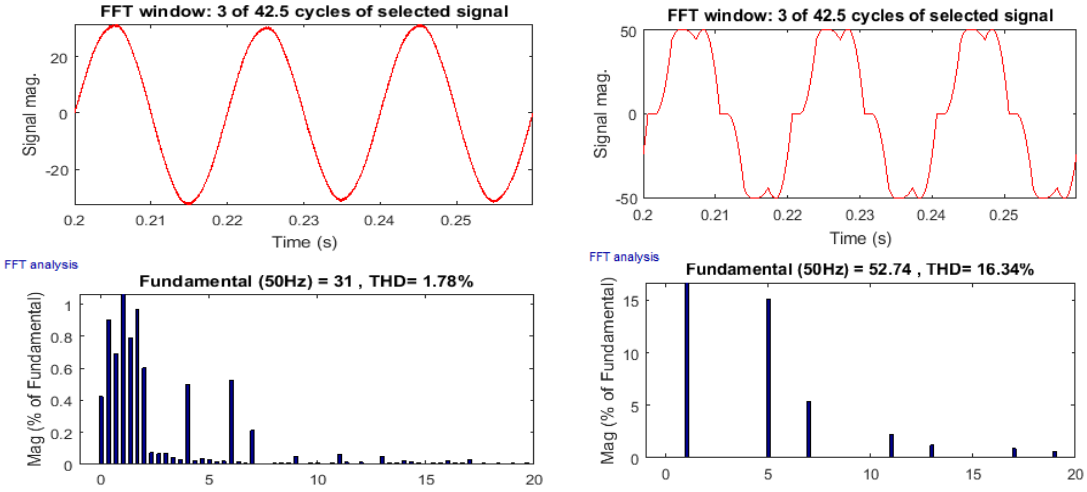

Fig.5.25 . Waveform and harmonic analysis for Grid Current (I_{grid}) and Load current (I_{Load}) for non- linear load

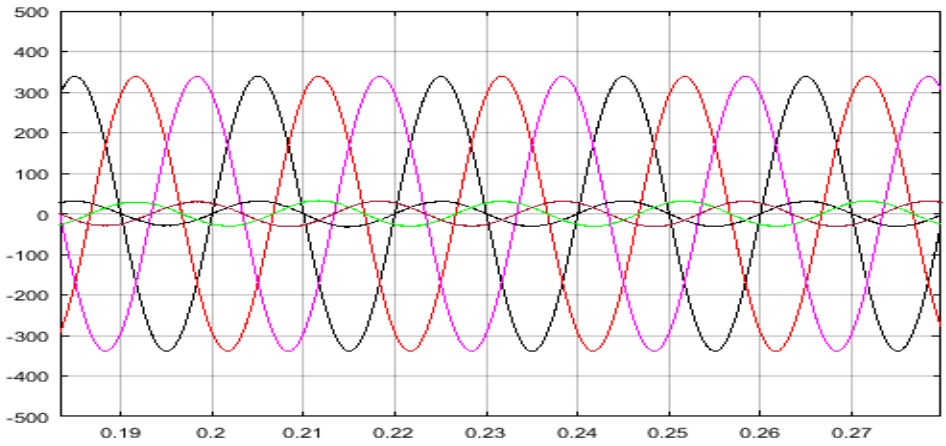

Fig.5.26 In phase grid side voltage and current for non-linear load conditions

C. Performance of grid connected Solar PV system with unbalanced non-linear load

The performance for non-linear unbalanced load condition is shown in Fig.5.27. From 0.3 sec to 0.5 sec 'a' phase of the load has been disconnected and at t=0.5 sec this 'a' phase load is again applied and the system again comes in the balanced mode. The effect of unbalanced load on the various parameters can be observed. V_{dc} remains constant and source current decreases to meet the load demand, but remains balanced, sinusoidal and the power factor is maintained to unity. From 0.6 sec. to 0.75 sec, irradiation of the SPV system is decreased from 1000 W/mm^2 to 600 W/mm^2 is also shown by fig 5.27. Under this condition, SPV power is reduced. So, the remaining load demand is supplied from the grid. Under all the above variable conditions, DC link and PCC voltages are maintained and grid current remains balanced. The THD level of grid current is 4.61% which is well within the IEEE limits as shown in Fig.5.28

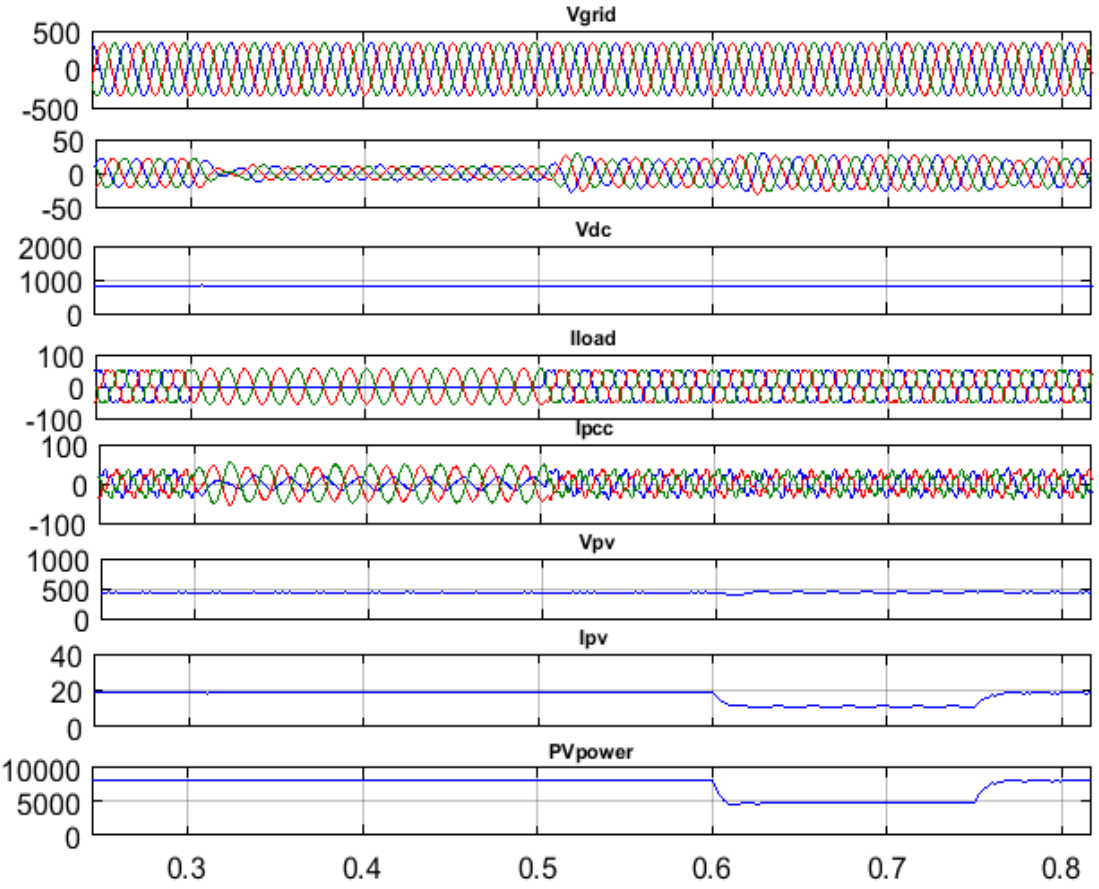

Fig. 5.27. Performance of grid connected SPV system for non-linear load under unbalancing with varying irradiation levels

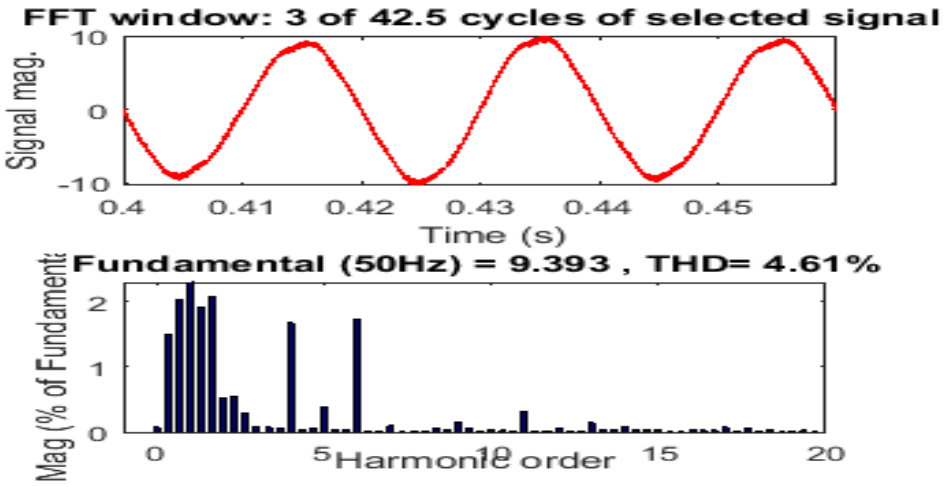

Fig.5.28. Waveform and harmonic analysis for Grid Current (I_{grid}) for non- linear load during unbalancing time

D. Performance of grid connected Solar PV system with dynamic load.

The performance for dynamic load is shown in Fig.5.29. At 0.3 sec torque of motor is increased to full load torque value i.e 20 N-m, after 5sec it is decreased to half of the load torque i.e 10N-m, and its effect on the various parameters can be seen. As seen from the graphs, V_{dc} remains constant, PCC voltage is regulated, current from the grid side decreases to meet the load. DC bus voltage and PCC voltage are well maintained and load currents are balanced and THD level of grid current is 3.57% and PCC current is 4.07%, which is well within IEEE limits as given by Fig. 5.30.

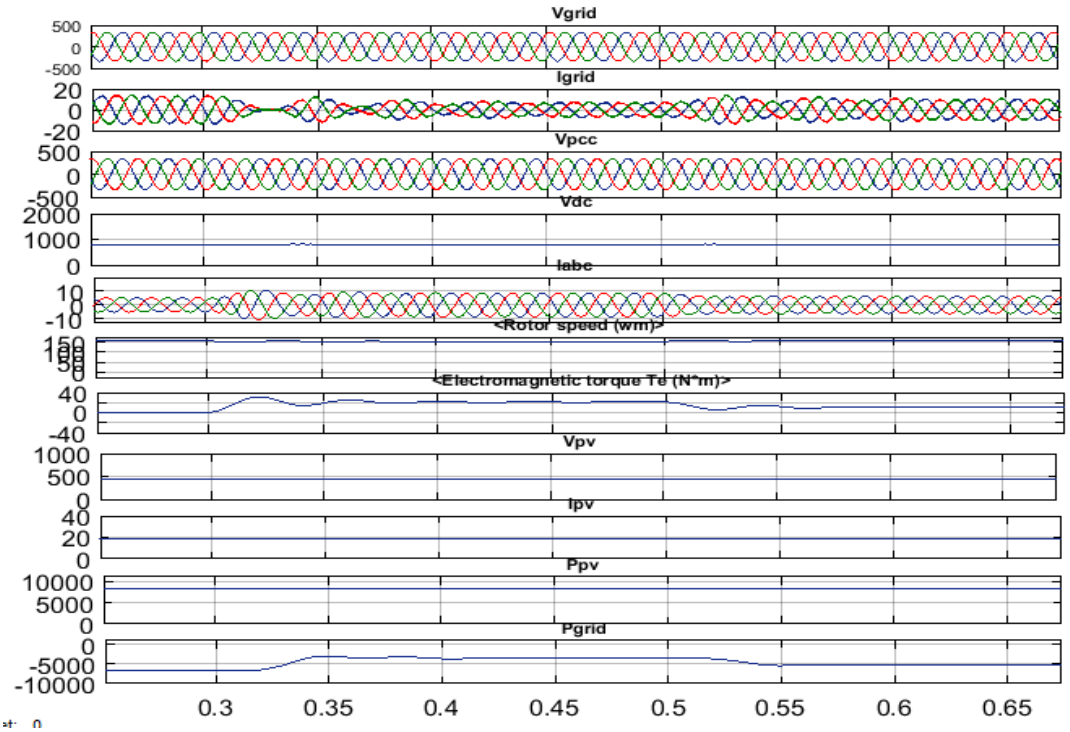

Fig. 5.29. Performance of grid connected SPV system for dynamic load under torque variation and varying irradiation level

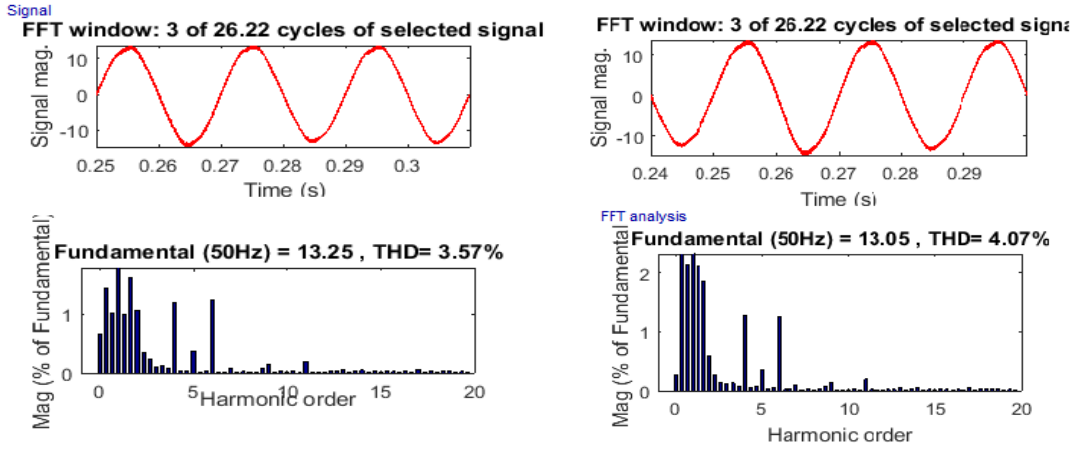

Fig.5.30. Waveform and harmonic analysis for Grid Current (I_{grid}) and PCC current (I_{PCC}) for dynamic load

5.3.3 Icosø Theory based control algorithm

The theory and its control technique is already explained in section 4.2.3. The Simulink model for the control technique is shown in Fig 5.31.

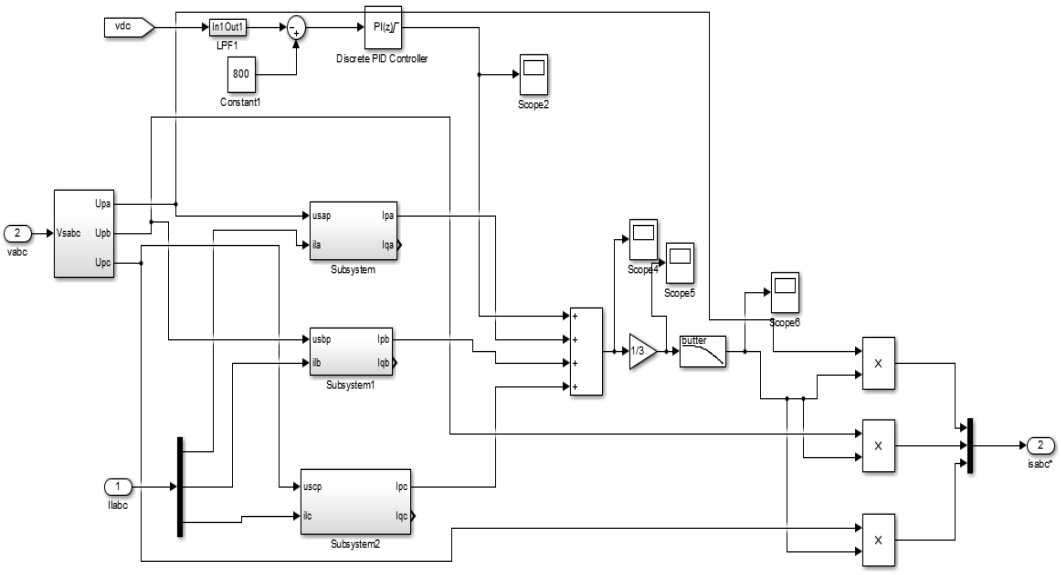

Fig.5.31. Icosø controller for reference current extraction

A. Performance of grid connected Solar PV system with balanced linear load

The simulation results of grid connected SPV system with balanced linear load are shown in Fig.5.32 and Fig.5.33. From 0.3sec to 0.5sec the load is suddenly decreased. The effect of load change on the various parameters can be seen. It is observed that, V_{dc} remains

constant and source current decreases to meet the load demand, but remains balanced, sinusoidal and the power factor is maintained to unity. From 0.6 sec. to 0.75 sec, irradiation of the Solar PV system is decreased from 1000 W/mm^2 to 600 W/mm^{2}as shown in Fig.5.32 and temperature is increased from 25^{0}C to 45^{0}C as shown in Fig. 5.33 respectively. Under these conditions, Solar PV power is reduced. So, the remaining load demand is supplied from the grid. Under all the above variable conditions, DC link and PCC voltages are maintained and grid current remains balanced. The THD level of grid current is 1.92% and PCC current is 1.07% as shown in Fig. 5.34, which is well within the IEEE limits. Also unity power factor is maintained for the grid side supply system as shown in Fig. 5.35.

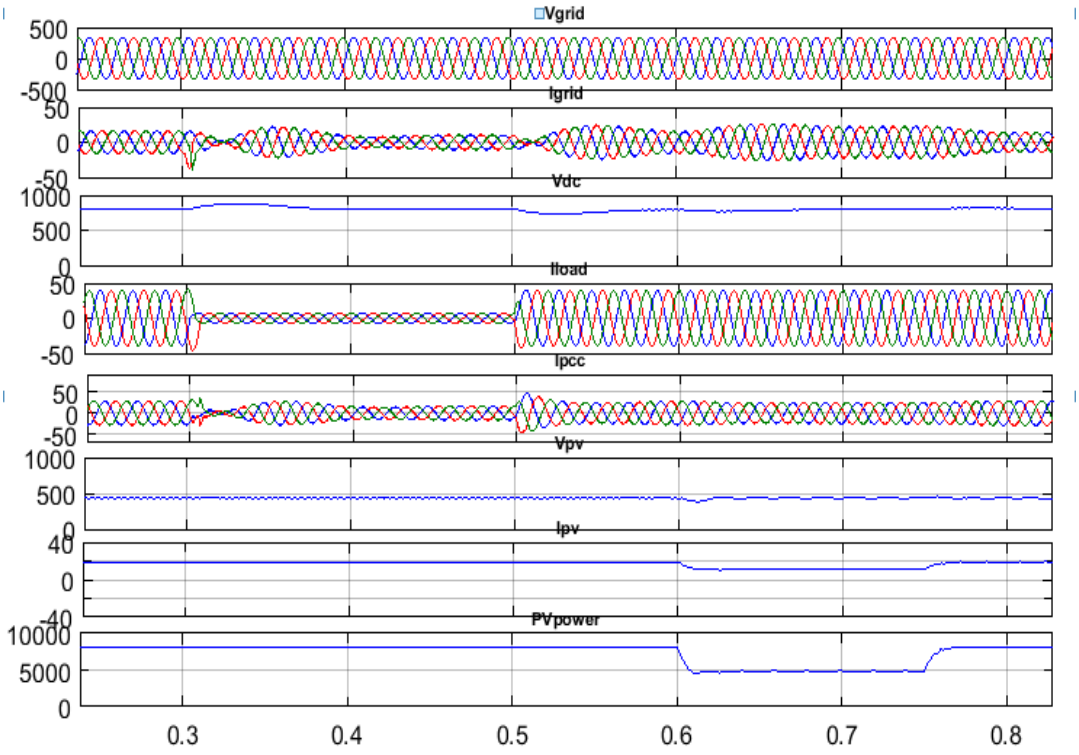

Fig. 5.32. Performance of grid connected SPV system for linear load under changing load with varying irradiation levels

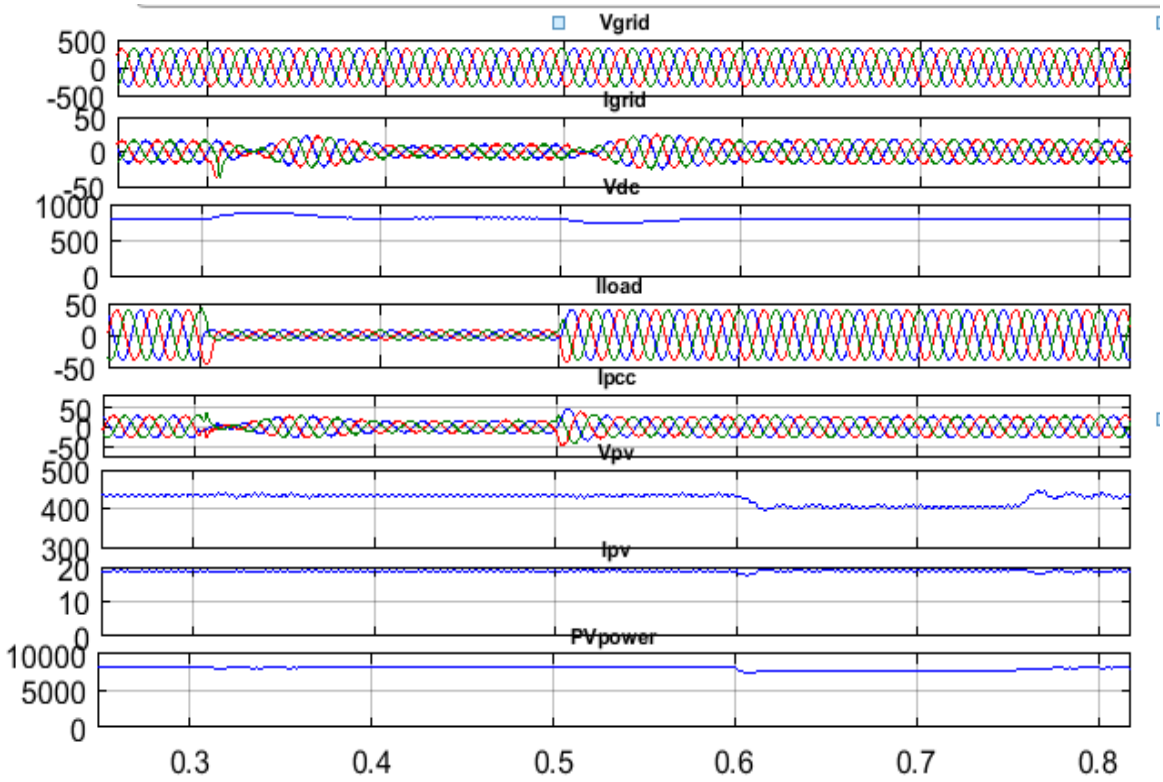

Fig 5.33. Performance of grid connected SPV system for linear load under changing load with varying temperature levels

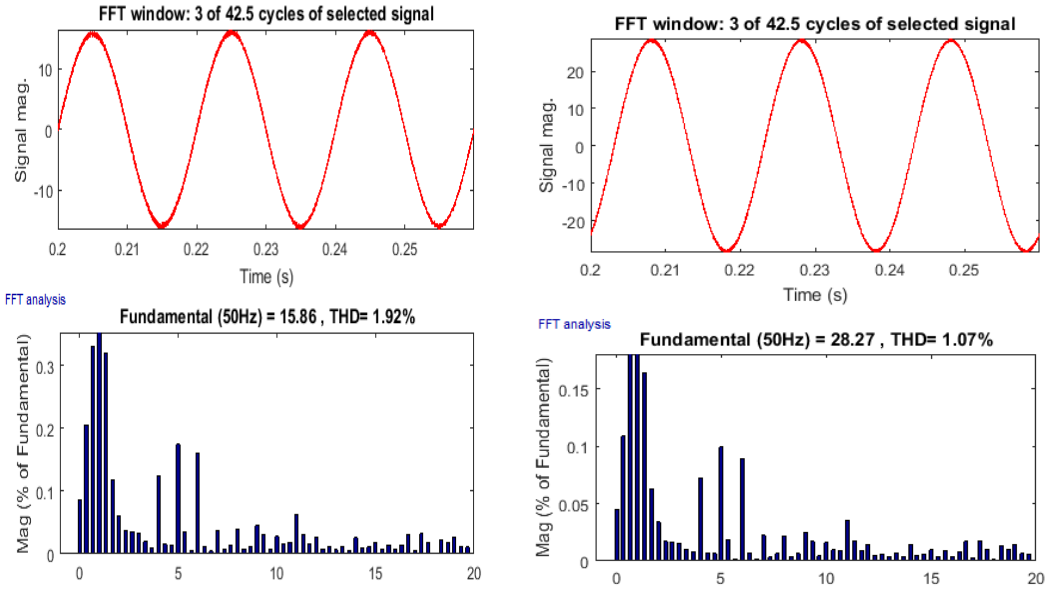

Fig.5.34. Waveform and harmonic analysis for Grid Current (I_{grid}) and PCC current (I_{PCC}) for linear load

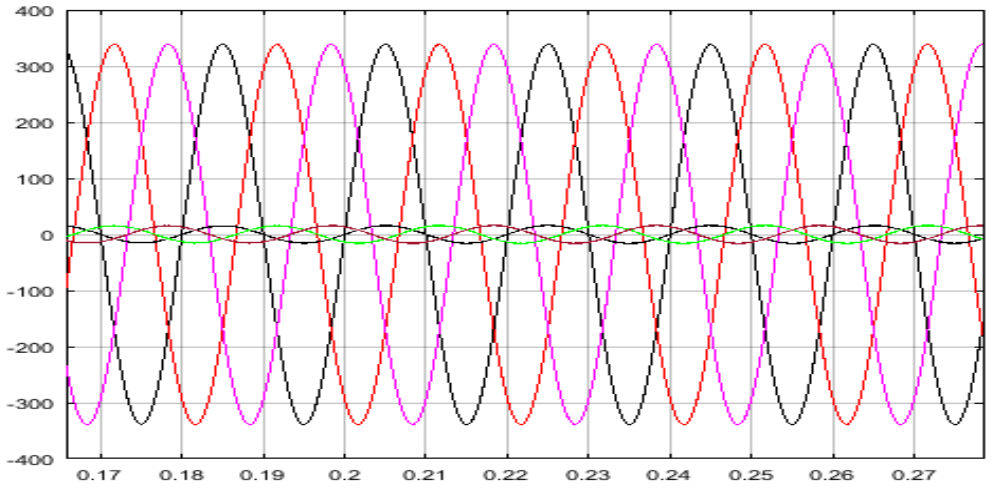

Fig. 5.35. In phase grid side voltage and current for linear load conditions.

B. Performance of grid connected Solar PV system with balanced non- linear load

The simulation results of grid connected SPV system with balanced non-linear load are shown in Fig. 5.36 and Fig.5.37. From 0.3sec to 0.5sec the load is suddenly decreased. The effect of load change on the various parameters can be observed as V_{dc} remains constant and source current decreases to meet the load demand, but remains balanced, sinusoidal and the power factor is maintained to unity. From 0.6 sec. to 0.75 sec, irradiation of the SPV system is decreased from 1000 W/mm^2 to 600 W/mm^2 as shown in Fig. 5.36 and temperature is increased from 25^{0}C to 45^{0}C as shown in Fig. 5.37 respectively. Under these conditions, Solar PV power is reduced. So, the remaining load demand is supplied from the grid. Under all the above variable conditions, DC link and PCC voltages are maintained and grid current remains balanced. The THD level of grid current is 0.92% and THD level of load current is 16.34% as shown in Fig.5.38, which is well within the IEEE limits. Also unity power factor is maintained for the grid side supply system as shown in Fig. 5.39.

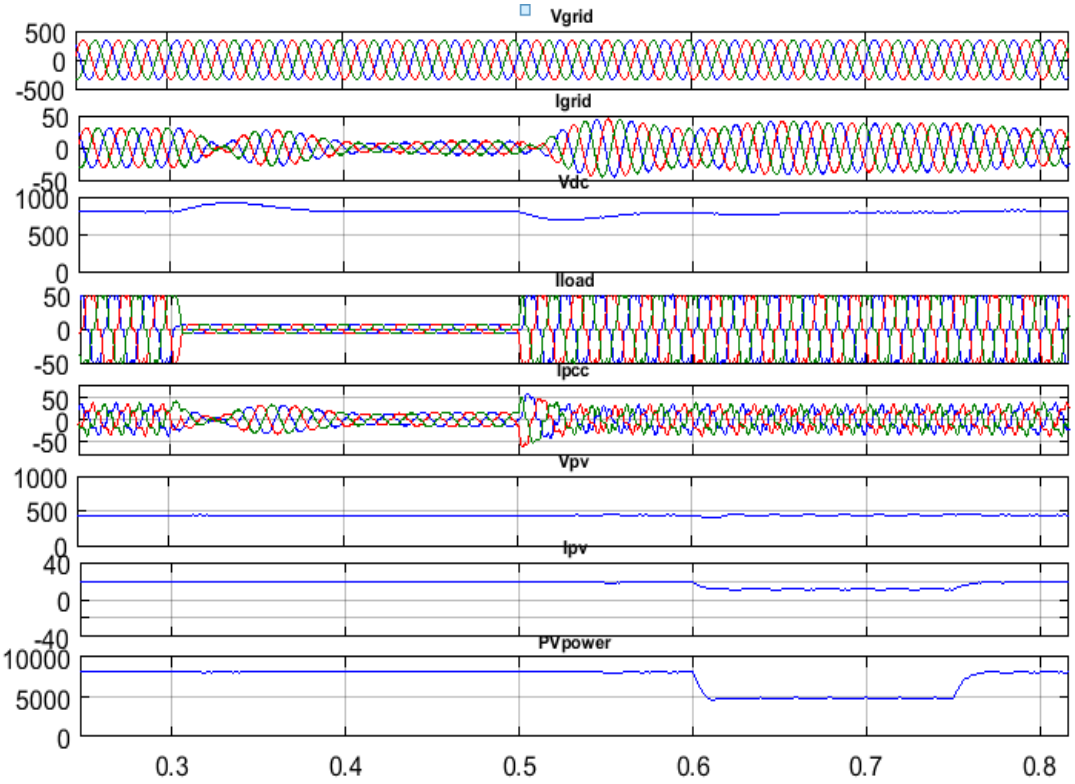

Fig. 5.36. Performance of grid connected SPV system for non-linear load under changing load with varying irradiation levels

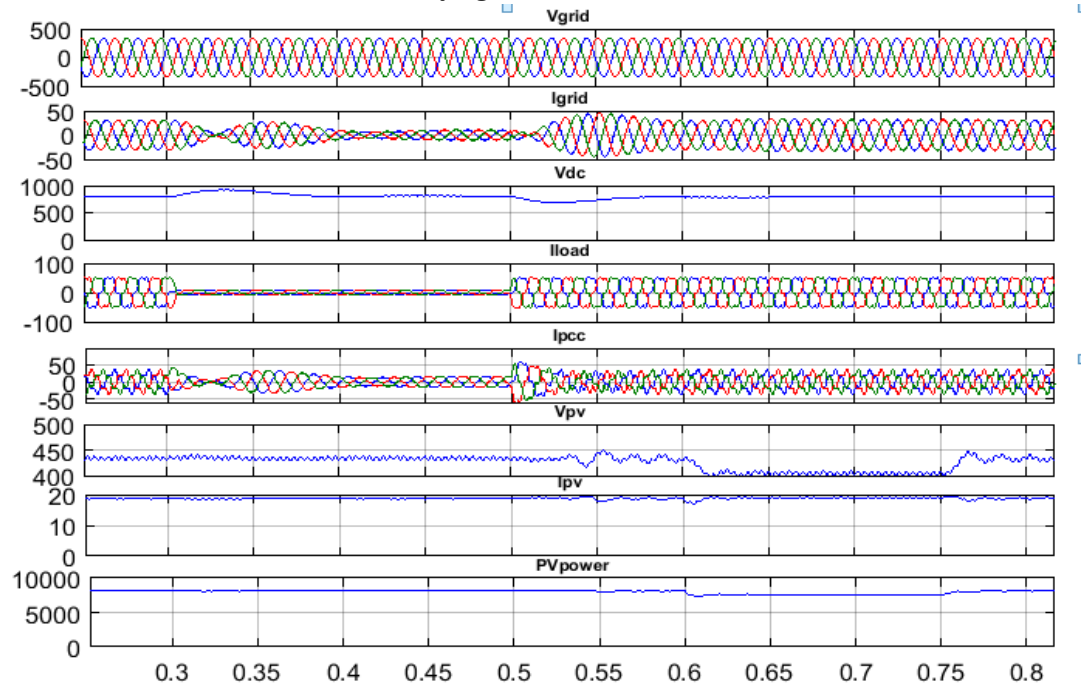

Fig.5.37. Performance of grid connected SPV system for non-linear load under changing load with varying temperature levels

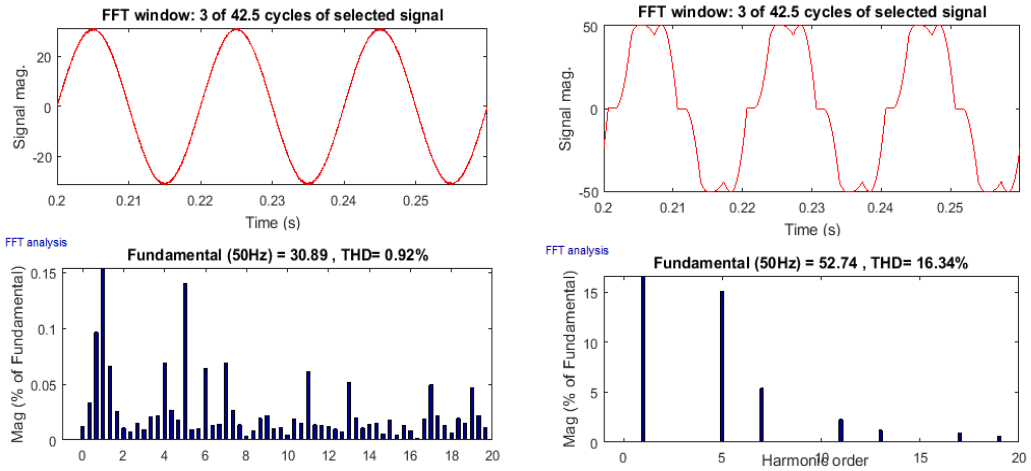

Fig.5.38. Waveform and harmonic analysis for Grid Current (I_{grid}) and Load current (I_{Load}) for non- linear load

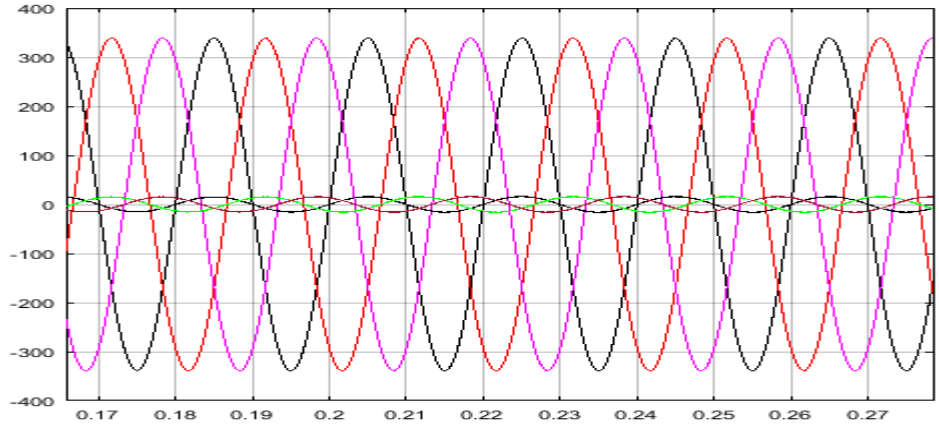

Fig. 5.39. In phase grid side voltage and current for non-linear load conditions

C. ***Performance of grid connected Solar PV system with unbalanced non-linear load***

The performance for non-linear unbalanced load condition is shown in Fig.5.40. From 0.3 sec to 0.5 sec 'a' phase of the load has been disconnected and at t=0.5 sec this 'a' phase load is again applied and the system again comes in the balanced mode. The effect of unbalanced load on the various parameters can be seen. It is observed that, V_{dc} remains constant and source current decreases to meet the load demand, but remains balanced, sinusoidal and the power factor is maintained to unity. From 0.6 sec. to 0.75 sec, irradiation of the SPV system is decreased from 1000 W/mm^2 to 600 W/mm^2 is also shown by fig 5.40. Under this condition, SPV power is reduced. So, the remaining load demand is supplied from the grid. Under all the above variable conditions, DC link and PCC voltages

are maintained and grid current remains balanced. The THD level of grid current is 2.92% which is well within the IEEE limits as shown in Fig.5.41

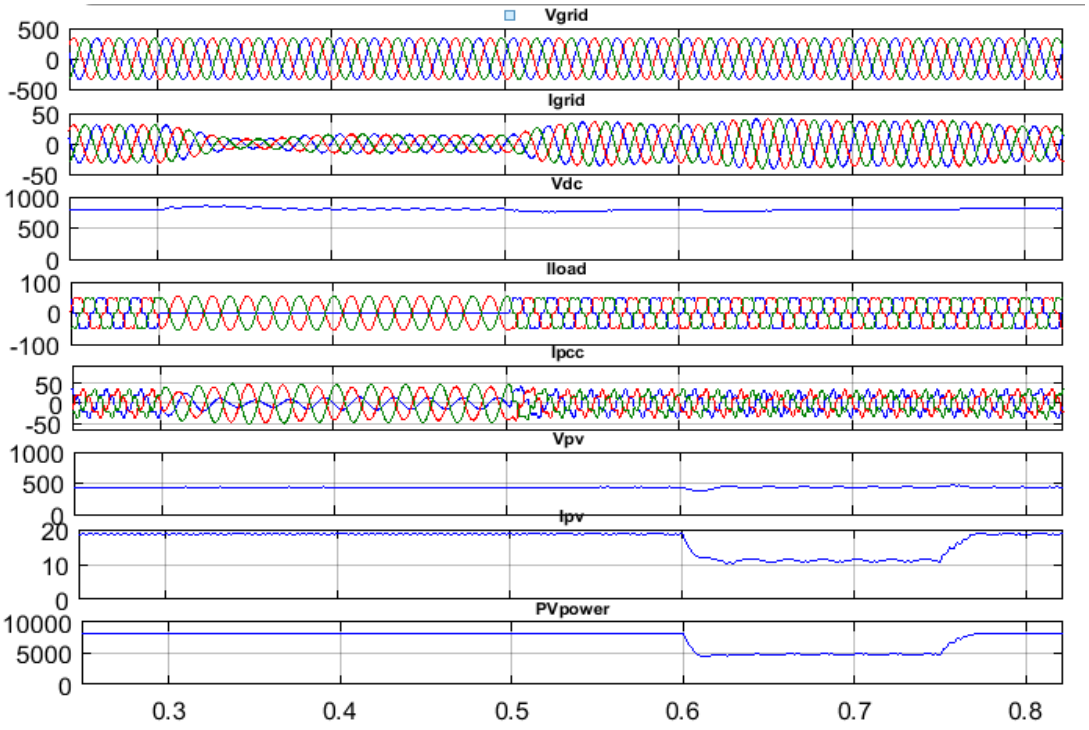

Fig.5.40. Performance of grid connected SPV system for non-linear load under unbalancing with varying irradiation levels

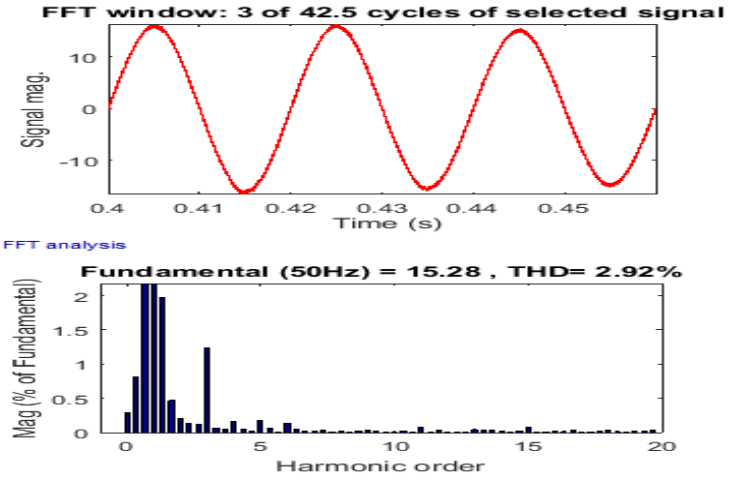

Fig.5.41. Waveform and harmonic analysis for Grid Current (I_{grid}) for non- linear load during unbalancing time

D. Performance of grid connected Solar PV system with dynamic load.

The performance for dynamic load is shown in Fig.5.42. At 0.3 sec torque of motor is increased to full load torque value i.e 20 N-m, after 5sec it is decreased to half of the load torque i.e.10 N-m, and its effect on the various parameters can be seen. As seen from the graphs, V_{dc} remains constant, current from the grid side decreases to meet the load. DC bus voltage and PCC voltage are well maintained and load currents are balanced and THD level of grid current is 2.67% and PCC current is 2.16%, which is well within IEEE limits as given by Fig. 5.43.

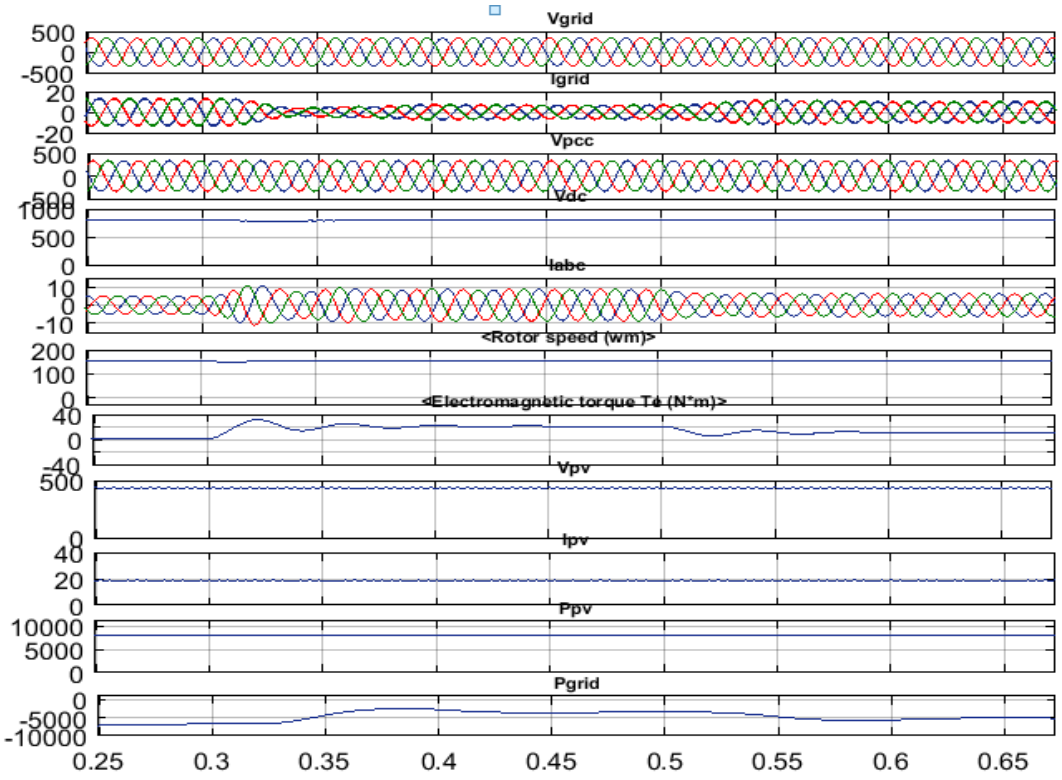

Fig. 5.42. Performance of grid connected SPV system for dynamic load under torque variation with varying irradiation levels

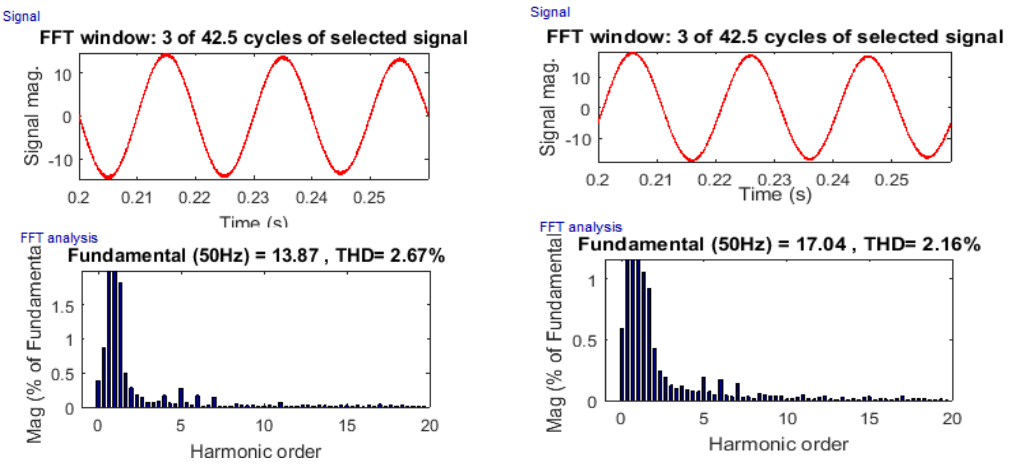

Fig.5.43. Waveform and harmonic analysis for Grid Current (I_{grid}) and PCC current (I_{PCC}) for dynamic load

5.4 Comparison of THD under SRF, ISC and Icosø Algorithms

Table II shows the performance of all three algorithms in terms of harmonic filtering. For all the algorithms source current THD is well maintained below 5%.

Table II. THD of source current, PCC current and load current under various loads

Control Algorithms	V_{dc}	Linear load		Non-linear load		Unbalanced Non-linear load	Dynamic load	
		Source current THD (in %)	PCC current THD (in %)	Source current THD (in %)	Load current THD (in %)	Source current THD during unbalancing time (in %)	Source current THD (in %)	PCC current THD (in %)
SRFT	799	2.30	1.32	1.18	16.34	3.85	3.32	2.96
ISCT	802	3.46	1.97	1.78	16.34	4.61	3.57	4.07
ICOSØ	798	1.92	1.07	0.92	16.34	2.92	2.67	2.16

5.5. Conclusion

The three control algorithm SRFT, ISCT and Icos ∅ are simulated in MATLAB/ SIMULINK and the simulation result for harmonic elimination in source current and power balancing under various loads and under different environment conditions are shown. Also the three algorithms are compared and it is observed that the THD in all the three control schemes for various loads is within IEEE Standard 519, 2014 and the unity power factor of the source side is maintained.

CHAPTER 6

CONCLUSIONS AND FUTURE SCOPE OF WORK

6.1 Conclusion

In this thesis, the design and simulation of grid connected PV system presented. The Power versus Voltage characteristics and Current versus Voltage characteristics of the solar PV array has been plotted and it is found that the PV output mainly depends upon the solar irradiation and temperature. When the irradiance decreases then, PV current decreases as I_{ph} depends on irradiance and this results in decrease in output power. When the temperature increases, the open circuit voltage decreases, hence the power of the solar PV array decreases. The PV array characteristics are non-linear in nature. So, to trace the maximum power output, P & O algorithm is used along with DC-DC boost converter.

The PV inverter is controlled using SRFT, ISCT, and IcosØ algorithms. Simulation studies are performed on the SPV system integrated with conventional grid. These studies are performed with different inverter control schemes under various load and environment conditions. Under all the conditions, the DC link voltage and power balance is maintained. The THD in source side current is well within IEEE standard and unity power factor of grid side is maintained.

6.2 Future scope

Further works that can be carried out in the field of grid connected solar PV system can be use of intelligent and adaptive control algorithms for maximum power point tracking as well as inverter control. Also, a prototype hardware model of the grid connected PV system can be developed for validating the simulation results.

The inverter should be tested for immunity to abnormal grid operation, e.g. voltage swells and sags, and phase jumps. Besides, the immunity to notches and spikes should be investigated. The impact on the grid performance (power quality) when multiple inverters are connected to a local grid may be analysed. Non-islanding inverter can be used to operate within a certain time after the islanding occurs.

REFERENCES

[1] "International Energy Outlook, 2008", Energy Information Administration, Available online: http://www.eia.doe.gov/oiaf/ieo/index.html. Retrieved February 2009 .

[2] Ministry of New and Renewable Energy (MNRE) *13 May 2015.*

[3] Gireesh Shrimali, Sunali Rohra,(2012, October), "India's solar mission: A review" *Renewable and Sustainable Energy Reviews, Vol.16, Issue 8, Pg 6317-6332.*

[4] Gupta, Sandeep Kumar, and Raghubir Singh Anand (2013) "Development of Solar Electricity Supply System in India: An Overview." *Journal of Solar Energy* 2013.

[5] Rachid Belaidi , A. Haddouche, "Shunt active power filter connected to a photovoltaic array for compensating harmonics and reactive power simultaneously" IEEE 4th International Conference on Power Engineering, Energy and Electrical Drives.

[6] Pritam Chowdhury, Indrajit Koley, Sougata Sen, Dr. Pradip Kumar Saha , Dr. Gautam Kumar Panda, "Modelling, Simulation And Control of A Grid Connected Non Conventional Solar Power Generation System Using Matlab" International Journal of Advanced Research in Electrical, Electronics and Instrumentation Engineering *Vol. 2, Issue 4, April 2013.*

[7] S. Sumathi, L. Ashok Kumar, P. Surekha, "Solar PV and Wind Energy Conversion Systems" an Introduction to Theory, Modeling with MATLAB/SIMULINK, and the Role of Soft Computing Techniques ISSN 1865-3529 ISSN 1865-3537 (electronic) Green Energy and Technology ISBN 978-3-319-14941-7 (eBook)

[8] Haitham Abu Rub, Mariusz Malinowski, Kamal Al-Hadad, "Power electronics of renewable energy systems, transportation, and industrial application.", First edition, IEEE press and john wiley and sons publication, 2014.

[9] S. Dasgupta, S. K. Sahoo, and S. K. Panda, "Single-phase inverter control techniques for interfacing renewable energy sources with microgrid—Part I: Parallel-connected

inverter topology with active and reactive power flow control along with grid current shaping," Power Electronics, IEEE Transactions on, vol. 26, pp. 717-731, 2011.

[10] Augustin McEvoy, Tom Markvart and Luis Castaner, “Practical Handbook of Photovoltaics-Fundamentals and Applications”, Second Edition, Elsevier, Wyman Street, USA, 2012

[11] B. Boukezata, A. Chaoui, J.P. Gaubert and M. Hachemi, “Improving the quality of energy in grid connected photovoltaic systems” IEEE Proceedings of the 3rd International Conference on Systems and Control, Algiers, Algeria, October 29-31, 2013.

[12] M. G. Villalva, J. R. Gazoli, and E. R. Filho, "Comprehensive Approach to Modeling and Simulation of Photovoltaic Arrays," *Power Electronics IEEE Transactions on*, vol. 24, pp. 1198-1208, 2009.

[13] J. A. Gow and C. D. Manning, “Development of a photovoltaic array model for use in power-electronics simulation studies,” *IEEE Proc. Elect. Power Appl.*, vol. 146, no. 2, pp. 193–200, 1999.

[14] Wei Jiang, Yu-fei Zhou and Jun-ning Chen, “Modeling and Simulation of Boost Converter in CCM and DCM,” *IEEE Conference on Power Electronics and Intelligent Transportation System (PEITS)*, pp. 288-291, 2009.

[15] Nikita Gupta, Rachana Garg and Parmod Kumar, “Characterization study of PV module connected to Microgrid”, *In IEEE India International Conference JM*I, DOI: 10.1109/INDICON.2015.7443356, India, 2015.

[16] Sachin Kumar Singh, Ahteshamul Haque, “Performance Evaluation of MPPT using Boost Converters for Solar Photovoltaic System” IEEE conf. INDICON 2015.

[17] Mukhtiar Singh, Vinod Khadkikar, Ambrish Chandra and Rajiv K. Varma, “Grid Interconnection of Renewable Energy Sources at the Distribution Level with Power Quality Improvement Features”, *IEEE Transactions on Power Delivery*, vol. 26, no. 1, pp. 307-315, 2011.

[18] S. Rustemli, F. Dincer, “Modeling of Photovoltaic Panel and Examining Effects of Temperature in Matlab/Simulink”, Electronics and Electrical Engineering, ISSN 1392-1215, no. 3(109), pp. 35-40,2012.

[19] Kinal Kachhiya, Makarand Lokhande, Mukesh Patel, “MATLAB/Simulink Model of Solar PV Module and MPPT Algorithm”, Proceedings of the National Conference on Recent Trends in Engineering and Technology, 2011.

[20] I.H. Atlas, A.M. Sharaf, “A Photovoltaic Array Simulation Model for Matlab-Simulink GUI Environment”, International Conference on Clean Power, pp. 341-345, 2007.

[21] Trishan Esram, “Comparison of Photovoltaic Array Maximum Power Point Tracking Techniques” *IEEE Transactions on Energy Conversion, Vol. 22, No. 2, June 2007.*

[22] Tarek Selmi, Mohamed Abdul-Niby, Laura Devis and Andrew Davis, “P&O MPPT Implementation Using MATLAB/Simulink” Ninth International Conference on Ecological Vehicles and Renewable Energies (EVER), IEEE 2014.

[23] M. A. Elgendy and B. Zahawi, “Assessment of perturb and observe MPPT algorithm implementation techniques for PV pumping applications,” *IEEE Transactions on Sustainable Energy*, vol. 3, no. 1, pp. 21-33, 2012.

[24] S. B. Kjaer, “Design and Control of an Inverter for Photovoltaic Applications,” Ph.D. dissertation, Inst. Energy Technol., Aalborg University, Aalborg East, Denmark.

[25] R. Mechouma, B.Azoui, M.Chaabane, “Three-Phase Grid Connected Inverter for PhotovoltaicSystems, a Review” pro. IEEE, 2012 First International Conference on Renewable Energies and Vehicular Technology.

[26] Bhim Singh, Sabha Raj Arya, “Design and control of a DSTATCOM for power quality improvement using cross correlation function approach” International Journal of Engineering, Science and Technology. Vol. 4, No. 1, 2012, pp. 74-86.

[27] B. N. Singh, P. Rastgoufard, B. Singh, A. Chandra, and K. A. Haddad, “Design, simulation and implementation of three pole/four pole topologies for active filters,” *Inst. Electr. Eng. Proc. Electr. Power Appl.*, vol. 151, no. 4, pp. 467–476, Jul. 2004

[28] El-Samahy and E. El-Saadany, "The effect of DG on power quality in a deregulated environment," IEEE Power Engineering Society General Meeting, vol. 3, Jun 2005, pp. 2969- 2976.

[29] Bhattacharya, S. Divan, and B. Benejee, “Synchronous Reference Frame HarmonicIsolator Using Series Active Filter”, 4th European Power Electronic Conf., Florence,vol. 3, 1991, pp. 30-35.

[30] A. K. Verma, B. Singh and D.T. Shahani, “Grid interfaced solar photovoltaic power generating system with power quality improvement at AC mains,” in IEEE ICSET-2012, 24-27 Sept. 2012, pp. pp.177-182.

[31] Reji, Anzari and Arun Kumar R, “Design and Simulation of Three Phase Shunt Active Power Filter Using SRF Theory”. Advance in Electronic and Electric Engineering. ISSN 2231-1297, Volume 3, Number 6 (2013), pp. 651-660

[32] Nikita Gupta, Rachana Garg and Parmod Kumar, “Asymmetrical fuzzy logic control to PV module connected micro-grid”, *In IEEE India International Conference JM*I, DOI: 10.1109/INDICON.2015.7443356, India, 2015.

[33] Ravi Nath Tripathi, Alka Singh , “SRF Theory Based Grid Interconnected Solar Photovoltaic (SPV) System with Improved Power Quality” Emerging Trends in Communication Control, Signal Processing & Computing Applications (C2SPCA), 2013 International Conference

[34] Da silva, Pereira, R.R., da silva, “A digital PLL scheme for three-phase system using modified synchronous reference frame”, IEEE Transactions Industrial Electronics, 2010, 57; 3814-21.

[35] http://in.mathworks.com/help/physmod/sps/powersys/ref/pll3ph.html

[36] Mohamayee Mohapatra, B.Chitti Babu, "Fixed and Sinusoidal-Band Hysteresis Current Controller for PWM Voltage Source Inverter with LC Filter" *IEEE Student's Technology Symposium* 2010,IIT Kharagpur,03-04/April/2010.

[37] U. Koteswara Rao, Mahesh K. Mishra, and Arindam Ghosh, "Control Strategies for Load Compensation Using Instantaneous Symmetrical Component Theory Under Different Supply Voltages," *IEEE Trans on Power Delivery,* vol.23, no.4, pp.2310-2317, 2008.

[38] Sunil Kumar and Bhim Singh, "Control of 4-Leg VSC Based DSTATCOM Using Modified Instantaneous Symmetrical Component Theory," *International Conf. on Power System (ICPS),* pp.1-6, 2009.

[39] Arindam Ghosh, and Avinash Joshi, "A New Approach to Load Balancing and Power Factor Correction in Power Distribution System," *IEEE Trans on Power Delivery,* vol.15, no.1, pp. 417-422, 2000.

[40] Mahesh K. Mishra, Arindam Ghosh, Avinash Joshi and Hiralal M. Suryawanshi, "A Novel Method of Load Compensation Under Unbalanced and Distorted Voltages," *IEEE Trans on Power Delivery,* vol.22, no.1, pp. 288-295, 2007.

[41] Naresh K. Kummari, Asheesh K. Singh and Pradeep Kumar, "Comparative Evaluation of DSTATCOM Control Algorithms for Load Compensation" conf. IEEE ICHQP, 2012.

[42] Dinesh Kumar, Rajesh, "Modelling, Analysis and Performance of a DSTATCOM for Unbalanced and Non-Linear Load" 2005 IEEE/PES Transmission and Distribution Conference & Exhibition: Asia and Pacific Dalian, China.

[43] Arun Kumar Verma, Bhim Singh, D.T Shahani, Ambrish Chandra and Kamal Al-Haddad, "Combined Operation of a VSC Based Grid Interfaced Solar Photovoltaic Power Generation System with Night Time Application". IEEE /PES General meeting, Conference & Exhibition 2014.

[44] Manoj Kumar, Mahesh K. Mishra, "A Grid-Connected Dual Voltage Source Inverter With Power Quality Improvement Features" *IEEE Trans.* on Sustainable Energy, Vol. 6, No. 2, April 2015.

[45] G. Bhuvaneswari and M.G. Nair , "Design, Simulation and Analog Circuit Implementation of a Three-phase Shunt Active Filter using the Icosφ Algorithm", *Conf. IEEE PEDS '05,* vol. 1, Jan. 2006, pp. 553 –55.

[46] B. Singh, and S. Kumar, "Control of DSTATCOM using IcosΦ Algorithm," *IEEE Conference in Industrial Electronics IECON'09,* pp. 322_327 (2009).

[47] Kamatchi Kannan V. and Rengarajan, N., "Photovoltaic Based Distribution Static Compensator for Power Quality Improvement," *International Journal of Electrical Power & Energy Systems,* Vol. 42, No. 1, pp.685_692 (2012).

[48] G. Bhuvaneswari, M.G. Nair and S. Kumar Reddy, "Comparison of Synchronous Detection and IcosΦ Shunt Active Filtering Algorithms", *Conf. IEEE PEDES,* Dec. 2006, pp. 1 – 5.

[49] G. Bhuvaneswari and M.G. Nair, "Design, Simulation, and Analog Circuit Implementation of a Three-Phase Shunt Active Filter Using the Icos∅ Algorithm," *IEEE Trans. on Power Delivery,* Volume 23, pp. 1222 –1235, April 2008.

[50] IEEE Recommended Practices and Requirements for Harmonics Control in Electric Power Systems, IEEE Standard 519, 2014.

Appendix 1

Data for SPV system:

Maximum power of array = 8 kW, Short circuit current of module= 8.32 A, open circuit voltage of module = 44.6 V, Cells per module=72, series resistance (R_s) =0.42018 Ω, shunt resistance (R_{sh}) =0.42018 Ω, Module current at MPP=7.78 A, Module voltage at MPP=36, q= 1.602 x 10^{-19} C, k =1.38 x 10^{-23} J K^{-1}, T_{ref}= 25 ^{0}C, T=25 ^{0}C to 70 ^{0}C, and K = 0.01 /^{o}C.

Data for DC-DC boost converter:

D=0.5, L=0.02 H, C=650 μF, fs=10 kHz

Data for PV inverter:

V_{dc} = 800 V, L_f =7 mF, C_d= 3000 μF.

Data for different loads:

i. Linear RL load with active power 16 kW and reactive power 12 kVAR and power factor 0.8.
ii. Changed Linear RL load from 0.3 sec to 0.5 sec in simulation analysis is 3 kW with active power and 2 kVAR with reactive power and power factor 0.83.
iii. Nonlinear load-universal bridge with 10Ω, 0.8mH RL load, and
iv. Changed Non-linear load from 0.3 sec to 0.5 sec in simulation is universal bridge with 100Ω, 200mH.
v. Dynamic load- 5 hp, induction motor load.

List of Publications

[1] M. Kumar, N. Gupta, R. Garg, “Unity Power Factor Control of Grid Connected SPV system using Instantaneous Symmetrical Component Theory”, In IEEE International Conference on Power Electronics, Intelligent control and Energy Systems (ICPEICES-2016), 4th - 6th July, DTU, Delhi.